

FLUTTER ANALYSIS OF FLAT RECTANGULAR ANISOTROPIC
PANELS/ IN A HIGH MACH NUMBER SUPERSONIC FLOW

by

R. L. RAMKUMAR

A thesis submitted to the Graduate Faculty of the
Virginia Polytechnic Institute and State University
in partial fulfillment of the requirements for the degree of
MASTER OF SCIENCE

in

Aerospace and Ocean Engineering

APPROVED:

T. A. Weisshaar, Chairman

F. H. Lutze

D. Frederick

July, 1974

Blacksburg, Virginia

ACKNOWLEDGMENTS

The author wishes to thank Dr. Weisshaar for his constant advice and help, without which this paper could not have been completed in this short period of time. Thanks are also due to Dr. Frederick, whose course in composites was of good assistance in doing this research. The encouragement from the author's parents, Mr. & Mrs. S.V.L.Narayanan, his brother, Mr.V.L.Sethuram, and his sister, Miss Lalitha, was a constant source of inspiration. The author is thankful to the Aerospace Dept. in VPI&SU for providing funds to work with the computer.

14

TABLE OF CONTENTS

	<u>Page</u>
ABSTRACT	ii
LIST OF TABLES	iv
LIST OF FIGURES	v
LIST OF SYMBOLS	viii
I. INTRODUCTION	1
II. TECHNICAL DISCUSSION	5
III. DISCUSSION OF RESULTS	21
IV. CONCLUSIONS	23
REFERENCES	25
APPENDIX A -- ELASTIC CONSTANTS FOR A LAMINATE	27
APPENDIX B -- COMPUTER PROGRAM FOR A,B,D MATRICES OF THE LAMINATE	30
APPENDIX C -- COMPUTER PROGRAM FOR STATIC BUCKLING LOADS	34
APPENDIX D -- COMPUTER PROGRAM TO SOLVE FOR FLUTTER FREQUENCIES AND MODE SHAPES	36
APPENDIX E	55
TABLES	57
FIGURES	62

LIST OF TABLES

	<u>Page</u>
1. Material Properties	58
2. Static Buckling Loads for a Boron-Epoxy Ply	59
3. Flutter Boundary of Boron-Epoxy Angle-Ply Panel for Various Numbers of Plies	60
4. Weak Coalescent Flutter Values for an Angle-Ply Panel . .	61

LIST OF FIGURES

	<u>Page</u>
1. Planform Geometry of a Ply	63
2. Angle - Ply Panel Layup	64
3. Flutter Boundary for a Boron-Epoxy Ply	65
4. Flutter Boundary for a Graphite-Epoxy Ply	66
5. Flutter Boundary for a Boron-Aluminium Ply	67
6. Effect of Damping on Flutter, Boron-Epoxy, $\phi=0^\circ$	68
7. Effect of Damping on Flutter, Boron-Epoxy, $\phi=10^\circ$	69
8. Effect of Damping on Flutter, Boron-Epoxy, $\phi=20^\circ$	70
9. Effect of Damping on Flutter, Boron-Epoxy, $\phi=30^\circ$	71
10. Effect of Damping on Flutter, Boron-Epoxy, $\phi=40^\circ$	72
11. Effect of Damping on Flutter, Boron-Epoxy, $\phi=50^\circ$	73
12. Effect of Damping on Flutter, Boron-Epoxy, $\phi=60^\circ$	74
13. Effect of Damping on Flutter, Boron-Epoxy, $\phi=70^\circ$	75
14. Effect of Damping on Flutter, Boron-Epoxy, $\phi=80^\circ$	76
15. Effect of Damping on Flutter, Boron-Epoxy, $\phi=90^\circ$	77
16. Effect of Damping on Flutter, Graphite-Epoxy, $\phi=0^\circ$	78
17. Effect of Damping on Flutter, Graphite-Epoxy, $\phi=10^\circ$	79
18. Effect of Damping on Flutter, Graphite-Epoxy, $\phi=20^\circ$	80
19. Effect of Damping on Flutter, Graphite-Epoxy, $\phi=30^\circ$	81
20. Effect of Damping on Flutter, Graphite-Epoxy, $\phi=40^\circ$	82
21. Effect of Damping on Flutter, Graphite-Epoxy, $\phi=50^\circ$	83
22. Effect of Damping on Flutter, Graphite-Epoxy, $\phi=60^\circ$	84

LIST OF FIGURES - continued

	<u>Page</u>
23. Effect of Damping on Flutter, Graphite-Epoxy, $\phi=70^\circ$. . .	85
24. Effect of Damping on Flutter, Graphite-Epoxy, $\phi=80^\circ$. . .	86
25. Effect of Damping on Flutter, Graphite-Epoxy, $\phi=90^\circ$. . .	87
26. Effect of Damping on Flutter, Boron-Aluminium, $\phi=0^\circ$. . .	88
27. Effect of Damping on Flutter, Boron-Aluminium, $\phi=10^\circ$. .	89
28. Effect of Damping on Flutter, Boron-Aluminium, $\phi=20^\circ$. .	90
29. Effect of Damping on Flutter, Boron-Aluminium, $\phi=30^\circ$. .	91
30. Effect of Damping on Flutter, Boron-Aluminium, $\phi=40^\circ$. .	92
31. Effect of Damping on Flutter, Boron-Aluminium, $\phi=50^\circ$. .	93
32. Effect of Damping on Flutter, Boron-Aluminium, $\phi=60^\circ$. .	94
33. Effect of Damping on Flutter, Boron-Aluminium, $\phi=70^\circ$. .	95
34. Effect of Damping on Flutter, Boron-Aluminium, $\phi=80^\circ$. .	96
35. Effect of Damping on Flutter, Boron-Aluminium, $\phi=90^\circ$. .	97
36. Variation in Flutter Boundary with Damping, Boron-Epoxy .	98
37. Variation in Flutter Boundary with Damping, Graphite-Epoxy	99
38. Variation in Flutter Boundary with Damping, Boron-Aluminium	100
39. Effect of Streamwise Inplane Compressive Stress on Flutter, Boron-Epoxy, $\phi=0^\circ$	101
40. Effect of Streamwise Inplane Compressive Stress on Flutter, Boron-Epoxy, $\phi=30^\circ$	102
41. Effect of Streamwise Inplane Compressive Stress on Flutter, Boron-Epoxy, $\phi=60^\circ$	103

LIST OF FIGURES - continued

	<u>Page</u>
42. Effect of Streamwise Inplane Compressive Stress on Flutter, Boron-Epoxy, $\phi=90^\circ$	104
43. Effect of Number of Plies on Flutter Boundary, Boron-Epoxy Angle-Ply Panel	105

LIST OF SYMBOLS

λ	flutter parameter defined as $\lambda = 2qa^3/D_{11} M^2 - 1$
q	freestream dynamic pressure
U_∞	freestream velocity
M_∞	freestream Mach number
M	Mach number
E_{11}, E_{22}	Young's moduli in the 1 and 2 principal directions of the ply
G_{12}	shear modulus in the 1-2 principal plane
ν_{12}	major Poisson's ratio
ν_{21}	defined as $\nu_{21} = \nu_{12} E_{22} / E_{11}$
a	streamwise length of panel
b	spanwise length of panel
x	streamwise direction
y	spanwise direction
$W(x, y)$	midplane deflection in the Z direction
ξ	nondimensional quantity = x/a
η	nondimensional quantity = y/b
$w(\xi, \eta)$	nondimensional quantity = $W(x, y)/a$
N_x, N_y	inplane normal stress resultant in the x and y directions
N_{xy}	inplane shear stress resultant in the x-y plane
M_x, M_y	bending moment resultants about the x and y axes
M_{xy}	twisting moment resultant in the x-y plane
$\epsilon_{0x}, \epsilon_{0y}, \epsilon_{oxy}$	midplane normal and shear strains

k_x, k_y, k_{xy}	plate curvatures and twist
n	number of plies
ϕ	orientation of principal ply axis with respect to the freestream direction
g	total damping in the panel, aerodynamic and/or structural
$K_{pq,mm}$	general stiffness element
$A_{pq,mm}$	general aerodynamic loading matrix element
$M_{pq,mm}$	general mass matrix element
m	mass density of panel = mass/area
\bar{m}	total mass of panel = mab
A_{ij}	defined as $\sum_{k=1}^n (\bar{Q}_{ij})_k (h_k - h_{k+1})$
B_{ij}	defined as $\sum_{k=1}^n (\bar{Q}_{ij})_k (h_k^2 - h_{k+1}^2)/2$
D_{ij}	defined as $\sum_{k=1}^n (\bar{Q}_{ij})_k (h_k^3 - h_{k+1}^3)/3$
Q_{ij}	stiffness of a ply referred to material principal axes
\bar{Q}_{ij}	stiffness of a ply referred to global axes (aligned with freestream direction)
h_k	distance from panel midplane to the top of the k'th ply
U_0	strain energy per unit area
U	total strain energy = $\int_0^a \int_0^b U_0 dx dy$
T	kinetic energy
λ_{crit}	critical flutter parameter

K_x

nondimensional inplane stress resultant in the
streamwise or x direction defined as :

$$K_x = (\pi^2 a^2 N_x) / (4D_{11})$$

I. INTRODUCTION

Panel flutter is a self-excited, aeroelastic, dynamic instability caused by the interaction among the aerodynamic, inertial and elastic forces of a panel (Ref. 1). It is seldom destructive because structural nonlinearities tend to limit the amplitude of the panel response. Nevertheless, panel flutter is undesirable because of the possibility of structural fatigue and the excessive noise levels generated by panel vibration.

Panel flutter has been observed on the X-15 (Ref. 2), on the X-20 (Ref. 3,4,5), on Titan II and III (Ref. 6), and on the S-IV B (Ref. 7). The structural damage due to panel flutter was destructive on the X-15 and the X-20. But, for the Titans and S-IV B, the flutter was non-destructive as the severity and duration of the flutter did not affect the structure of the panel very much.

The contributors and their contributions to the panel flutter problem are many and varied. Surveys on panel flutter have been written by Fung (Ref. 8,9), Johns (Ref. 10,11), Dowell (Ref. 12) and others (Ref. 13). The two documents mentioned in References 1 and 14 are widely available for design purposes. While Reference 1 helps in the identification of panels likely to encounter flutter, Reference 14 gives simplified criteria in graphical form for most of the parameters affecting panel flutter design. This introduction is based on the material given in References 1,12,14.

The present problem is essentially an extension of the

basic problem that Hedgepeth solved (Ref. 15). Hedgepeth analysed an isolated, simply supported, rectangular, isotropic plate of uniform thickness subjected to supersonic flow over one surface. Perlmutter (Ref. 16) studied panel flutter on orthotropic wings with the model being simply supported along the two spanwise edges and free along the leading and trailing edges. Bohon (Ref. 17) analysed the flutter of flat, orthotropic panels with biaxial inplane loading and arbitrary flow direction. A theoretical analysis of the flutter of flat, rectangular, orthotropic panels at various angles of orientation with respect to the flow direction was carried out by Gaspers and Redd (Ref. 18). The effect of rotating the material principal axes of the panel with respect to the panel edges was studied by Calligeros and Dugundgi (Ref. 19). The problem in the present study extends the latter work. Unlike the latter study the present study assumes the panel material to be generally anisotropic rather than orthotropic.

A continuous fiber composite material is a heterogeneous material consisting of fibers embedded in a matrix material. Composites possess manifold improvements in stiffness and strength over ordinary materials. Composite structures are normally fabricated by a lamination process in which the individual plies are oriented in a predetermined manner. The plies that build up the laminate are called unidirectional layers, and are generally orthotropic.

In an isotropic material the material properties at a point are the same for all planes passing through the point. An orthotropic material has three mutually orthogonal planes of material property

symmetry, while an anisotropic material has different material properties for different planes passing through a point.

Composite materials have had a steadily increasing impact on the aerospace materials field. Many interesting details given in Reference 20 support this fact, and a few of these are recalled here. Lockheed engineers estimated that substitution of an organic composite in a 50% resin content by volume could provide a weight reduction of 25 to 30% (Ref. 20). Six different primary and secondary parts for Northrop's F-5A fighter were designed and fabricated from various graphite systems. Most of these parts, including a landing gear door, leading and trailing edge flaps, and horizontal stabilizer, performed well. A landing gear door, flown in an actual aircraft, was 36% lighter than its aluminium counterpart and exceeded all static and flight test structural requirements (Ref. 20). The F-15 fighter has a composite horizontal stabilizer with boron epoxy skins. F-111 test parts have been made from a number of composites including boron and graphite. A graphite box beam assembly has been designed by Grumman Aircraft. The demand for fiberglass has been predicted to increase this decade. Composite materials may also be used in aircraft engine parts very soon. The use of boron/polymide blades instead of titanium blades could effect a weight saving of 51% (Ref. 20). Space applications have led to the development of composites using a resin system called Ryton, which is practically insoluble and appears to be completely inert. All these successes in the field of composite materials are bound to boost their use in actual aircraft components in the near future.

As mentioned earlier, the present problem is similar to that analysed by Calligeros and Dugundgi in Reference 19. The main difference between the two problems is that our panel is not restricted to special orthotropy but is assumed to be a midplane symmetric, angle-ply laminate, with alternating orthotropic plies having the same angle of orientation, ϕ , but alternating signs. Figure 1 shows the planform geometry of an individual orthotropic ply, defining its coordinates and orientation angle. Figure 2 shows the angle-ply panel layup with the necessary notations used in the derivation of the laminate constitutive equation (Appendix A). Thus, our panel is generally anisotropic, and midplane symmetry eliminates, as will be explained in the technical discussion, the bending-membrane coupling which would otherwise be present.

II. TECHNICAL DISCUSSION

The panel model used in this analysis is a midplane symmetric angle-ply laminate, built up of individual orthotropic, rectangular plies simply supported at the edges. Above and below the midplane of the angle-ply panel, alternate plies are crossed at the same angle with respect to the freestream direction, one having a positive orientation and the other a negative orientation of the same magnitude (Fig.2). The plies above the midplane are a mirror image of those below the midplane. The ensuing analysis will determine the effect of the orientation of orthotropicity of various plies on the flutter boundary. The effect of damping, compressive inplane stresses in the streamwise direction, and the number of plies in the panel is also studied. The plies of different stiffness ratios, used in our analysis, are boron-epoxy, graphite-epoxy and boron-aluminium plies.

Reference 12 classifies most panel flutter analyses in one of four categories based on the structural and aerodynamic theories employed: (1) Linear structural theory and quasi-steady aerodynamic theory; (2) Linear structural theory and full, linearised (inviscid, potential) aerodynamic theory; (3) Nonlinear structural theory and quasi-steady aerodynamic theory; (4) Nonlinear structural theory and full, linearised (inviscid, potential) aerodynamic theory.

The present analysis is a type (1) analysis which is the simplest of the four. One of the two drawbacks of this approach is that it gives no information about the magnitude of the panel flutter

oscillation itself though it does determine the flutter boundary. The other drawback is that the use of quasi-steady aerodynamics neglects the three-dimensionality and the unsteadiness the flow. A type (4) analysis represents the most advanced state-of-the-art as it remedies both these drawbacks. For further details on these analyses the reader is referred to Reference 12 and the references mentioned therein.

The panel in this thesis is made elastically and geometrically symmetrical about its midplane to eliminate bending-membrane elastic coupling, though coupling will still be present between bending and twisting and, for membrane behaviour, between normal and shearing strains. This is so because, in the laminate equation (Ref. 21,22):

$$\begin{Bmatrix} N \\ M \end{Bmatrix} = \begin{bmatrix} A & B \\ B & D \end{bmatrix} \begin{Bmatrix} \epsilon_0 \\ k \end{Bmatrix} \quad (1)$$

the coupling matrix [B] becomes a null matrix when the laminate is midplane symmetric (Ref. 22). In equation (1)

$$\{N\} = \begin{Bmatrix} N_x \\ N_y \\ N_{xy} \end{Bmatrix} \quad (2)$$

is the stress resultant vector, where N_x and N_y are the inplane normal stress resultants in the x and y directions, and N_{xy} is the inplane shear stress resultant in the x-y plane.

$$M = \begin{Bmatrix} M_x \\ M_y \\ M_{xy} \end{Bmatrix} \quad (3)$$

is the moment resultant vector, where M_x and M_y are the bending moment

resultants due to normal stresses in the x and y directions, and M_{xy} is the twisting moment resultant due to shear stresses in the x-y plane (Ref. 21,22).

$$\{\epsilon_0\} = \begin{Bmatrix} \epsilon_{0x} \\ \epsilon_{0y} \\ \epsilon_{0xy} \end{Bmatrix} \quad (4)$$

is the midplane strain vector, where ϵ_{0x} and ϵ_{0y} are the midplane normal strains in the x and y directions, and ϵ_{0xy} is the midplane shear strain in the x-y plane.

$$\{k\} = \begin{Bmatrix} k_x \\ k_y \\ k_{xy} \end{Bmatrix} = - \begin{Bmatrix} W_{,xx} \\ W_{,yy} \\ 2W_{,xy} \end{Bmatrix} \quad (5)$$

is the plate curvature vector, where $w_{,xx}$ etc. are the second partial derivatives of $W(x,y,t)$ with respect to the subscripts, taken in order, from left to right (Ref. 21,22). $W(x,y,t)$ is the plate midplane deflection.

Elements of the A,B,D matrices of the panel are defined in Appendix A.

Hence, for a midplane symmetric panel, the laminate constitutive equation yields:

$$\begin{Bmatrix} M_x \\ M_y \\ M_{xy} \end{Bmatrix} = \begin{bmatrix} D_{11} & D_{12} & D_{16} \\ D_{12} & D_{22} & D_{26} \\ D_{16} & D_{26} & D_{66} \end{bmatrix} \begin{Bmatrix} k_x \\ k_y \\ k_{xy} \end{Bmatrix} \quad (6)$$

When $D_{16} = D_{26} = 0$, bending and twisting are uncoupled, and the panel is said to be specially orthotropic or simply orthotropic. When either D_{16} or D_{26} is non-zero, bending and twisting are coupled and the panel

is generally anisotropic. The coupling terms D_{16} and D_{26} become negligibly small in comparison to D_{11} in an angle-ply panel composed of a large number of built-up layers. In this case the panel behaviour approaches that of an orthotropic panel (Ref. 22).

Midplane symmetry also uncouples the inplane and out-of-plane equations of motion of the panel, and makes feasible an explicit solution for the deflection $W(x,y,t)$ of the panel (sec. 2.5, Ref. 22). This uncoupled partial differential equation of motion for a midplane symmetric anisotropic laminate is (Ref. 22):

$$D_{11}W_{,xxxx} + 4D_{16}W_{,xxxxy} + 2(D_{12}+2D_{66})W_{,xxyy} + 4D_{26}W_{,xyyy} + D_{22}W_{,yyyy} = p(x,y) + N_x W_{,xx} + 2N_{xy} W_{,xy} + N_y W_{,yy} \quad (7)$$

where $W_{,xxxx}$ etc. are the fourth partial derivatives of $W(x,y)$ with respect to the subscripts. $p(x,y)$ is the sum of the aerodynamic and inertial loadings (per unit area).

The D_{ij} terms for the panel are defined in Appendix A. D_{11} and D_{22} are a measure of the streamwise and spanwise rigidities of the panel, while $(D_{12}+2D_{66})$ is a measure of its torsional rigidity. D_{16} and D_{26} are the elastic coupling terms which give a measure of the bending-torsion elastic coupling in the midplane symmetric panel. The presence of D_{16} and D_{26} in the equilibrium equation seems to preclude the possibility of an exact solution, as explained later. Because of this an approximate solution technique must be used. The approximate solution technique used here is the well-known Rayleigh-Ritz procedure.

The aerodynamic loads on the panel are based on two-dimensional "piston theory" (Ref. 23), which relates the local

pressure generated by the panel motion to the local normal component of fluid velocity. Piston theory may be employed for large flight Mach numbers ($M > 2$) or high reduced frequencies of unsteady motion whenever the surface is nearly plane and not inclined too sharply to the direction of flow of the freestream. For $M > 2$, the point function aerodynamic theories such as the piston theory or Ackeret theory offer reasonable approximations to the local aerodynamic pressure and greatly simplify the analyses (Ref. 23). The use of piston theory aerodynamics limits the present analysis to freestream Mach numbers greater than two ($M_\infty > 2$).

In the equilibrium equation,

$$p(x,y) = p_A(x,y) + p_I(x,y) \quad (8)$$

Two-dimensional piston theory predicts the aerodynamic loading to be (Ref. 23):

$$p_A(x,y) = - \frac{2q}{U_\infty \sqrt{M_\infty^2 - 1}} [U_\infty W_{,x} + \frac{M_\infty^2 - 2}{M_\infty^2 - 1} W_{,t}] \quad (9)$$

where q is the freestream dynamic pressure,

U_∞ is the freestream velocity, and

M_∞ is the freestream Mach number.

The inertial loading is given by:

$$p_I(x,y) = - m W_{,tt} \quad (10)$$

where m is the mass density (mass per unit area) of the panel.

Inplane stresses (N) may result from in-flight heating, flight loads or manufacturing and installation procedures. This analysis includes compressive stresses in one of the cases analysed because

compressive stresses degrade the flutter speed. Tensile stresses, on the other hand, increase the stiffness of the panel and hence raise the flutter speed.

To solve the panel flutter problem non-dimensional quantities ξ, η and $w(\xi, \eta, t)$ are introduced by normalizing the dimensional panel midplane deflection $W(x, y, t)$ and the coordinate x with respect to a , and the coordinate y with respect to b . Here a and b are the streamwise and spanwise panel dimensions, respectively (Fig. 1).

$$\xi = x/a ; \eta = y/b ; w(\xi, \eta, t) = W(x, y, t)/a \quad (11)$$

The resulting nondimensional equation of motion for the panel is given in Appendix E.

The deflection function is assumed to be mathematically separable and harmonic with respect to time:

$$w(\xi, \eta, t) = w(\xi, \eta) e^{i\omega t} \quad (12)$$

In the Rayleigh-Ritz procedure, an approximation to the deflection function $w(\xi, \eta)$ is chosen such that it satisfies the geometric boundary conditions of the panel. For a simply supported panel these geometric boundary conditions specify that the deflection $w(\xi, \eta)$ of the panel along all the four edges should be zero. That is

$$w(\xi, \eta) = 0 \text{ at } \xi=0,1; \eta=0,1 \quad (13)$$

The assumed solution satisfying these geometric boundary conditions is taken to be:

$$w(\xi, \eta) = \sum_{m=1}^M \sum_{n=1}^N a_{mn} \sin m\pi\xi \sin n\pi\eta \quad (14)$$

where m and n are integers. These integers define the assumed modes of

vibration. The twenty mode analysis used in this thesis assumes modes with $(m, n) = (1, 1), (1, 2), (2, 1), (2, 2), \dots, (10, 1)$ and $(10, 2)$.

Alternatively, a Galerkin solution may be attempted for our problem. In this case, the assumed approximate series solution is substituted into the governing equation of motion for the panel and the resulting error is minimized using weighting functions. These weighting functions are generally the different modes assumed in equation (14). This yields a set of algebraic equations which may be solved for the required eigenvalues.

If a Galerkin solution is attempted, a function satisfying the full boundary conditions must be present in the series solution for $w(\xi, \eta)$ if the Rayleigh-Ritz and Galerkin techniques are to be equivalent. That is, a function must satisfy the zero-moment condition in addition to the zero-deflection condition on all four edges of the panel. The complexity involved in this is seen by looking at equation (6) which expresses the moment resultants in terms of the plate rigidities and plate curvatures. As the panel is generally anisotropic (D_{16} and/or D_{26} is non-zero) and not specially orthotropic ($D_{16} = D_{26} = 0$), the derivative $W_{,xy}$ in the expressions for M_x and M_y makes it difficult to choose a function $W(x,y)$ satisfying the zero-moment condition on all four edges of the panel. Hence the preference of the Rayleigh-Ritz procedure over Galerkin's method.

In the Rayleigh-Ritz procedure, the chosen approximate solution (eqn.14) is used with the Lagrange equations formed with Hamilton's principle as basis. This yields a system of linear algebraic

equations which may be written in matrix form as:

$$-\Omega^2 [M]_{ij,rs} \{a\}_{mn} + ([K]_{ij,rs} - \lambda[A]_{ij,rs}) \{a\}_{mn} = \{0\} \quad (15)$$

[M], [K] and [A] are termed the mass, stiffness and aerodynamic loading matrices. These matrix expressions will be developed subsequently. Ω^2 is an eigenvalue of the problem related to ω as shown in Appendix E.

$$\lambda = \frac{2qa^3}{D_{11}\sqrt{M_\infty^2-1}} \text{ is the nondimensional flutter parameter.} \quad (16)$$

Expressions for the general element in the mass, stiffness and aerodynamic loading matrices are now derived, dropping the $e^{i\omega t}$ term.

(a) Stiffness Matrix

The strain energy in the panel, per unit area, U_0 , is given by:

$$U_0 = 1/2 \{k\}^T \{M\} + 1/2 \{k\}^T [D] \{k\} \quad (17)$$

The curvatures $\{k\}$ are made non-dimensional through a transformation matrix, and U_0 is integrated over the surface area of the panel to give the total strain energy, U , in terms of the second derivatives in $w(\xi, \eta)$ and panel properties. The assumed deflection function is introduced into this expression for U , and dummy variables p and q are used to take care of products of second order derivatives. For example, the $w_{,\xi\xi}^2$ term is written as:

$$w_{,\xi\xi}^2 = \sum \sum \sum \sum \{ \pi^4 m^2 p^2 a_{mn} a_{pq} \sin m\pi\xi \sin n\pi\eta \sin p\pi\xi \sin q\pi\eta \} \quad (18)$$

The stiffness element $K_{ij,rs}$ is now determined from the total strain energy, U , given in Appendix E, as follows:

$$K_{ij,rs} = \frac{\partial^2 U}{\partial a_{ij} \partial a_{rs}}$$

$$= U_{,a_{ij} a_{rs}} \quad (19)$$

This, in our analysis, reduces to:

$$K_{pq,mn} = (\pi^4/4) [m^4 + m^2 n^2 (2C_1 + C_2) + n^4 E]$$

when $m=p$ and $n=q$

$$K_{pq,mn} = \frac{-4\pi^2 pqmn}{(m^2 - p^2)(n^2 - q^2)} [B(m^2 + p^2) + D(n^2 + q^2)] \quad (20)$$

when $m \neq p$ and $n \neq q$, and $(m+p)$ and $(n+q)$ are odd

$$K_{pq,mn} = 0 \quad \text{otherwise}$$

The constants B, C₁, C₂, D and E are defined as:

$$B = 2D_{16}/D_{11}$$

$$C_1 = D_{12}/D_{11}$$

$$C_2 = 4D_{66}/D_{11} \quad (21)$$

$$D = 2D_{26}/D_{11}$$

$$E = D_{22}/D_{11}$$

The above computation does not include the effect of inplane stresses on the stiffness of the panel. This is found separately and added to the stiffness expression for $K_{pq,mn}$ just derived to give the general stiffness matrix element, with the inclusion of inplane stresses. The stiffness due to inplane stresses alone reduces to:

$$K_{pq,mn} = (\pi^2 a^2/4) [mpN_x/D_{11} + nq(a/b)^2 N_y/D_{11}]$$

when $m=p$ and $n=q$

$$K_{pq, mn} = \frac{-8a^2 pqmn}{(m^2 - p^2)(n^2 - q^2)} (a/b) N_{xy} / D_{11} \quad (22)$$

when $m \neq p$ and $n \neq q$, and $(m+p)$ and $(n+q)$ are odd

$$K_{pq, mn} = 0 \quad \text{otherwise}$$

(b) Mass Matrix

The expression for the kinetic energy, T , in the panel is:

$$T = (1/2) m a^3 b \int_0^1 \int_0^1 (\dot{w})^2 d\xi d\eta \quad (23)$$

where m is the mass density of the panel and \dot{w} is the time derivative of the deflection function $w(\xi, \eta, t)$. If $b_{mn} = a_{mn} e^{i\omega t}$, equations 12&14 give:

$$\dot{w}(\xi, \eta, t) = \sum_m \sum_n \dot{b}_{mn} \sin m\pi\xi \sin n\pi\eta \quad (24)$$

Using the dummy variables p and q for the $(\dot{w})^2$ expression, and replacing (mab) by \bar{m} , the total mass of the panel, the kinetic energy equation yields the general mass matrix element from:

$$M_{ij, rs} = \frac{\partial^2 T}{\partial b_{ij} \partial b_{rs}} = T_{, b_{ij} b_{rs}} \quad (25)$$

In our case, this reduces to:

$$M_{ij, rs} = \bar{m} a^2 / 4 \quad \text{when } m=p \text{ and } n=q$$

$$M_{ij, rs} = 0 \quad \text{otherwise} \quad (26)$$

(c) Aerodynamic Loading Matrix

When damping is neglected, the aerodynamic loading given by the piston theory (eqn. 9) reduces to:

$$p(\xi, \eta, t) = - \frac{\lambda D_{11}}{a^3} w, \xi \quad (27)$$

The variance of the work done by this loading on the panel is:

$$\begin{aligned} \delta \text{Work} &= \int_0^a \int_0^b p \delta w \, dx \, dy \\ &= - \lambda D_{11} (b/a) \int_0^1 \int_0^1 w, \xi \delta w \, d\xi \, d\eta \end{aligned} \quad (28)$$

$$\text{where } \delta w = \sum_p \sum_q \delta b_{pq} \sin p\pi\xi \sin q\pi\eta \quad (29)$$

$$\text{and } w, \xi = \sum_m \sum_n m\pi b_{mn} \cos m\pi\xi \sin n\pi\eta \quad (30)$$

Substituting these into the expression for δWork ,

$$\delta \text{Work} = \sum_m \sum_n \sum_p \sum_q b_{mn} \delta b_{pq} \lambda A_{pq, mn} \quad (31)$$

where $A_{pq, mn}$ is a double integral that is easily evaluated. The aerodynamic loading matrix element is given by:

$$\begin{aligned} \frac{\partial^2 (\delta \text{Work})}{\partial a_{mn} \partial (\delta a_{pq})} &= \delta \text{Work}, b_{mn} \delta b_{pq} \\ &= \lambda A_{pq, mn} \end{aligned} \quad (32)$$

In our case, we get:

$$A_{pq, mn} = mp / (p^2 - m^2) \quad \text{when } n=q \text{ and } (m+p) \text{ is odd}$$

$$A_{pq,mm} = 0 \text{ otherwise} \quad (33)$$

As the expressions for the general elements in the mass, stiffness and aerodynamic loading matrices have been derived, a computer program is set up (Appendix D) to evaluate all the elements in each of these matrices. This program also solves for the complex eigenvalues of the flutter equations (15), for some assumed value of the flutter parameter λ .

Panel flutter is determined by the coalescence of the frequencies of any two modes of vibration. Aerodynamic coupling drives the free vibration frequencies of the twenty assumed modes toward each other. The lowest value of λ corresponding to the coalescence of any two frequencies is the critical flutter parameter, λ_{crit} . Above $\lambda = \lambda_{crit}$ the eigenvalues are complex conjugate pairs. Hence, for a chosen ply and its orientation ϕ , the value of λ is increased from zero till the eigenvalues corresponding to any two modes become a complex conjugate pair. The latter indicates that these two modes have coalesced. A plot of λ against the frequencies may be drawn to find the exact value of λ_{crit} at which the two frequencies coalesce. The orientation ϕ affects the flutter boundary through the rigidities D_{ij} defined in Appendix A.

The ratio of the absolute value of the imaginary part of the complex eigenvalue pair to the square root of its real part gives the value of the total damping, g , present in the panel. The total damping includes the aerodynamic and/or structural damping in the

panel. Damping always raises the value of the critical flutter parameter, the amount of increase depending on the ply material, its aspect ratio and its orientation. Apart from raising the flutter boundary, the damping present in the panel may also transfer the flutter condition to a new pair of coalescent modes. Generally the first two modes coalesce to cause flutter. If we consider the complex eigenvalue pair/pairs at $\lambda > \lambda_{crit}$ for the undamped case, the value of λ corresponding to the damping g is the λ_{crit} value for a panel with a total damping of g .

The panel aspect ratio, the orientations of the individual plies, and their relative stiffnesses affect the spacing of the frequencies and their magnitudes. Thus two coupled modes may be driven very close together resulting in a "weak coalescence". The addition of a slight amount of damping usually eliminates weak coalescence and raises the flutter boundary significantly.

Though the analysis provides for the inclusion of all inplane stresses, only the effect of a compressive inplane stress resultant in the streamwise direction, N_x , is studied. The flutter instability of compressed panels is apparently influenced by static buckling. The static buckling loads are determined using the computer program in Appendix C, which is written using the information in Ref. 22. A non-dimensional stress parameter is defined as:

$$K_x = \frac{\pi^2 a^2 N_x}{4D_{11}} \quad (34)$$

Our panel model, however, fails to account for the fact that a buckled

panel exhibits dynamic behaviour that cannot be taken into account using flat plate theory. Our analysis is thus restricted to finding the trend in the decrease of the critical flutter parameter, λ_{crit} , with an increase in the compressive inplane stresses. Flutter analysis of the buckled panel may be carried out at a later time and the results superimposed on the flat panel results to give an idea of the variation of the flutter boundary with inplane compressive stresses, when the panel is free to buckle. Reference 24 provides the necessary details for such a study.

The orientation of the principal axis of the individual orthotropic ply with respect to the freestream (Fig. 1) and the relative stiffnesses of various fiber-matrix combinations for the plies play an important part in determining the critical flutter parameter for the panel. The material properties of the boron-epoxy, graphite-epoxy and boron-aluminium plies are given in Table I and taken from Ref. 25.

The present analysis also incorporates a means of analysing the effect of the panel aspect ratio on the flutter boundary. The aspect ratio of the panel is defined as the ratio of the streamwise length of the panel to its spanwise length. All the results presented here are for panels with an aspect ratio of unity. A different aspect ratio would modify the preferred orientation of the plies in the panel, where the flutter speed is maximum.

The number of orthotropic plies in the panel also influences the flutter boundary. When the number of plies, n , in an angle-ply panel is increased, the terms D_{16}/D_{11} and D_{26}/D_{11} become smaller. This weakens

the bending-twisting coupling in the panel and hence degrades the flutter characteristics.

The foregoing discussion has named a few of the many parameters that affect panel flutter. Panel surface curvature, edge conditions other than simple supports, cavity effect, boundary layer effect, etc. may also be realised in a practical case, making the analysis more sophisticated. The effects of these parameters are discussed qualitatively in Reference 14.

The various objectives of the present analysis are given below. Results are presented in the section which follows.

(a) Single-ply panels without inplane stresses and damping

This part of the analysis is concerned with the effect of the orientation, ϕ , of the single-ply panel on the flutter boundary, neglecting damping. ϕ varies from 0° to 90° in increments of 10° . Plots of λ_{crit} versus ϕ are obtained for boron-epoxy, graphite-epoxy and boron-aluminium plies.

(b) Single-ply panels without inplane stresses but with damping

The effect of damping, g , on the flutter boundary is studied by analysing the results obtained for the preceding case (a), where the eigenvalues are computed for undamped single-ply panels at different ϕ values, with λ varying from zero to above λ_{crit} . For $\lambda > \text{undamped } \lambda_{crit}$, the variation of λ_{crit} with g is obtained as explained earlier. "Weak coalescence" is easily spotted here when the damping g increases initially for $\lambda > \text{undamped } \lambda_{crit}$, and soon drops down to zero. Plots of λ_{crit} versus g , for various ϕ values, are

drawn for boron-epoxy, graphite-epoxy and boron-aluminium plies. From these plots, graphs of λ_{crit} versus ϕ , for various g values, are obtained.

(c) Single-ply panels with inplane stresses but without damping

The influence of the static buckling loads on flutter instability is studied. The static buckling loads for a boron-epoxy ply are given in Table II. The variation of λ_{crit} with K_x (eqn. 34) is then studied for a boron-epoxy ply at 0° , 30° , 60° and 90° . K_x is varied from zero to about K_{xcrit} (static buckling load).

(d) Effect of number of plies on the flutter boundary of a boron-epoxy angle-ply panel

This part of the analysis is similar to what was done in case (a). Plots of λ_{crit} versus ϕ are obtained for an angle-ply panel, built up of boron-epoxy plies, for different numbers of layers, n . The various values of n used in our case are: 1, 3, 5, 9, 15 and 49. Table III gives the λ_{crit} values for all these cases.

III. DISCUSSION OF RESULTS

Figures 3, 4 and 5 show the flutter boundaries of boron-epoxy, graphite-epoxy and boron-aluminium plies, for ϕ varying from 0° to 90° , and $g=0$. It is evident from these plots that a ply need not necessarily have the best flutter characteristics (maximum λ_{crit} value) when its principal axis is aligned with the freestream direction ($\phi = 0$). The three plies chosen for the analysis have different stiffness ratios (Table I). Hence their flutter boundaries are also seen to be different from one another, qualitatively and quantitatively.

Figures 6 to 35 show the variation in λ_{crit} with g , for the three different plies at various orientations. λ_{crit} is seen to increase monotonically with g in all cases. The magnitude of the increase in λ_{crit} with an increase in g depends on the ply material and its orientation, ϕ .

Figures 36 to 38 show the variation in the flutter boundaries for different damping values, for single-ply boron-epoxy, graphite-epoxy and boron-aluminium panels. The increase in λ_{crit} with an increase in g , at a particular ϕ , is not negligible, though it is quite small at low damping values.

"Weak coalescence" is observed in a single-ply boron-epoxy panel at 10° and 20° , and in a single-ply graphite-epoxy panel at 20° . It is also observed in a boron-epoxy angle-ply panel with alternate plies at $+20^\circ$ and -20° with respect to the freestream direction. Table IV compares these "weak coalescence" flutter values with the

actual flutter values. A small amount of damping is sufficient to get rid of "weak coalescence".

Figures 39 to 42 show the variation in λ_{crit} with K_x for a boron-epoxy ply at 0° , 30° , 60° and 90° . λ_{crit} decreases with an increase in the inplane compressive stress ($-N_x$) in the streamwise direction. While this decrease is gradual for $\phi = 0^\circ$, 30° and 90° , it is of a different nature for $\phi = 60^\circ$. When $\phi = 60^\circ$, λ_{crit} increases with an increase in compression ($-K_x$) for a range of K_x values. Thus, in this range, compression improves the flutter characteristics of the panel.

Figure 43 shows the effect of the number of plies, n , on the flutter boundary, for a boron-epoxy angle-ply panel. Through λ_{crit} decreases with an increase in n , the magnitude of decrease is seen to be negligibly small.

In figures 3 to 5 and 36 to 43, the points shown on the curves are the points obtained through the present analysis. The curves are drawn through these points using visual judgement.

IV. CONCLUSIONS

The flutter boundaries of the single-ply panels are affected by the ply material and ply orientation. The relative stiffnesses of the different plies change the qualitative and quantitative nature of the flutter boundary. Figures 3 to 5 show that the stiffness ratio E_{11}/E_{22} of the individual orthotropic ply affects the qualitative shape of the flutter boundary only after a ϕ value of about 50° . Till then the critical flutter parameter is seen to increase with ϕ . The effect on the flutter boundary of the stiffness ratio for the boron-epoxy ($E_{11}/E_{22} = 11$), graphite-epoxy ($E_{11}/E_{22} = 26$) and boron-aluminium ($E_{11}/E_{22} = 2$) plies is significant beyond a ϕ value of about 50° .

An important conclusion is that the alignment of the ply principal axis with the freestream direction ($\phi=0^\circ$) does not necessarily yield the best flutter characteristics (maximum λ_{crit}). As the panel aspect ratio is known to be an important parameter affecting the flutter boundary, it is suggested that the present analysis be carried out for aspect ratios other than unity.

Damping increases the flutter speed and also helps eliminate "weak coalescence". In the case of a single-ply graphite-epoxy panel, the addition of damping tends to flatten out the undamped flutter boundary beyond a ϕ value of about 50° , reducing the number of peaks from two to one. The addition of damping is seen to have a relatively negligible effect on the flutter boundary for a boron-

aluminium ply. Inplane compressive stresses generally decrease the flutter speed. But for a boron-epoxy ply at 60° , an increase in the compressive stress is seen to increase the flutter speed within a range of K_x values. It is further suggested that a "buckled panel" flutter analysis be carried out and the results be superimposed over the λ_{crit} versus K_x graphs to give an idea of the flutter instability of a panel that is free to buckle.

Increasing the number of plies in a boron-epoxy angle-ply panel reduces the critical flutter parameter by a negligible magnitude. Hence such an angle-ply panel may, for all practical purposes, be treated as an orthotropic panel. The analysis may also be done more accurately by assuming nonlinear structural theory and full, linearised (inviscid, potential) aerodynamic theory.

REFERENCES

1. " Panel Flutter ", NASA Space Vehicle Design Criteria, NASA SP-8004, July 1964, Revised June 1972.
2. Bohon, H. L., " Panel flutter tests on full-scale X-15 lower vertical stabilizer at Mach number of 3 ", NASA TN D-1385, 1962.
3. Rich, R. L., " Preliminary skin panel flutter tests ", The Boeing Company, Document D2-8148, 1962.
4. Mortvedt, R. L. and Wagner, R. T., " Transonic, supersonic panel flutter test ", The Boeing Company, Document D2-81095, 1964.
5. Golden, C. T., Hager, T. R. and Sherman, L. L., " Orthotropic panel flutter analysis correlation, X-20 ", The Boeing Company, Document D2-81301, 1964.
6. Anon, " 624A Panel flutter analysis ", U.S.A.F., Space Systems Divisions, CR-64-87, May 1964.
7. Nichols, J. J., " Final report: Saturn V, S-IVB ", Panel flutter qualification test, NASA TN D-5439, 1969.
8. Fung, Y. C., " A summary of the theories and experiments on panel flutter ", Guggenheim Aeronautical Lab., CIT, Pasadena, Calif., AFOSR TN 60-224, May 1960.
9. Fung, Y. C., " Some recent contributions to panel flutter research", AIAA Journal, Vol. 1, No. 4, April 1963.
10. Johns, D. J., " The present status of panel flutter ", Rept. 484, 1961, Advisory group for aeronautical research and development.
11. Johns, D. J., " A survey on panel flutter ", Advisory Rept. 1, Nov. 1965, Advisory group for aeronautical research and development.
12. Dowell, E. H., " Panel flutter : A review of the aeroelastic stability of plates and shells ", AIAA Journal, March 1970, Vol. 8, No. 3.
13. Mirowitz, L. I., Zimmerman, N. H. and Schweiker, J. W., " Panel flutter survey and design criteria ", Aerospace Industries Association of America, ATC Rept., ARTC-32, Aug. 1962.

14. Lemley, C. E., " Design criteria for the prediction of panel flutter ", TR 67-140, Vols. I and II, August 1968, Air Force Flight Dynamics Lab.
15. Hedgepeth, J. M., " Flutter of rectangular, simply supported panels at high supersonic speeds ", J Ae S, Vol. 24, No. 8, August 1957.
16. Perlmutter, A. A., " On the aeroelastic stability of orthotropic panels in supersonic flow ", J Ae S, Vol. 29, No. 11, Nov. 1962.
17. Bohon, H. L., " Flutter of flat, rectangular orthotropic panels with biaxial loading and arbitrary flow direction ", NASA TN D-1949.
18. Gaspers, P. A., Jr., and Bass Redd, " A theoretical analysis of the flutter of orthotropic panels exposed to a high supersonic stream of arbitrary direction ", NASA TN D-3551.
19. Calligeros, J. M. and Dugundgi, J., " Supersonic flutter of rectangular orthotropic panels with arbitrary orientation of orthotropicity ", USAF Contract No. AF49(638)-219, MIT Aeroelastic and Structures research lab., June 1963.
20. Irwin Stambler, " Bright future forecast for composites in aerospace ", Interavia, December 1972.
21. Ashton, J. E., Halpin, J. C. and Petit, P. H., " Primer on composite materials : Analysis ", Technomic publication.
22. Ashton, J. E. and Whitney, J. M., " Theory of laminated plates ", Progress in materials science series, Volume IV, Technomic publication.
23. Holt Ashley and Garabed Zartarian, " Piston theory - A new aerodynamic tool for the aeroelastician ", J Ae S, Dec. 1956.
24. Holt Ashley and Bisplinghoff, R. L., " Principles of aeroelasticity" John Wiley and sons, Inc.
25. " Structural design guide for advanced composite applications ", 3rd edn., Jan. 1973, Advanced composite division, AF Materials Lab., Wright - Patterson AFB, Ohio.

APPENDIX A

ELASTIC CONSTANTS FOR A LAMINATE

The laminate is built up of individual orthotropic plies, each of which has four independent elastic constants E_{11} , E_{22} , ν_{12} and G_{12} . These constants depend on the fiber - matrix properties of the ply. The planform geometry of the ply is shown in Fig. 1. The laminate layup is as shown in Fig. 2, except that alternate layers need not be crossed at the same orientation angle. The stiffnesses of each of these plies, referred to the principal axes of the material, are defined by (Ref. 21) :

$$Q_{11} = \frac{E_{11}}{(1 - \nu_{12}\nu_{21})}$$

$$Q_{22} = \frac{E_{22}}{(1 - \nu_{12}\nu_{21})}$$

$$Q_{12} = \frac{\nu_{12}E_{22}}{(1 - \nu_{12}\nu_{21})} = \frac{\nu_{21}E_{11}}{(1 - \nu_{12}\nu_{21})}$$

$$Q_{66} = G_{12}$$

$$Q_{16} = Q_{26} = 0$$

(A-1)

These stiffnesses are transformed to the global axes (Ref. 21) as shown below :

$$\bar{Q}_{11} = Q_{11}m^4 + 2(Q_{12} + 2Q_{66})m^2n^2 + Q_{22}n^4$$

$$\bar{Q}_{22} = Q_{11}n^4 + 2(Q_{12} + 2Q_{66})m^2n^2 + Q_{22}m^4$$

$$\bar{Q}_{12} = (Q_{11} + Q_{22} - 4Q_{66})m^2n^2 + Q_{12}(m^4 + n^4)$$

$$\bar{Q}_{66} = (Q_{11} + Q_{22} - 2Q_{12} - 2Q_{66})m^2n^2 + Q_{66}(m^4 + n^4)$$

$$\bar{Q}_{16} = (Q_{11} - Q_{12} - 2Q_{66})m^3n + (Q_{12} - Q_{22} + 2Q_{66})mn^3$$

$$\bar{Q}_{26} = (Q_{11} - Q_{12} - 2Q_{66})mn^3 + (Q_{12} - Q_{22} + 2Q_{66})m^3n \quad (\Lambda-2)$$

where $m = \cos \phi$; $n = \sin \phi$

Q_{ij} is the stiffness referred to the principal axes, and \bar{Q}_{ij} is the stiffness referred to the global axes. The streamwise and spanwise directions of our panel form the global axes.

The laminate equation may be written as (Ref. 21,22) :

$$\begin{Bmatrix} N \\ M \end{Bmatrix} = \begin{bmatrix} A & B \\ B & D \end{bmatrix} \begin{Bmatrix} \epsilon_0 \\ k \end{Bmatrix} \quad (\Lambda-3)$$

$$\text{where } A_{ij} = \sum_{k=1}^n (\bar{Q}_{ij})_k (h_k - h_{k+1})$$

$$B_{ij} = \sum_{k=1}^n (\bar{Q}_{ij})_k (h_k^2 - h_{k+1}^2) / 2$$

$$D_{ij} = \sum_{k=1}^n (\bar{Q}_{ij})_k (h_k^3 - h_{k+1}^3) / 3 \quad (\Lambda-4)$$

$\{N\}$ and $\{M\}$ are the stress and moment resultant vectors, $\{\epsilon_0\}$ is the midplane strain vector, and $\{k\}$ is the plate curvature vector.

The D_{ij} terms are thus functions of the material properties of the plies, the orientations of the plies, the stacking sequence in the laminate, the number of plies in it, and the thickness of each ply. A computer program to compute the A, B and D matrices for any general laminate layup is given in Appendix B.

APPENDIX B -- COMPUTER PROGRAM FOR A,B,D MATRICES OF THE LAMINATE

```

C*****
C      PROGRAM TO SOLVE FOR THE A,B,D MATRICES
C*****
C
C      ODIMENSION D(6,6),T(2),Q(3,3),E11(2),E22(2),G12(2),GNU12(2),
C      1GNU21(2),THETA(2),H(3),QB(3,3)
C PROGRAM FOR ABD MATRIX OF COMPOSITE PLATE
C N IS THE NUMBER OF LAMINAE
C      READ(5,100)N
C      100 FORMAT(I3)
C INITIALIZE D(6,6) WHICH IS THE ABD MATRIX
C      DO12 I=1,6
C      DO12J=1,6
C      12 D(I,J)=0.00
C THICKNESS OF LAMINATE IS NAMED DEPTH
C      DEPTH=0.00
C      DO 3 M=1,N
C T(M) IS THE THICKNESS OF THE M*TH LAMINA
C      READ(5,101) T(M)
C      101 FORMAT(10F8.0)
C      3 DEPTH=DEPTH+T(M)
C Q MATRIX OF EACH LAMINA
C      DO 10 I=1,N
C      READ(5,102)E11(I),E22(I),G12(I),GNU12(I),THETA(I)
C      102 FORMAT(3E14.6,F6.0,F6.0)
C      GNU21(I)=GNU12(I)*E22(I)/E11(I)
C      GNU2=GNU12(I)*GNU21(I)
C      Q(1,1)=E11(I)/(1.00-GNU2)
C      Q(2,2)=E22(I)/(1.00-GNU2)
C      Q(1,2)=E11(I)*GNU21(I)/(1.00-GNU2)
C      Q(3,3)=G12(I)

```

2
3
1
4
5
6
7
8
9
10
11
12
13
14
15
17
18
19
20
22
23
24
25
26
27

```

C THETA +VE FROM GLOBAL TO LAMINA PRINCIPAL AXES
  IF(THETA(I).EQ.90.0)GO TO 50
  ANGL=(THETA(I)/180.00)*3.1415927
  C=COS(ANGL)
  S=SIN(ANGL)
  GO TO 60
50 C=0.00
  S=1.00
60 C2=C**2
  S2=S**2
  C3=C*C2
  S3=S*S2
  C4=C*C3
  S4=S*S3
C THE QB MATRIX OF EACH LAMINA
  QB(1,1)=Q(1,1)*C4+2.0*(Q(1,2)+2.00*Q(3,3))*S2*C2+Q(2,2)*S4
  QB(2,2)=Q(1,1)*S4+2.00*(Q(1,2)+2.00*Q(3,3))*S2*C2+Q(2,2)*C4
  QB(1,2)=(Q(1,1)+Q(2,2)-4.00*Q(3,3))*S2*C2+Q(1,2)*(S4+C4)
  QB(1,3)=(Q(1,1)-Q(1,2)-2.0*Q(3,3))*S*C3+(Q(1,2)-Q(2,2)+2.0*
1Q(3,3))*S3*C
  QB(2,3)=(Q(1,1)-Q(1,2)-2.0*Q(3,3))*S3*C+(Q(1,2)-Q(2,2)+2.0*
1Q(3,3))*S*C3
  QB(3,3)=(Q(1,1)+Q(2,2)-2.00*Q(1,2)-2.00*Q(3,3))*S2*C2
1+Q(3,3)*(S4+C4)
  QB(2,1)=QB(1,2)
  QB(3,1)=QB(1,3)
  QB(3,2)=QB(2,3)
  IF(I-1)15,14,15
C H(I) IS DISTANCE FROM MIDPLANE TO TOP OF I'TH LAMINA
14 H(I)=DEPTH/2.00
20 H(I)=DEPTH/2.00
15 H(I+1)=H(I)-T(I)

```

28
29
30
31
32
33
34
35
36
37
38
39
40
41
42
43
44

49
50
51
52
53
54
55
56
57
58

D1=H(I)-H(I+1)	59
D2=(H(I)**2-H(I+1)**2)/2.00	60
D3=(H(I)**3-H(I+1)**3)/3.00	61
DO 25 K=1,3	62
DO 25 J=1,3	63
D(K,J)=D(K,J)+D1*QB(K,J)	64
JJ=J+3	65
D(K,JJ)=D(K,JJ)+D2*QB(K,J)	66
KK=K+3	67
25 D(KK,JJ)=D(KK,JJ)+D3*QB(K,J)	68
DO 30 K=1,3	69
DO 30 J=4,6	70
30 D(J,K)=D(K,J)	71
10 CONTINUE	72
WRITE(6,110)N	73
110 FORMAT(1H1///10X,'COMPOSITE PLATE RESULTS'///2X,'N=',I3)	74
WRITE(6,211)	75
211 FORMAT(///2X,'INPUT VARIABLES OF EACH LAMINA'///)	76
DO 201 I=1,N	77
WRITE(6,111)T(I),E11(I),E22(I),G12(I),GNU12(I),THETA(I)	78
111 FORMAT(1X,F6.4,3E14.6,F6.4,F6.2//)	79
201 CONTINUE	80
WRITE(6,212)	81
212 FORMAT(///2X,'THE ABD MATRIX IS'///)	82
WRITE(6,112)((D(K,J),J=1,6),K=1,6)	83
112 FORMAT('D',6E13.7//)	84
C RATIOS OF D VALUES FOR COMPUTATION OF STIFFNESS, MASS, AND AERODYNAMIC MATRICES	
C AR IS THE ASPECT RATIO OF THE LAMINATE AND IS=A/B	
AR=1.0	
CFT1=D(4,5)/D(4,4)*AR*AR	
CFT2=2.0*D(4,6)/D(4,4)*AR	
CFT3=D(5,5)/D(4,4)*AR**4	

```
CFT4=2.0*D(5,6)/D(4,4)*AR**3
CFT5=4.0*D(6,6)/D(4,4)*AR*AR
WRITE(6,300)CFT2,CFT1,CFT5,CFT4,CFT3
300 FORMAT(/' B=',E15.7// ' C1=',E15.7// ' C2=',E15.7// ' D=',E15.7//
1' E=',E15.7/1H1)
STOP
END.
```

85

86

C*****

APPENDIX C -- COMPUTER PROGRAM FOR STATIC BUCKLING LOADS

```

C *****
C   PROGRAM TO SOLVE FOR STATIC BUCKLING LOADS
C *****
C
C
C   DIMENSION AK(20,20),B(20,20),M(20),N(20),XL(20),X(20,20)
C   READ(5,110)AB,C1,C2,D,E
110  FORMAT(5E15.7)
C   WRITE(6,120)AB,C1,C2,D,E
120  FORMAT(5X,'CONSTANTS B,C1,C2,D,E'//5E16.7//)
C   NSETS IS THE NUMBER OF MODES CHOSEN
C   READ(5,140)NSETS
140  FORMAT(2I5)
C   DO 150 I=1,NSETS
C   READ(5,140)M(I),N(I)
150  WRITE(6,140)M(I),N(I)
C   PI=ARCCOS(-1.)
C   PI2=4.*PI**2
C   PI4=PI**4/4.
C   CNX=PI**2*A**2*NX/D11/4
C   DO 280 II=1,NSETS
C   NN=N(II)
C   MM=M(II)
C   DO 280 I=1,NSETS
C   IQ=N(I)
C   IP=M(I)
C   IF(MM.EQ.IP.AND.NN.EQ.IQ)GO TO 240
C   IF(MM.NE.IP.AND.NN.NE.IQ.AND.(MM+IP)/2*2.NE.(MM+IP).AND.
C   1(NN+IQ)/2*2.NE.(NN+IQ))GO TO 250
C   AK(I,II)=0.
C   B(I,II)=0.0
C   GO TO 280

```

```

240 AK(I,II)=PI4*(MM**4+(2.*C1+C2)*(MM*NN)**2+E*NN**4)
    B(I,II)=MM*IP
    GO TO 280
250 DR=(MM*MM-IP*IP)*(NN*NN-IQ*IQ)
    AK(I,II)=-IP*IQ*MM*NN*PI2*(AB*(MM*MM+IP*IP)+D*(NN*NN+IQ*IQ))/DR
    B(I,II)=0.0
280 CONTINUE
    CALL NROOT(NSETS,AK,B,XL,X)
    WRITE(6,300){XL(I),I=1,NSETS)
300 FORMAT(1H1,' THE EIGENVALUES (-CNX) ARE'//(F10.0/))
    STOP
    END
C*****

```

APPENDIX D -- COMPUTER PROGRAM TO SOLVE FOR FLUTTER FREQUENCIES AND MODE SHAPES

```

C*****
C      PROGRAM TO SOLVE FOR FLUTTER FREQUENCIES AND MODE SHAPES
C*****
C
C
C MAIN PROGRAM
C
C
C      DIMENSION TITLE(20)
C      DIMENSION A(25,25),AK(25,25),ANET(25,25)
C      DIMENSION M(25),N(25)
C      COMPLEX CMPLX,CSQRT
C      COMPLEX B(25,25),Z,CMPLX,RT(25)
C      COMPLEX CV,ADETER(25,25),CABS
C      COMMON/C43/NSETS
C      COMMON/C42/DL,LV,CV(25)
C      WRITE(6,100)
100  FORMAT(1H1)
C      READ(5,98)TITLE
C      98  FORMAT(20A4)
C      WRITE(6,99)TITLE
C      99  FORMAT(5X,20A4//)
C      READ(5,110)AB,C1,C2,D,E
110  FORMAT(5E15.7)
C XPLATE IS IN INCHES,NX ETC. IN PSI,D11 IN LB.IN.
C      READ(5,115)CNX,CNY,CNXY
115  FORMAT(3F10.0)
C      READ(5,116)IGNVCT
116  FORMAT(11)
C      WRITE(6,120)AB,C1,C2,D,E
120  FORMAT(5X,'CONSTANTS B,C1,C2,D,E'//5E16.7//)
C      WRITE(6,125)CNX,CNY,CNXY

```

```

125 FORMAT(// ' CNX,CNY,CNXY FOR THE LAMINATE'//3F10.0//)
      READ(5,130)ALAM,DLAM
130 FORMAT(2F8.2)
C NSETS IS THE NUMBER OF MODES CHOSEN
      READ(5,140)NSETS,MODE
140 FORMAT(2I5)
      DO 150 I=1,NSETS
        READ(5,140)M(I),N(I)
150 WRITE(6,140)M(I),N(I)
        READ(5,140)KKK
        DO 220 II=1,NSETS
          NN=N(II)
          MM=M(II)
          DO 210 I=1,NSETS
            IQ=N(I)
            IP=M(I)
            IF(NN.EQ.IQ.AND.(MM+IP)/2*2.NE.(MM+IP))GO TO 180
            A(I,II)=0.0
            GO TO 210
180 A(I,II)=MM*IP/FLQAT(IP*IP-MM*MM)
210 CONTINUE
220 CONTINUE
        PI=ARCOS(-1.)
        PI2=4.*PI**2
        PI4=PI**4/4.
C CNX=PI**2*A**2*NX/D11/4
C CNY=PI**2*A**2*NY*(AR)**2/(4*D11)
C CNXY=-8*A**2*AR*NX/D11
        DO 280 II=1,NSETS
          NN=N(II)
          MM=M(II)
          DO 280 I=1,NSETS

```

```

      IQ=N(I)
      IP=M(I)
      IF(MM.EQ.IP.AND.NN.EQ.IQ)GO TO 240
      IF(MM.NE.IP.AND.NN.NE.IQ.AND.(MM+IP)/2*2.NE.(MM+IP).AND.
1(NN+IQ)/2*2.NE.(NN+IQ))GO TO 250
      AK(I,II)=0.
      GO TO 280
240 AK(I,II)=PI4*(MM**4+(2.*C1+C2)*(MM*NN)**2+E*NN**4)+CNX*MM*IP+
      ICNY*NN*IQ
      GO TO 280
250 AK(I,II)=IP*IQ*MM*NN/((MM*MM-IP*IP)*(NN*NN-IQ*IQ))*(CNXY-PI2*(AB*
      1(MM*MM+IP*IP)+D*(NN*NN+IQ*IQ)))
280 CONTINUE
      DO 340 K=1,KKK
      WRITE(6,290)ALAM
290 FORMAT(1H1,'LAMBDA=',F8.2)
      DO 310 II=1,NSETS
      DO 310 I=1,NSETS
310 ANET(I,II)=4.*(AK(I,II)+ALAM*A(I,II))
      Z=(0.,0.)
      DO 320 I=1,NSETS
      DO 320 J=1,NSETS
      AIJ=ANET(I,J)
      B(I,J)=CMLX(AIJ,0.)
      ADETER(I,J)=B(I,J)
320 CONTINUE
      CALL EIG4(B,NSETS,25,NSETS,RT,Z)
      WRITE(6,330)(RT(L),L=1,NSETS)
330 FORMAT(//' THE EIGENVALUES ARE'//(2E18.7//))
340 ALAM=ALAM+DLAM
      IF(IGNVCT.EQ.0)GO TO 850
      DO 740 I=1,NSETS

```

```
740 ADETER(I,I)=ADETER(I,I)-RT(MODE)
    CALL DETER(2,ADETER,0)
    WRITE(6,770)LV,DL
770 FORMAT(////' LV AND DL VALUES'//I12,E20.7)
    WRITE(6,760)MODE,(CV(I),M(I),N(I),I=1,NSETS)
760 FORMAT(1H1,'THE EIGENVECTOR CORRESPONDING TO THE EIGENVALUE RT(',
    1I2,') IS GIVEN BELOW'//(2E16.7,5X,'FOR THE MODE (',I2,',',I2,')'/'
    2))
850 WRITE(6,350)
350 FORMAT(1H1)
    STOP
    END
```

```

C*****
C      SUBROUTINE EIG4(A,N,ND,M,RT,Z)
C*****
C
C      EIG4  NYU MATH UTILITY  12/01/63  EIGENVALUES OF COMPLEX MATRICES      A   2
C      THIS PROGRAM CALCULATES THE EIGENVALUES OF GENERAL COMPLEX MATRICE   A   3
C      IT WAS DEVELOPED BY BERESFORD PARLETT AT NYU AND CONTAINS MINOR      A   4
C      MODIFICATIONS BY P.A. GASPERIS JR. OF NASA, AMES RESEARCH CENTER.    A   5
C      A=INPUT MATRIX                                                         A   6
C      N=SIZE OF MATRIX                                                         A   8
C      ND=DIMENSION, NOT CURRENTLY USED.                                     A   9
C      M=NUMBER OF EIGENVALUES COMPUTED.                                     A  10
C      RT=VECTOR CONTAINING THE EIGENVALUES IN THE ORDER COMPUTED.          A  11
C      Z=POINT IN COMPLEX PLANE WHERE EIGENVALUE ITERATION IS STARTED.      A  12
C      IF Z=0, THE EIGENVALUES WILL BE FOUND APPROXIMATELY IN ORDER OF AB   A  13
C      VALUE STARTING WITH THE SMALLEST.                                     A  14
C                                                                              A  15
C                                                                              A  16
C      COMPLEX CSQRT,S,R,E,X,TRACE                                           A  17
C      COMPLEX Z,RT(25),A(25,25)
C      DIMENSION KCOOFX(70)
C      TRACE=A(1,1)
C      DO 1 I=2,N
1      TRACE=TRACE+A(I,I)
C      CALL CXTRI (A,1.E-8,N,ND,KCOOFX)
C      TRACE=A(1,1)
C      DO 2 I=2,N
2      TRACE=TRACE+A(I,I)
C      NU=0
C      NV=0
3      IF (NV-N) 4,12,4
C                                                                              A  19
C                                                                              A  20
C                                                                              A  21
C                                                                              A  22
C                                                                              A  23
C                                                                              A  24
C                                                                              A  25
C                                                                              A  26
C                                                                              A  27
C                                                                              A  28
C                                                                              A  29

```

4	NV=NV+1	A	30
	NU=NV	A	31
5	IF (KCOOFX(NV)) 6,7,6	A	32
6	NV=NV+1	A	33
	GO TO 5	A	34
7	IF (NV-NU) 9,8,9	A	35
8	RT(NU)=A(NU,NU)	A	36
	X=RT(NU)	A	37
	GO TO 3	A	38
9	IF (NV-NU-1) 10,11,10	A	39
10	NP=MINO(M,NV)	A	40
	CALL CXLG (A,1.E-4,NP,NU,NV,ND,RT,Z)	A	41
	GO TO 3	A	42
11	R=(.5,.0)*(A(NU,NU)+A(NV,NV))	A	43
	E=R**2-A(NU,NU)*A(NV,NV)+A(NU,NV)*A(NV,NU)	A	44
	S=CSQRT(E)	A	45
	RT(NU)=R+S	A	46
	RT(NV)=R-S	A	47
	X=RT(NU)	A	48
	E=RT(NV)	A	49
	GO TO 3	A	50
12	X=(.0,.0)	A	51
	DO 13 J=1,M	A	52
13	X=X+RT(J)	A	53
	RETURN	A	54
	END	A	55
C*****			

```

C*****
SUBROUTINE CXLAG(A, EPS, N1, NU, N, ND, RT, Z)
C*****
C
C
COMPLEX RT(25), A(25, 25)
COMPLEX CMLX, CSQRT
COMPLEX DUM
COMPLEX B1, Z, P, S2, S1, R
COMPLEX SUM2, SUM1, Q2
COMPLEX CSQRT, D, T, SPUR2, SPUR1, Q1
COMPLEX F1, DELZ, E, B3, B2

DIMENSION P(3, 71), S1(1), S2(1), R(1), Z(1), B1(1), B2(1), B3(1),
1E(1), DELZ(1), F1(1), Q1(1)
AFUN(DUM)=ABS(REAL(DUM))+ABS(AIMAG(DUM))
BL1=1.0
NUQ=NU-1
LLY=0
ZZ=0.0
DELOLD=1.0
ROLD=1.0
SUM1=(0.0, 0.0)
SUM2=(0.0, 0.0)
CALL OVERFL (IOVER)
P(1, NU)=(1.0, .0)
P(2, NU)=(.0, .0)
P(3, NU)=(.0, .0)
NU1=NU+1
CUP=0.0
DO 1 J=NU1, N
R(1)=A(J-1, J)

```

```

A 3
A 4
A 5
A 6
A 7
A 8
A 9
A 10
A 11
A 12
A 13
A 14
A 15
A 16
A 17
A 18
A 19
A 20
A 21
A 22
A 23
A 24
A 25
A 26
A 27

```

1	CUP=CUP+AFUN(B(1))	A	28
	CUP=CUP/FLOAT(N-NU)	A	29
	CAP=0.0	A	30
C		A	31
C	FIND THE TRACE OF A AND A**2	A	32
C		A	33
	SPUR1=A(NU,NU)	A	34
	SPUR2=SPUR1**2	A	35
	DO 2 J=NU1,N	A	36
	T=A(J,J)	A	37
	SPUR1=SPUR1+T	A	38
2	SPUR2=SPUR2+T**2+(2.0,C.0)*A(J-1,J)*A(J,J-1)	A	39
	S1(1)=-SPUR1	A	40
	S2(1)=SPUR2	A	41
C		A	42
C	INITIAL ITERATE (EITHER GIVEN OR FROM INFINITY)	A	43
C		A	44
	IF (REAL(Z(1))-1.E35) 6,3,3	A	45
3	F1(1)=CMPLX(FLOAT(N-NUQ),0.0)	A	46
	IF (AFUN(S1(1))+AFUN(S2(1))-1.E-6*CAP) 4,4,5	A	47
4	Z(1)=CMPLX(CUP,0.0)	A	48
	GO TO 6	A	49
5	D=(F1(1)-(1.0,0.0))*(F1(1)*S2(1)-S1(1)**2)	A	50
	Z(1)=(CSQRT(D)-S1(1))/F1(1)	A	51
C		A	52
C	EVALUATE POLYNOMIAL AND DERIVATIVES	A	53
C		A	54
6	P(1,NU)=(1.0,0.0)	A	55
	IF (LLY+NUQ-NU) 7,7,8	A	56
7	P(1,NU)=(1.E-20,0.0)	A	57
8	DO 15 K=NU,N	A	58
	T=-A(K,K+1)	A	59

	DO 15 L=1,3	A	60
	S=FLOAT(MCD(L-1,3))	A	61
	R(1)=-((Z(1)*P(L,K)+S*P(L-1,K))	A	62
	DO 9 J=NU,K	A	63
9	R(1)=R(1)+P(L,J)*A(K,J)	A	64
	CALL OVERFL (IOVER)	A	65
	GO TO (10,12,12), IOVER	A	66
10	P(1,NU)=P(1,NU)*1.E-15	A	67
	IF (REAL(P(1,NU))) 11,11,8	A	68
11	F=0.9*FLOAT(K-NU)/FLOAT(N-NU+1)	A	69
	WRITE (6,46) Z(1)	A	70
	Z(1)=F*Z(1)	A	71
	P(1,NU)=(1.0,0.0)	A	72
	GO TO 8	A	73
12	IF (N-K) 13,13,14	A	74
13	P(L,K+1)=R(1)	A	75
	GO TO 15	A	76
14	P(L,K+1)=R(1)/T	A	77
15	CONTINUE	A	78
C		A	79
C	SCALE DOWN THESE VALUES IF REQUIRED TO AVOID OVERFLOW	A	80
C		A	81
	B1(1)=P(1,N+1)	A	82
	B2(1)=P(2,N+1)	A	83
	B3(1)=P(3,N+1)	A	84
	G1=AFUN(B1(1))	A	85
	G2=AFUN(B2(1))	A	86
	G3=AFUN(B3(1))	A	87
	S=AMAX1(G1,G2)	A	88
	S=AMAX1(S,G3)	A	89
	IF (S-1.E19) 17,17,16	A	90
16	B1(1)=B1(1)/(1.E+19,0.0)	A	91

	B2(1)=B2(1)/(1.E+19,0.0)	A 92
	B3(1)=B3(1)/(1.E+19,0.0)	A 93
C		A 94
C	REMOVE EFFECT OF KNOWN ROOTS FROM S1,S2 THE LOG DERIVATIVES.	A 95
C		A 96
17	Q1(1)=(.0,.0)	A 97
	Q2=(.0,.0)	A 98
	IF (NUQ-NU) 20,18,18	A 99
18	DO 19 J=NU,NUQ	A 100
	D=(1.0,C.0)/(RT(J)-Z(1))	A 101
	Q1(1)=Q1(1)+D	A 102
19	Q2=Q2+D**2	A 103
20	IF (G1) 22,22,21	A 104
21	S1(1)=Q1(1)+B2(1)/B1(1)	A 105
	S2(1)=(B2(1)/B1(1))**2-B3(1)/B1(1)-Q2	A 106
C		A 107
C	FIND NEXT ITERATE	A 108
C		A 109
	LLY=LLY+1	A 110
	IF (1.E7-ZZ*AFUN(S1(1))) 22,22,23	A 111
22	MARK=1	A 112
	GO TO 42	A 113
23	G=N-NUQ	A 114
24	IF (BL1) 25,25,26	A 115
25	H=0.5*(G-2.0)	A 116
	GO TO 27	A 117
26	H=G-1.0	A 118
27	D=H*(G*S2(1)-S1(1)**2)	A 119
	E(1)=CSQRT(D)	A 120
	IF (REAL(S1(1))*REAL(E(1))+AINAG(S1(1))*AINAG(E(1))) 28,29,29	A 121
28	E(1)=-E(1)	A 122
29	DEL2(1)=-G/(S1(1)+E(1))	A 123

	Z(1)=Z(1)+DELZ(1)	A 124
	DELNEW=AFUN(DELZ(1))	A 125
	RNEW=DELNEW/DELOLD	A 126
	ZZ=AFUN(Z(1))	A 127
C		A 128
C	TEST FOR CYCLING AT 57 AND FOR LINEAR CONVERGENCE AT 571	A 129
C		A 130
	IF (LLY-3) 38,38,30	A 131
30	IF (DELNEW-AMAX1(3.0*DELOLD,.5*ZZ)) 33,33,31	A 132
31	IF (BL1) 33,33,32	A 133
32	DELOLD=CAP+1.0	A 134
	ROLD=3.0	A 135
	IF (LLY-15) 3,3,42	A 136
33	IF (RNEW-.7*ROLD) 38,34,34	A 137
34	MARK=3	A 138
	IF (DELNEW-.1*EPS*AMAX1(ZZ,.01*CAP)) 41,35,35	A 139
35	IF (BL1) 37,37,36	A 140
36	Z(1)=Z(1)-DELZ(1)	A 141
	BL1=0.0	A 142
	GO TO 24	A 143
37	BL1=1.0	A 144
	GO TO 39	A 145
C		A 146
C	TEST FOR AN EIGENVALUE	A 147
C		A 148
38	IF (DELNEW-10.0*EPS*AMAX1(ZZ,.001*CAP)) 40,40,39	A 149
39	DELOLD=DELNEW	A 150
	ROLD=RNEW	A 151
	IF (LLY-15) 6,6,42	A 152
40	MARK=2	A 153
41	BL1=1.0	A 154
C		A 155

C	WE ACCEPT Z AS A ROOT	A 156
C		A 157
42	NUQ=NUQ+1	A 158
	RT(NUQ)=Z(1)	A 159
	LLY=0	A 160
	CAP=AMAX1(ZZ,CAP)	A 161
	DELOLD=1.0	A 162
	ROLD=1.0	A 163
	SUM1=SUM1+RT(NUQ)	A 164
	SUM2=SUM2+RT(NUQ)**2	A 165
	S1(1)=SUM1-SPUR1	A 166
	S2(1)=SUM2-SPUR2	A 167
	IF (NUQ-N1) 43,45,45	A 168
C		A 169
C	A NEWTON STEP TOWARDS NEXT ROOT	A 170
C		A 171
43	IF (AFUN(Q1(1))*AMAX1(ZZ,.001*CAP)-1.E4) 44,44,3	A 172
44	Z(1)=Z(1)-B2(1)/((.5,.0)*B3(1)-B2(1)*Q1(1))	A 173
	GO TO 6	A 174
45	RETURN	A 175
46	FORMAT (8H ITERATE,20X,2E20.8,12X,9H OVERFLOW)	A 176
	END	A 177

C*****

SUBROUTINE CXTRI(A, EPS, N, ND, KOOOFX)

C*****

C
C

COMPLEX A(25,25)

COMPLEX U,C

A 3

C

DIMENSION C(1)

A 4

DIMENSION KOOOFX(70)

A 5

N1=N-1

A 6

N2=N-2

A 7

DO 19 J=1,N1

A 8

J1=J+1

A 9

J2=J+2

A 10

L=J1

A 11

NJ1=N-J1

A 12

C(1)=A(J,J1)

A 13

S=ABS(REAL(C(1)))+ABS(AIMAG(C(1)))

A 14

IF (NJ1) 7,7,1

A 15

1

DO 3 K=J2,N

A 16

C(1)=A(J,K)

A 17

T=ABS(REAL(C(1)))+ABS(AIMAG(C(1)))

A 18

IF (T-S) 3,3,2

A 19

2

L=K

A 20

S=T

A 21

3

CONTINUE

A 22

IF (L-J1) 4,7,4

A 23

4

DO 5 K=1,N

A 24

C(1)=A(K,J+1)

A 25

A(K,J+1)=A(K,L)

A 26

5

A(K,L)=C(1)

A 27

A 28

```

        DO 6 K=1,N
        C(1)=A(J+1,K)
        A(J+1,K)=A(L,K)
6       A(L,K)=C(1)
7       R=0.0
        DO 8 K=1,J
        C(1)=A(J,K)
        T=ABS(REAL(C(1)))+ABS(AIMAG(C(1)))
8       R=AMAX1(R,T)
        IF (S-EPS*R) 9,9,10
9       L=0
        NJ1=0
        GO TO 12
10      C(1)=A(J,J+1)
        IF (J2.GT.N) GO TO 12
        DO 11 K=J2,N
11      A(J,K)=A(J,K)/C(1)
12      DO 18 I=1,N
        M=AMINO(J,I-2)
        U=(0.0,0.0)
        IF (NJ1) 15,15,13
13      DO 14 K=J2,N
14      U=U+A(K,I)*A(J,K)
15      IF (M) 18,18,16
16      DO 17 K=1,M
17      U=U-A(K,I)*A(J+1,K+1)
18      A(J+1,I)=A(J+1,I)+U
19      KOODOFX(J)=L
        KOODOFX(N)=0
        RETURN
        END

```

```

A 29
A 30
A 31
A 32
A 33
A 34
A 35
A 36
A 37
A 38
A 39
A 40
A 41
A 42
A 43
A 44
A 45
A 46
A 47
A 48
A 49
A 50
A 51
A 52
A 53
A 54
A 55
A 56
A 57
A 58
A 59

```

```

C *****
C SUBROUTINE DETER(IV,A,ND)
C *****
C
C
C NP09AH THIS PROGRAM COMPUTES THE LOG (TO THE BASE 10) OF THE A 2
C ABSOLUTE VALUE OF THE DETERMINANT OF THE COMPLEX MATRIX A A 3
C BY BACKWARD GAUSSIAN ELIMINATION WITHOUT INTERCHANGES. A 4
C THE ASSOCIATED VECTOR IS ALSO COMPUTED. A 5
C IF IV=0, ONLY THE DETERMINANT OF A IS EVALUATED. IF IV IS NOT EQU A 6
C ZERO, BOTH THE DETERMINANT AND THE EIGENVECTOR ARE EVALUATED. A 7
C TO OBTAIN THE EIGENVECTOR OF A MATRIX B CORRESPONDING TO EIGENVALU A 8
C SET A=B-XI, WHERE I IS THE IDENTITY MATRIX. THE EIGENVECTOR IS DE A 9
C CV AND IS LOCATED IN THE LABELED COMMON BLOCK C42. A 10
C THE EIGENVECTOR IS NORMALIZED SO THAT THE COMPONENT WITH THE LARGE A 11
C ABSOLUTE VALUE HAS ITS REAL PART EQUAL TO ONE AND IMAGINARY PART E A 12
C ZERO. A 13
C THE ARGUMENT ND IS NOT USED. A 14
C FIRST=1.0 A 15
C COMPLEX A,CV,R,C,CVL A 16
C COMPLEX CMLX,CSQRT
C DIMENSION A(25,25)
C COMMON /C42/ DL,LV,CV(25)
C COMMON /C43/ N7 A 19
C N8=N7-1 A 20
C DO 3 K=1,N8 A 21
C DO 2 L=K,N8 A 22
C N9=N7-K+1 A 23
C N5=N7-L A 24
C R=-A(N5,N9)/A(N9,N9) A 25
C N6=N7-K A 26
C DO 1 N=1,N6 A 27

```

```

1  A(N5,N)=A(N5,N)+R*A(N9,N)
2  CONTINUE
3  CONTINUE
   DL=0.0
   DO 4 J=1,N7
     AJJ=CABS(A(J,J))
     IF (AJJ.LE.0.0) GO TO 4
     DL=DL+ALOG10(AJJ)
4  CONTINUE
   IF (IV.EQ.0) GO TO 9
   CA=1.0
   CV(1)=CMPLX(1.0,0.0)
   L=1
   CV(2)=-A(2,1)/A(2,2)
   CM=CABS(CV(2))
   IF (CM.GT.1.0) L=2
   IF (L.EQ.2) CA=CM
   IF (N7.EQ.2) GO TO 7
   DO 6 I=3,N7
     C=-A(I,1)
     I1=I-1
     DO 5 J=2,I1
5    C=C-A(I,J)*CV(J)
     CV(I)=C/A(I,I)
     CM=CABS(CV(I))
     IF (CM.GT.CA) L=I
     IF (L.EQ.I) CA=CM
6  CONTINUE
7  CONTINUE
   LV=L
   IF (L.EQ.1) GO TO 9
   CVL=CV(L)

```

```

A 28
A 29
A 30
A 31
A 32
A 33
A 34
A 35
A 36
A 37
A 38
A 39
A 40
A 41
A 42
A 43
A 44
A 45
A 46
A 47
A 48
A 49
A 50
A 51
A 52
A 53
A 54
A 55
A 56
A 57
A 58
A 59

```

```
      DO 8 I=1,N7  
8     CV(I)=CV(I)/CVL  
      CV(L)=CMPLX(1.0,0.0)  
9     RETURN  
      END
```

```
      A 60  
      A 61  
      A 62  
      A 63  
      A 64
```

```

C*****
C          SAMPLE DATA SET
C*****
C
C TITLE FOR THE PROBLEM
C
C BORON-EPOXY;N=3;PHI=20
C
C RIGIDITY RATIOS B,C1,C2,D,E (5E15.7)
C
C   0.12      E+00  0.212      E+00  0.65      E+00  1.24      E+00  0.07      E+00
C
C CNX,CNY,CNXY (3F10.0)
C
C 0.0        0.0        0.0
C
C EIGENVECTOR PARAMETER: C-NO EIGENVECTOR (I5)
C
C
C ALAM,DLAM (2F8.2)
C 421.0      0.5
C
C NSETS,MODE OF LARGEST AMPLITUDE (2I5)
C 20        1
C
C ASSUMED MODES :M AND N (2I5)
C 1         1
C 1         2
C 2         1
C 2         2
C 3         1
C 3         2

```

4	1
4	2
5	1
5	2
6	1
6	2
7	1
7	2
8	1
8	2
9	1
9	2
10	1
10	2

C
C KKK (I5)
C
10

C*****

APPENDIX E

The nondimensional form of the differential equation of motion for a midplane symmetric anisotropic laminate (Eqn. 7) is:

$$\begin{aligned}
 & w_{,\xi\xi\xi\xi} + 4 (D_{16}/D_{11}) (a/b) w_{,\xi\xi\xi\eta} + 2 (D_{12} + 2D_{66})/D_{11} (a/b)^2 w_{,\xi\xi\eta\eta} + \\
 & 4 (D_{26}/D_{11}) (a/b)^3 w_{,\xi\eta\eta\eta} + (D_{22}/D_{11}) (a/b)^4 w_{,\eta\eta\eta\eta} + \lambda w_{,\xi} + \\
 & \lambda (a/U_\infty) (M_\infty^2 - 2)/(M_\infty^2 - 1) w_{,t} + (ma^4/D_{11}) w_{,tt} = (a^2 N_x/D_{11}) w_{,\xi\xi} + \\
 & (2a^2/D_{11}) (a/b) N_{xy} w_{,\xi\eta} + (a^2/D_{11}) (a/b)^2 N_y w_{,\eta\eta} \quad (E1)
 \end{aligned}$$

The eigenvalue Ω^2 of the flutter problem (Eqn. 15) is related to ω in equation 12 as:

$$\Omega^2 = \omega^2 - ig\omega \quad (E2)$$

where g is the aerodynamic and/or structural damping present in the panel. From equation 12 we see that:

$$\text{For instability, } \omega_I < 0 \quad (E3)$$

where ω_I is the imaginary part of ω .

Solving equation E2 for ω , the condition of instability reduces to the following (Ref. 19):

$$g^2 \Omega_R^2 < \Omega_I^2 \quad (E4)$$

$$\text{where } \Omega^2 = \Omega_R^2 + i\Omega_I \quad (E5)$$

The expression for the total strain energy in the panel, U , in terms of the second derivatives in $w(\xi,\eta)$ and panel properties is:

$$\begin{aligned}
 U = & (D_{11}/2) (b/a) \int_0^1 \int_0^1 [w_{,\xi\xi}^2 + 4(a/b) (D_{16}/D_{11}) w_{,\xi\xi} w_{,\xi\eta} + \\
 & 2(a/b)^2 (D_{12}/D_{11}) w_{,\xi\xi} w_{,\eta\eta} + 4(a/b)^2 (D_{66}/D_{11}) w_{,\xi\eta}^2 + \\
 & 4(a/b)^3 (D_{26}/D_{11}) w_{,\eta\eta} w_{,\xi\eta} + (a/b)^4 (D_{22}/D_{11}) w_{,\eta\eta}^2] d\xi d\eta \quad (E6)
 \end{aligned}$$

TABLES

TABLE 1

MATERIAL PROPERTIES

Material \	Boron/Epoxy AVCO 5505/4	Graphite/Epoxy AS/3002	Boron/Aluminium B ₄ /Al 6061-F
E ₁₁ (psi)	30 x 10 ⁶	18.5 x 10 ⁶	32 x 10 ⁶
E ₂₂ (psi)	2.7 x 10 ⁶	0.7 x 10 ⁶	18 x 10 ⁶
v ₁₂	0.21	0.21	0.23
G ₁₂ (psi)	0.93 x 10 ⁶	0.83 x 10 ⁶	9.5 x 10 ⁶
Thickness of each ply (in.)	0.0052	0.00525	0.0052

TABLE 2

STATIC BUCKLING LOADS FOR A BORON - EPOXY PLY

Orientation, ϕ (degrees)	Static Buckling Load, K_{xcrit}
0	- 30
10	- 33
20	- 41
30	- 62
40	- 101
50	- 167
60	- 251
70	- 269
80	- 231
90	- 209

TABLE 3

FLUTTER BOUNDARY OF BORON-EPOXY ANGLE-PLY PANEL FOR VARIOUS NUMBERS OF PLYS

ϕ (degrees)	λ_{crit} for					
	n = 1	n = 3	n = 5	n = 9	n = 15	n = 49
0	356.4	356.4	356.4	356.4	356.4	356.4
10	372.7	372.5	371.65	371.35	371.25	371.25
20	424.65	423.75	421.25	420.25	419.75	419.75
30	513.7	513.3	512.9	513.05	513.35	513.75
40	693.8	691.5	682.7	679.05	677.75	677.15
50	955.7	951.1	934.7	927.5	925.25	924.15
60	1191.0	1185.5	1164.9	1155.7	1152.85	1151.45
70	1060.9	1056.9	1042.9	1036.9	1035.25	1034.35
80	662.8	662.1	659.7	658.65	658.35	658.25
90	494.3	494.3	494.3	494.3	494.25	494.25

TABLE 4

WEAK COALESCENT FLUTTER VALUES FOR AN ANGLE-PLY PANEL

Number of Plies n	Orientation, ϕ (degrees)	Material	Critical Flutter Value, λ_{crit}	
			Weak Coalescent Value	Actual Value
1	10	Boron/Epoxy	351.0	372.7
1	20	Boron/Epoxy	400.5	424.65
3	20	Boron/Epoxy	400.9	423.75
5	20	Boron/Epoxy	403.15	421.25
9	20	Boron/Epoxy	405.1	420.25
15	20	Boron/Epoxy	406.25	419.75
49	20	Boron/Epoxy	407.65	419.75
1	20	Graphite/ Epoxy	385.5	421.95

FIGURES

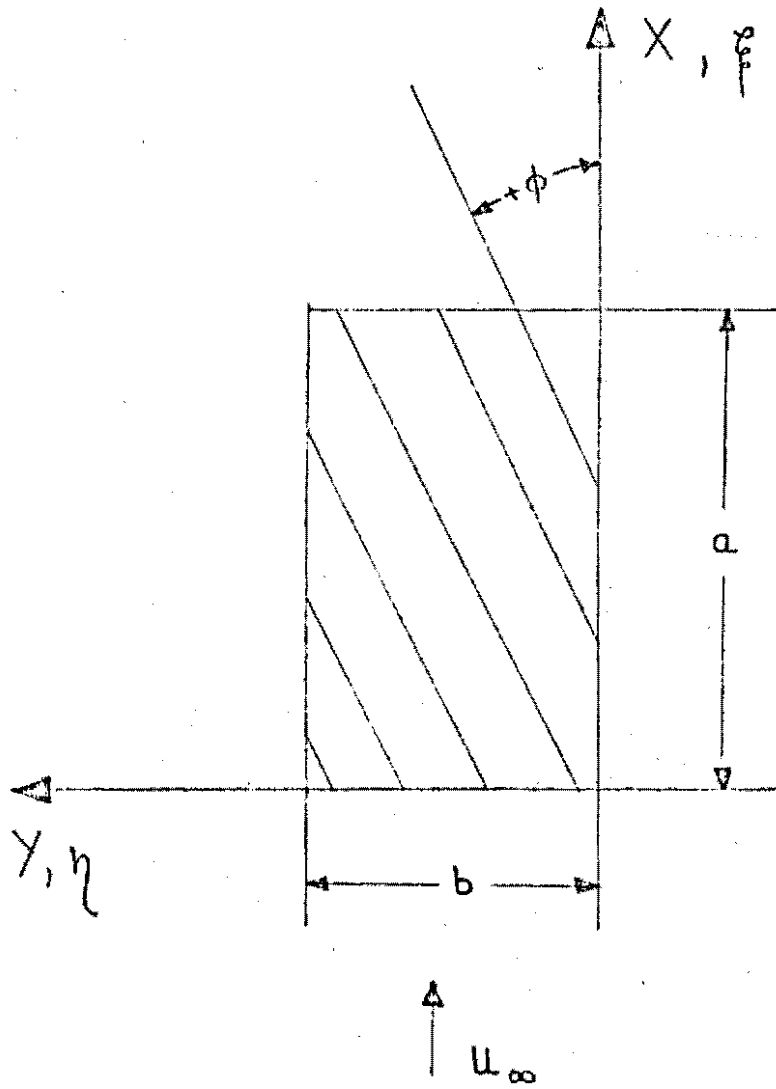


Figure 1. Planform Geometry of a Ply

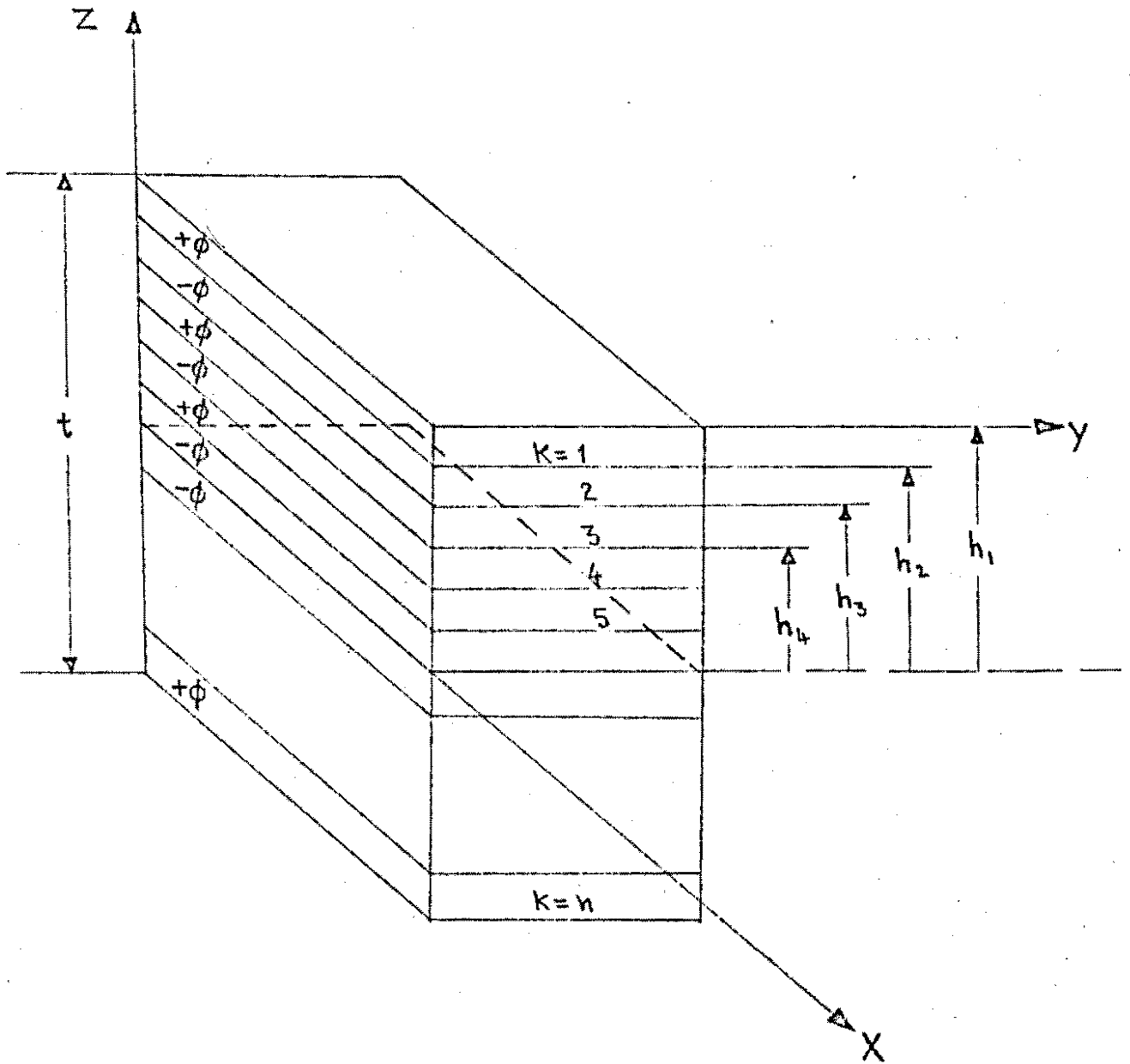


Figure 2. Angle-Ply Panel Layup

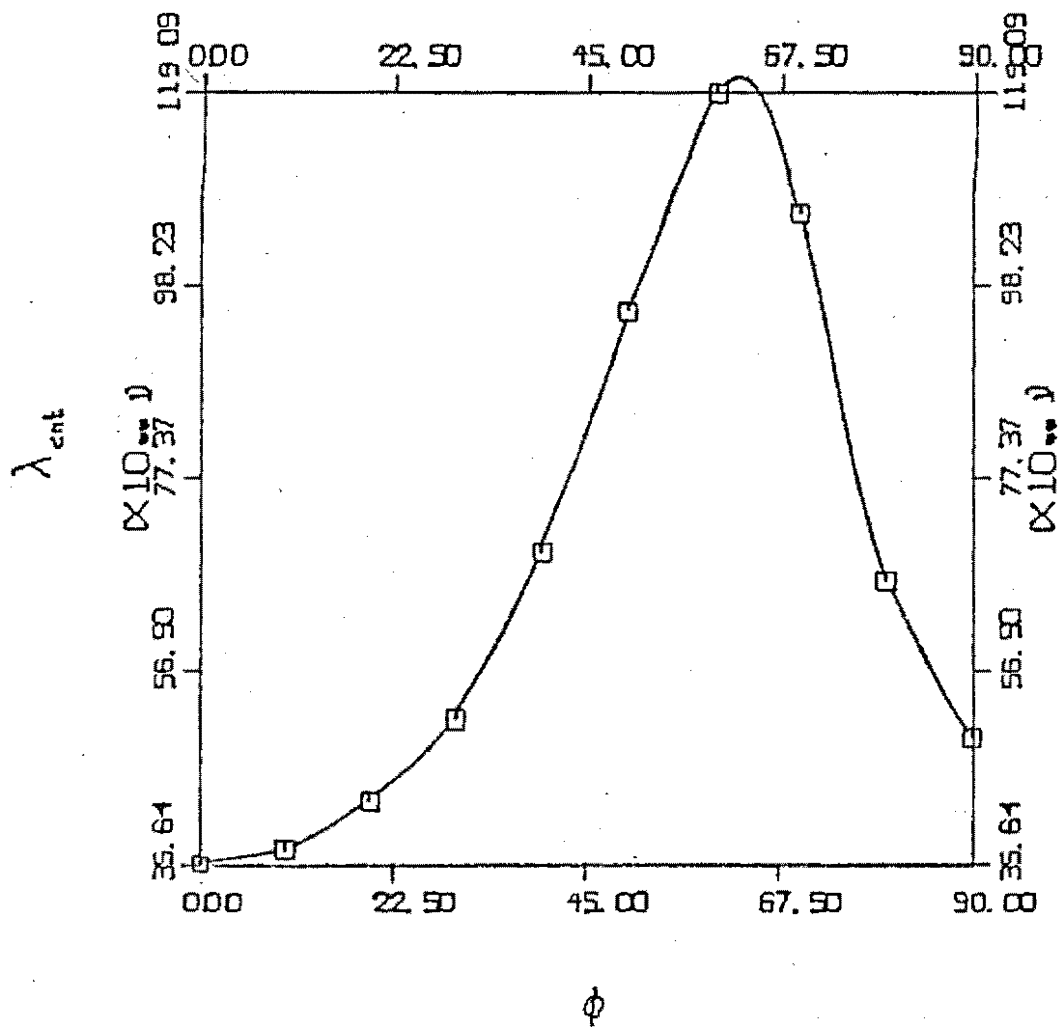


Figure 3. Flutter Boundary for a Boron-Epoxy Ply; $g=0$

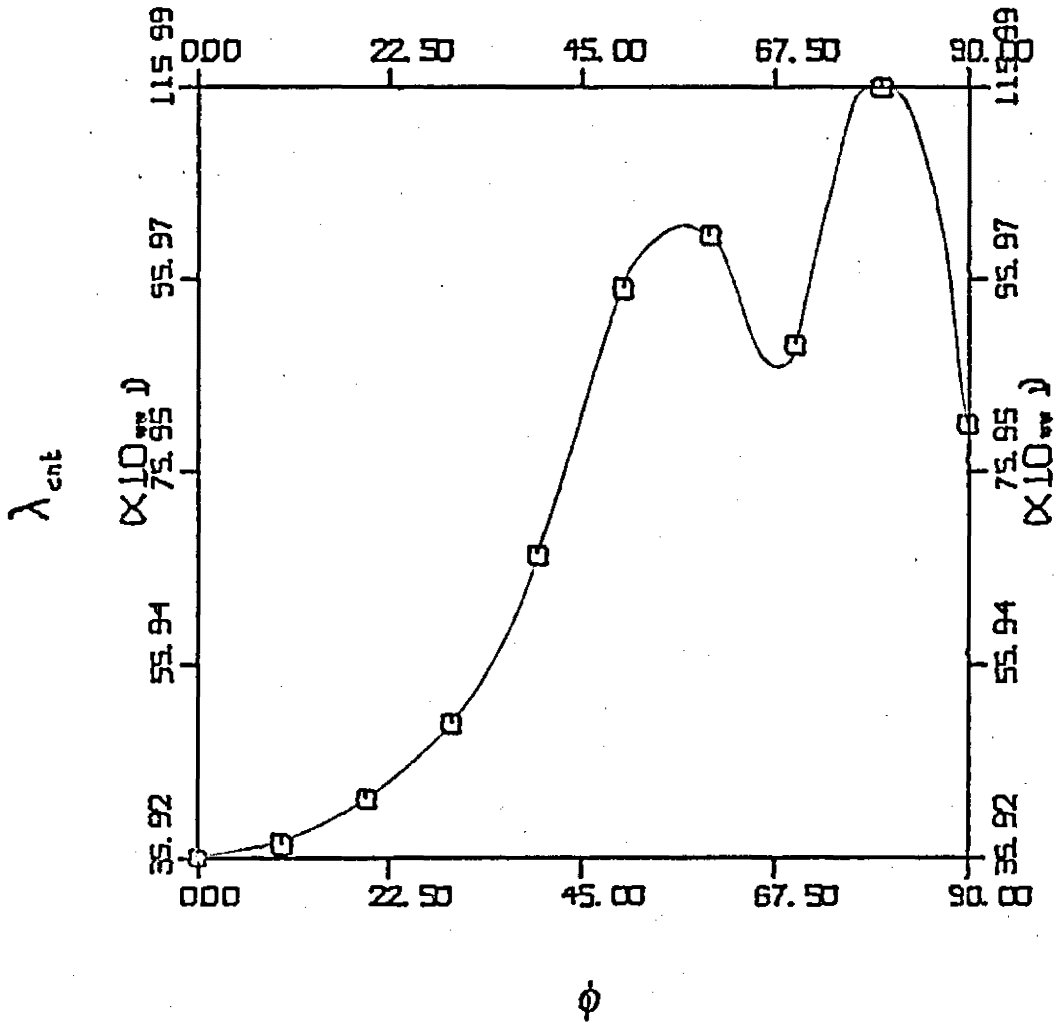


Figure 4. Flutter Boundary for a Graphite-Epoxy Ply; $g=0$

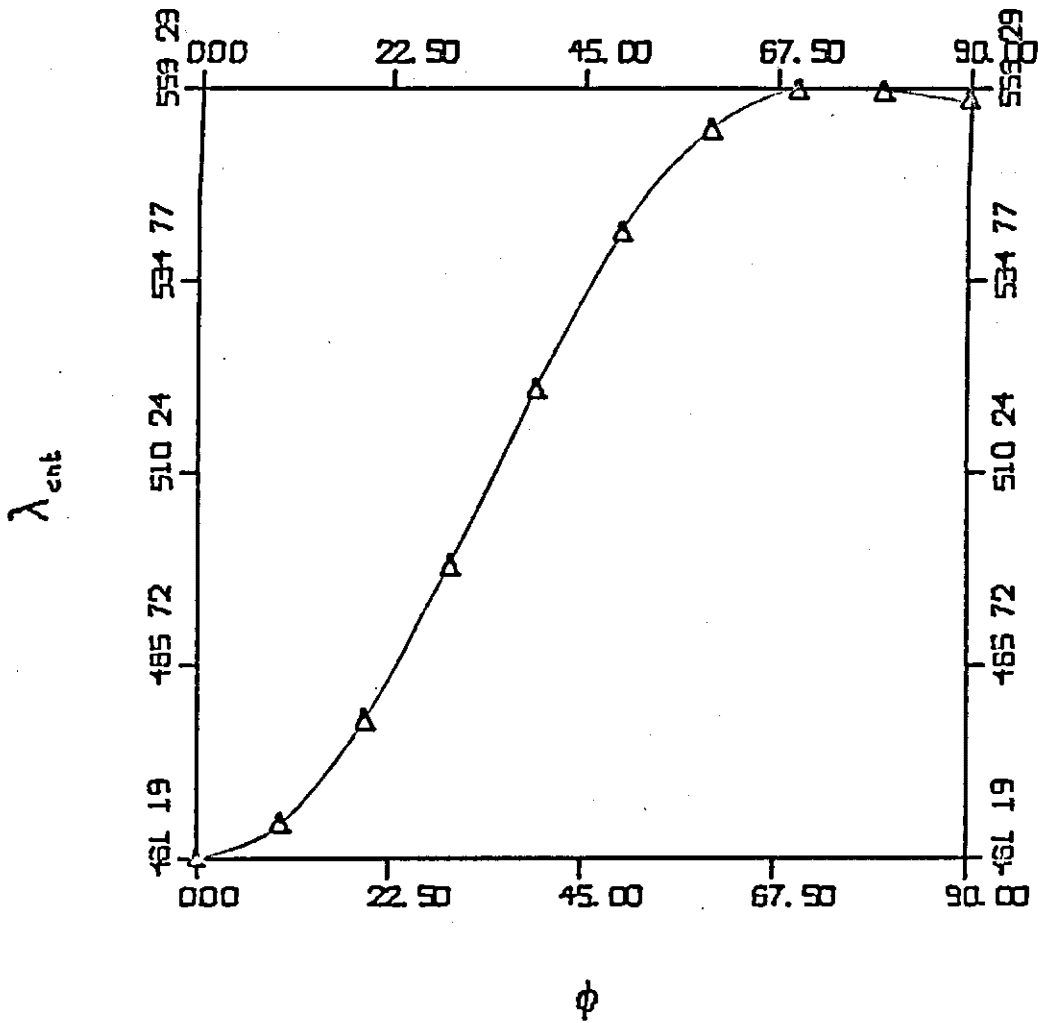


Figure 5. Flutter Boundary for a Boron-Aluminium Ply; $g=0$

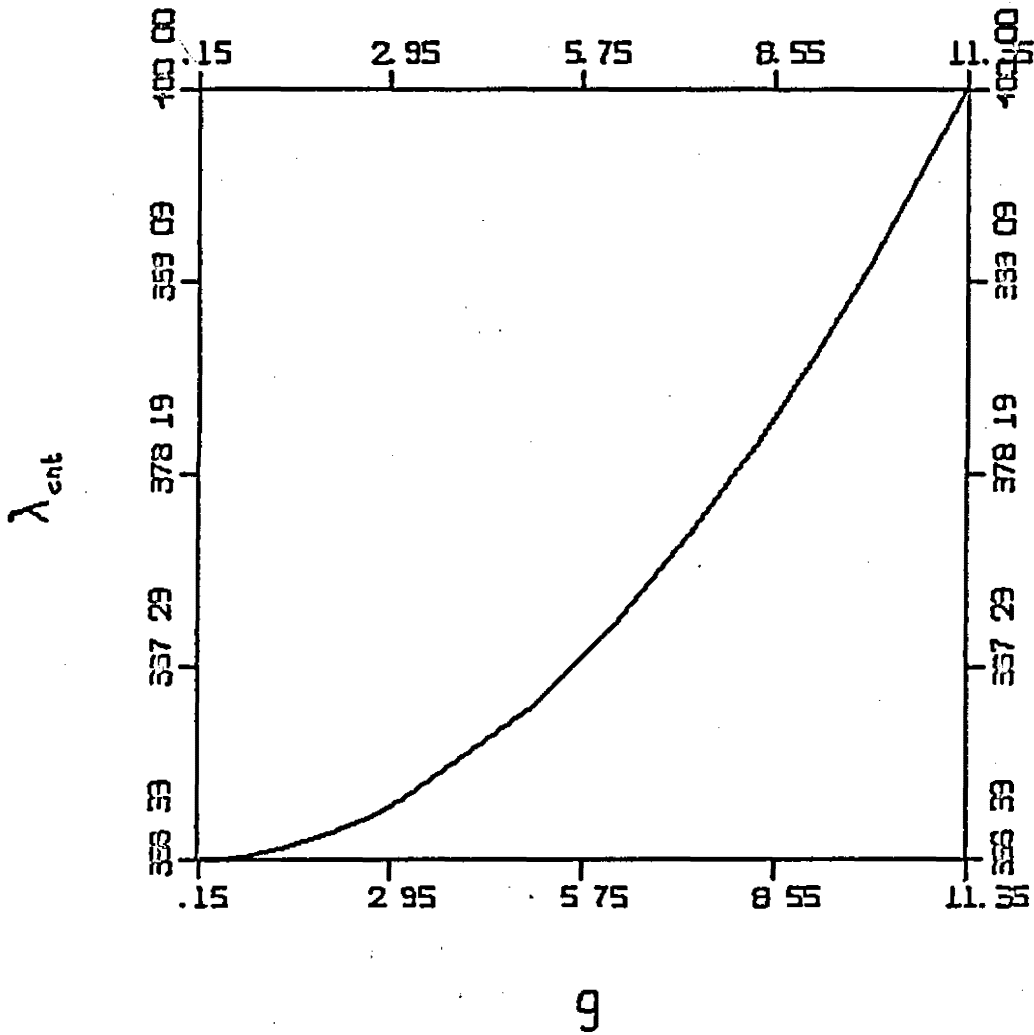


Figure 6. Effect of Damping on Flutter, Boron-Epoxy, $\phi=0^\circ$

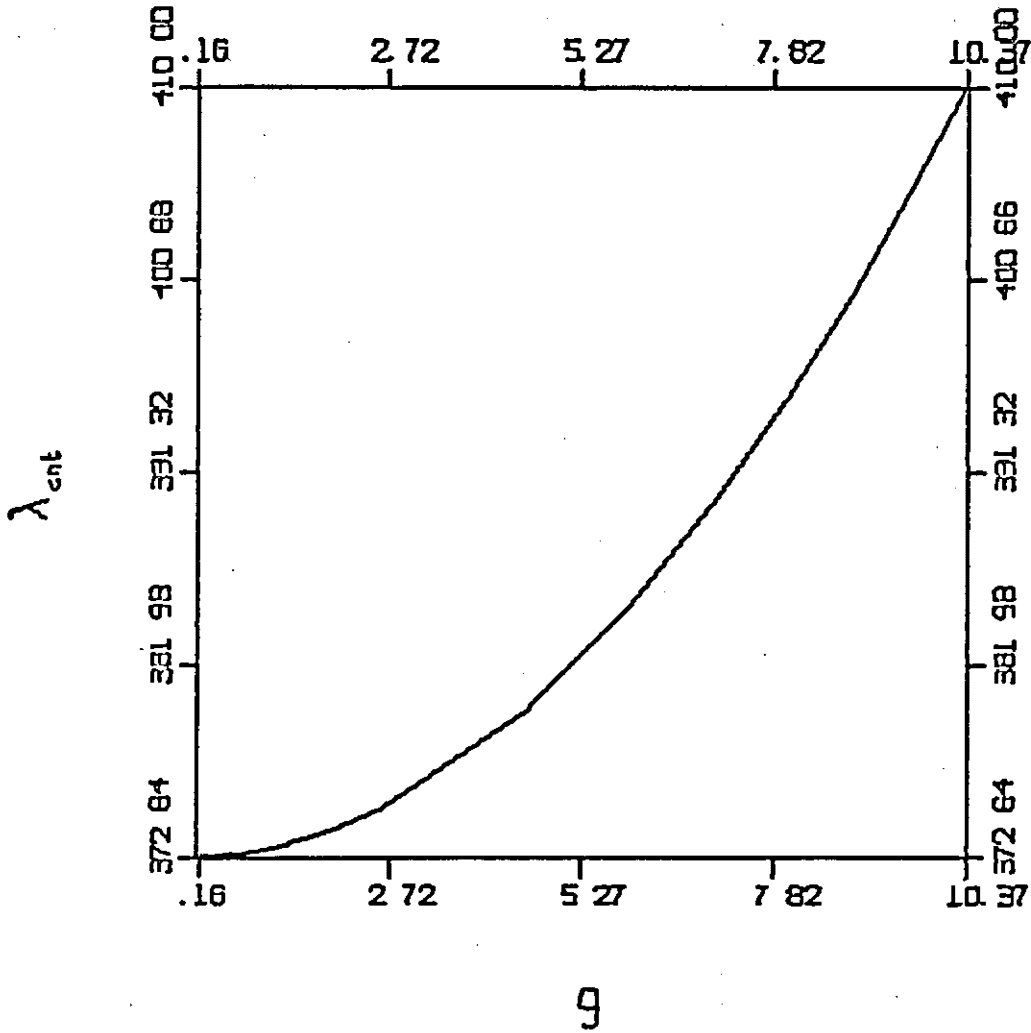


Figure 7. Effect of Damping on Flutter, Boron-Epoxy, $\phi=10^\circ$

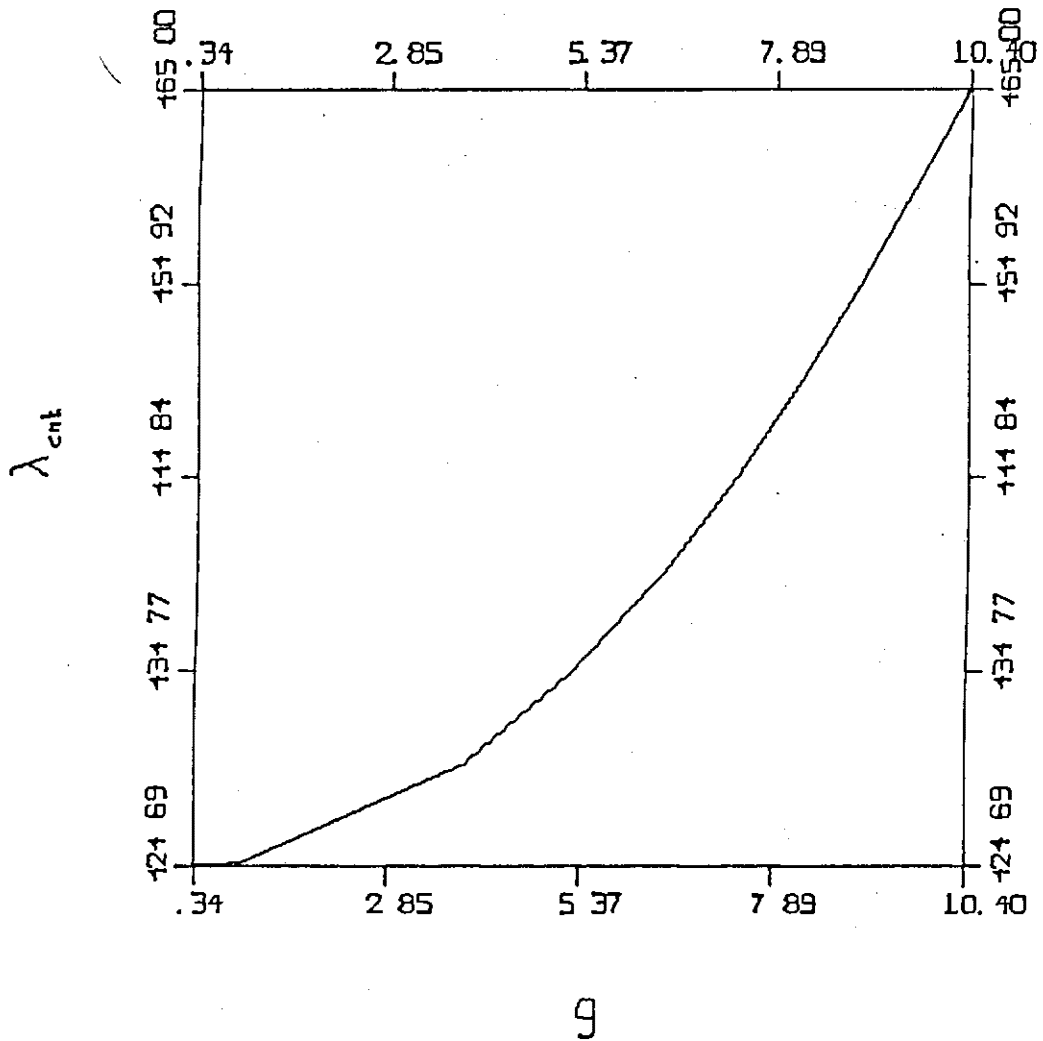


Figure 8. Effect of Damping on Flutter, Boron-Epoxy, $\phi=20^\circ$

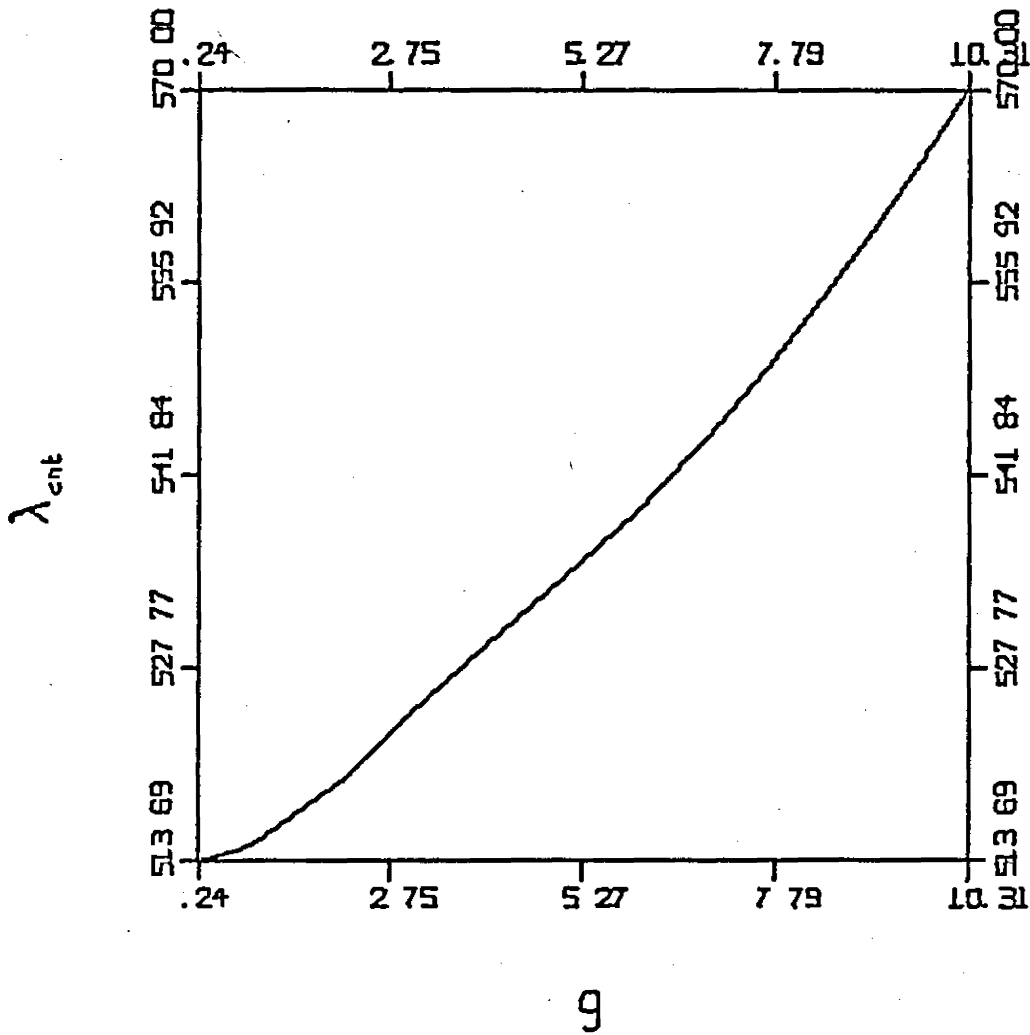


Figure 9. Effect of Damping on Flutter, Boron-Epoxy, $\phi=30^\circ$

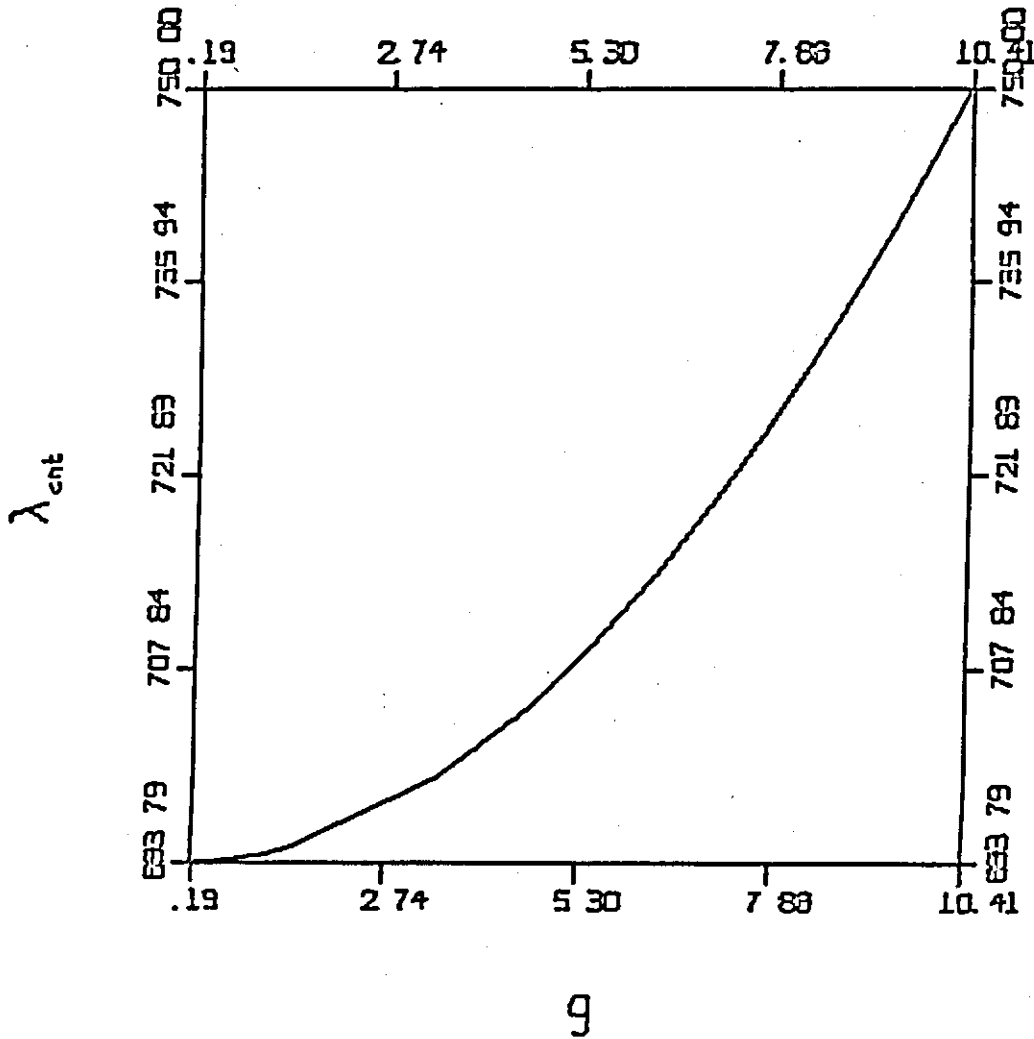


Figure 10. Effect of Damping on Flutter, Boron-Epoxy, $\phi=40^\circ$

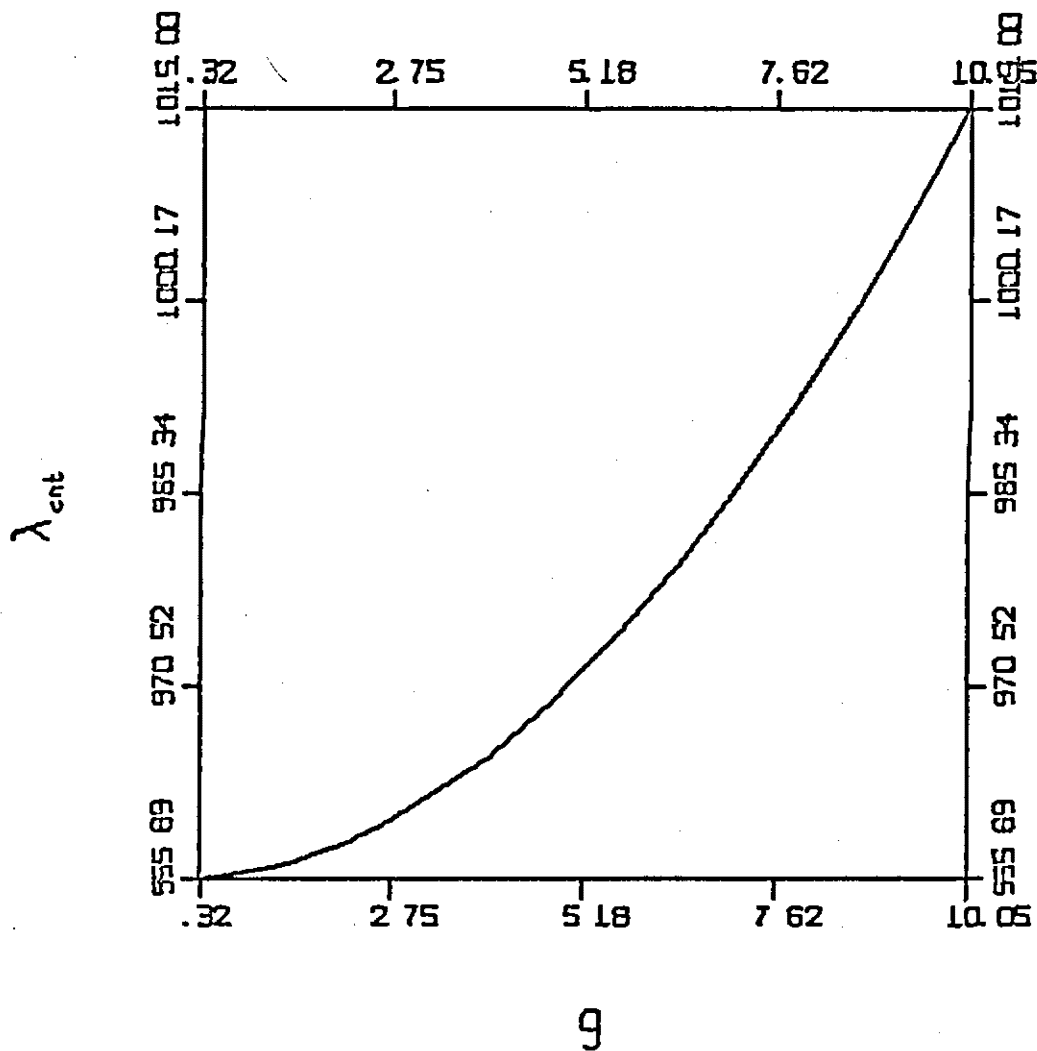
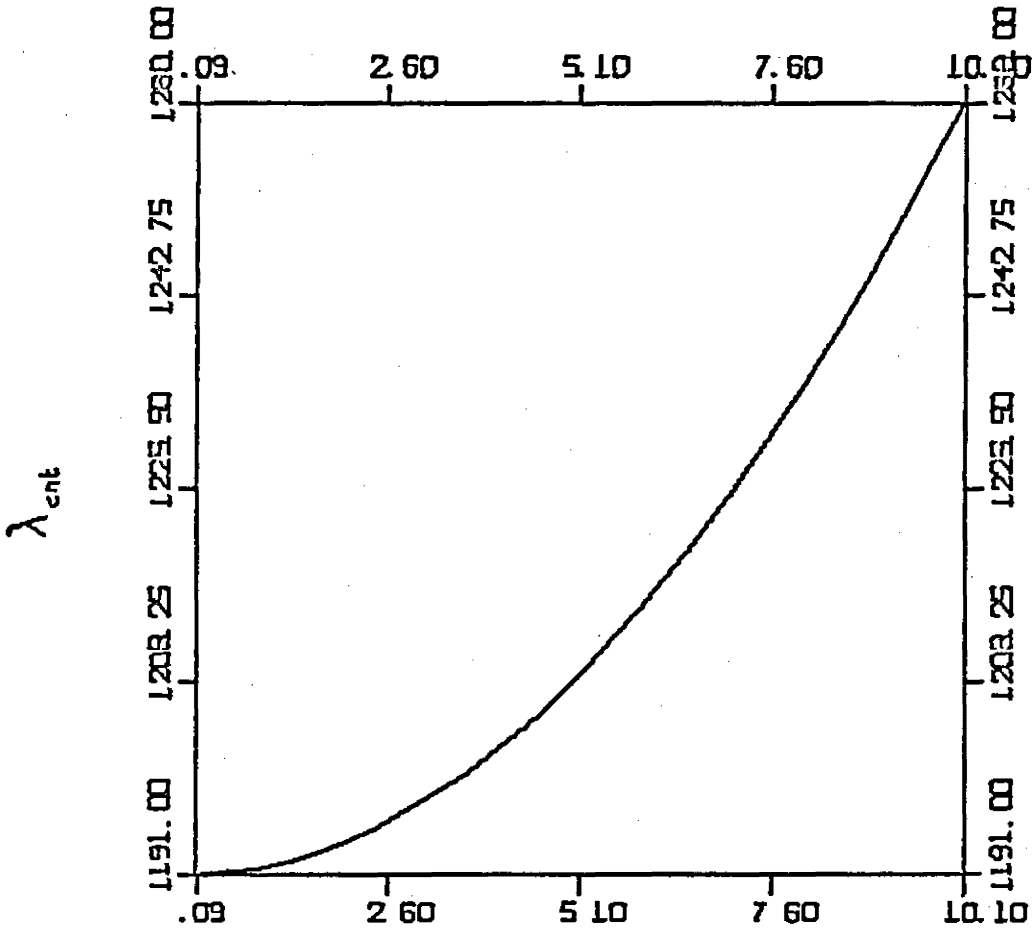


Figure 11. Effect of Damping on Flutter, Boron-Epoxy, $\phi=50^\circ$



9

Figure 12. Effect of Damping on Flutter, Boron-Epoxy, $\phi=60^\circ$

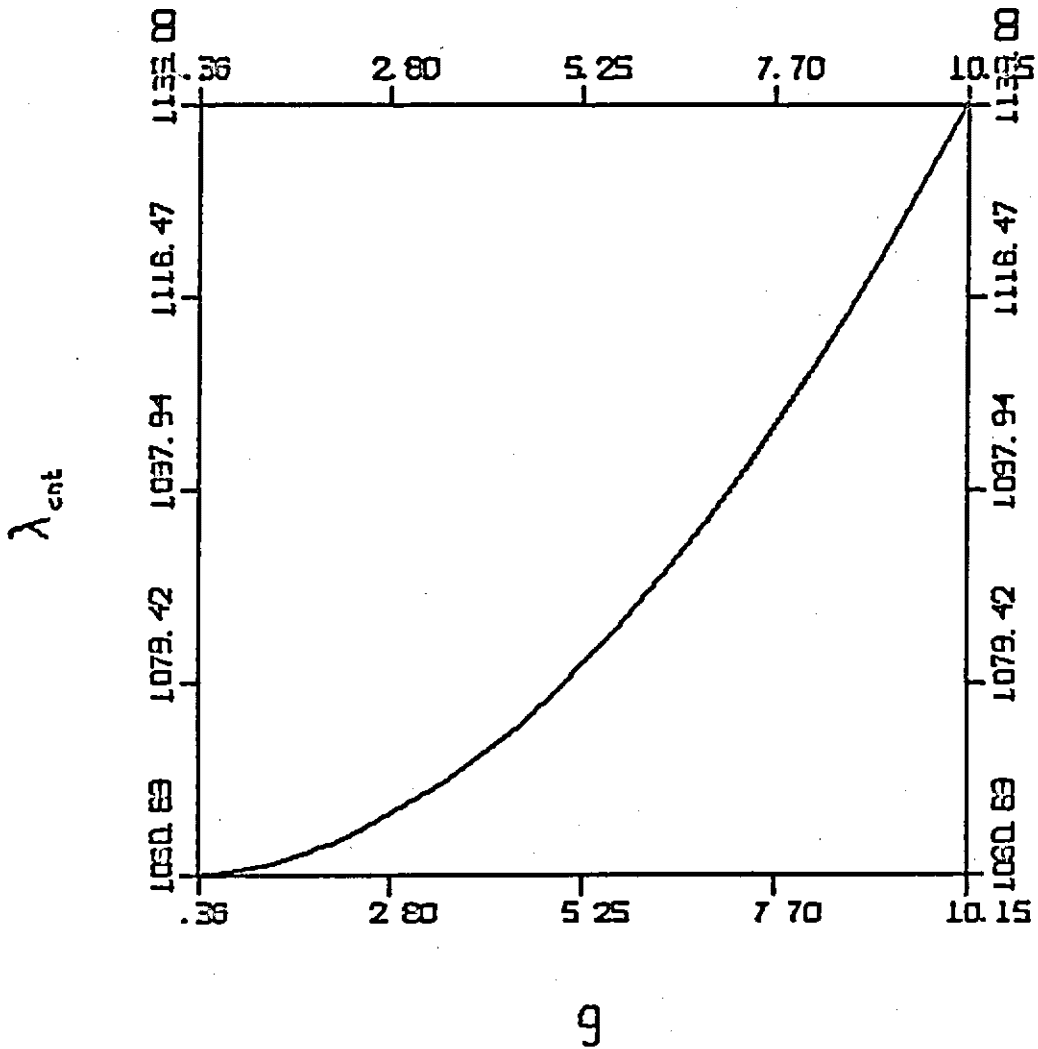


Figure 13. Effect of Damping on Flutter, Boron-Epoxy, $\phi=70^\circ$

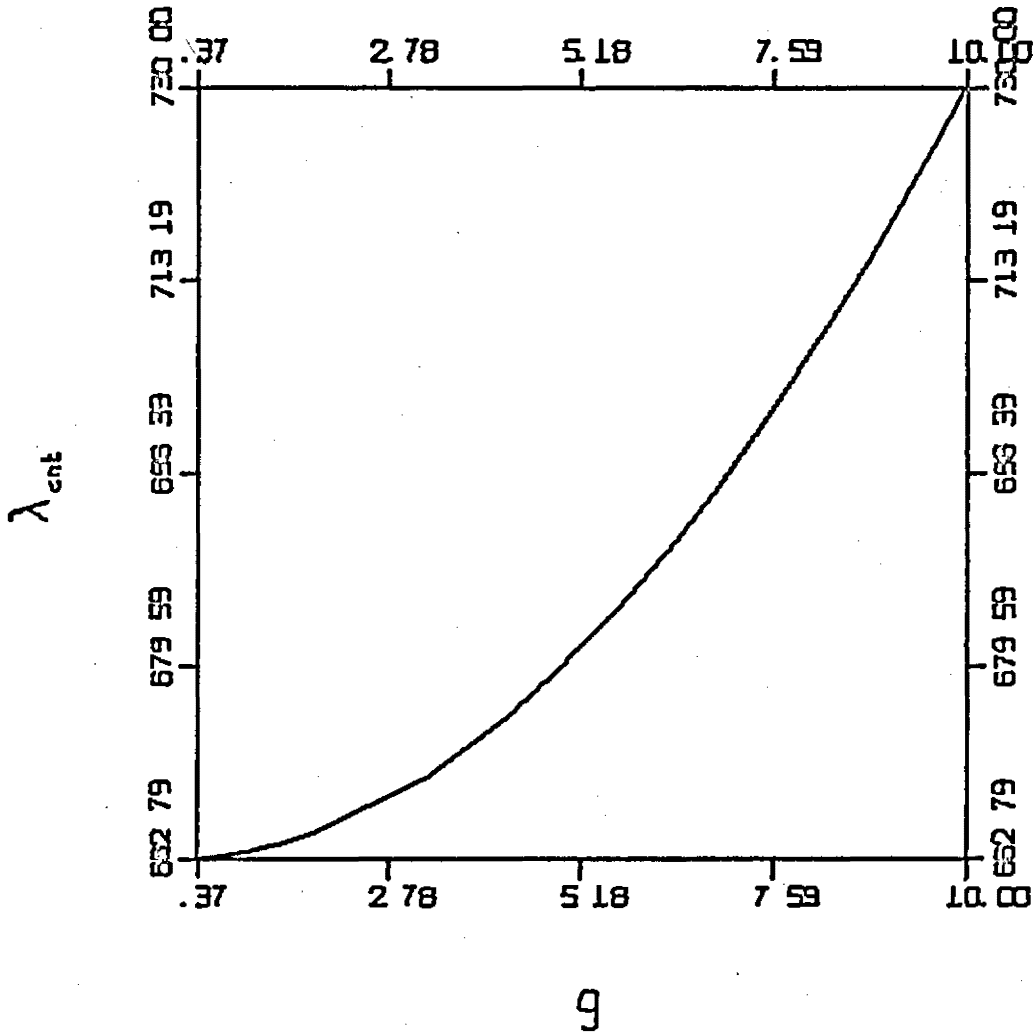


Figure 14. Effect of Damping on Flutter, Boron-Epoxy, $\phi=80^\circ$

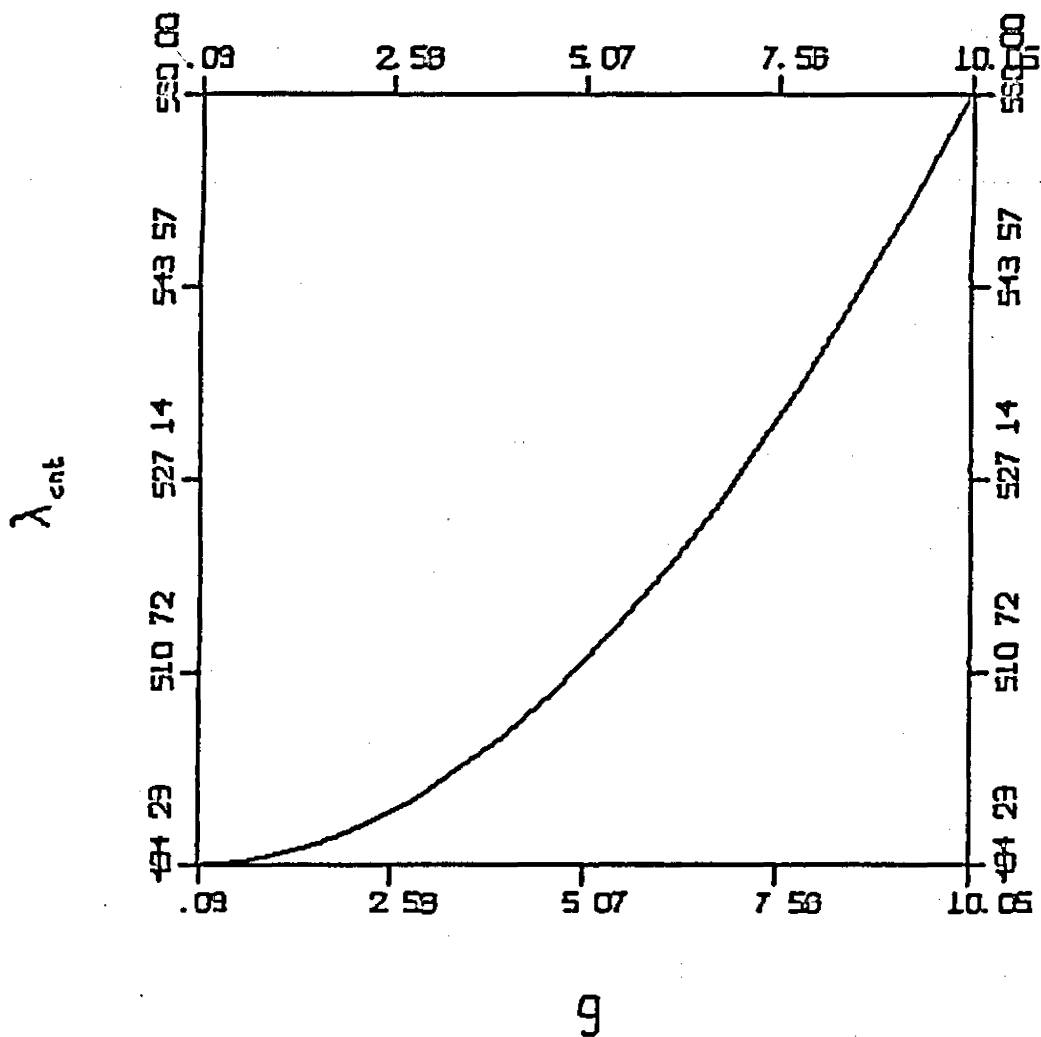
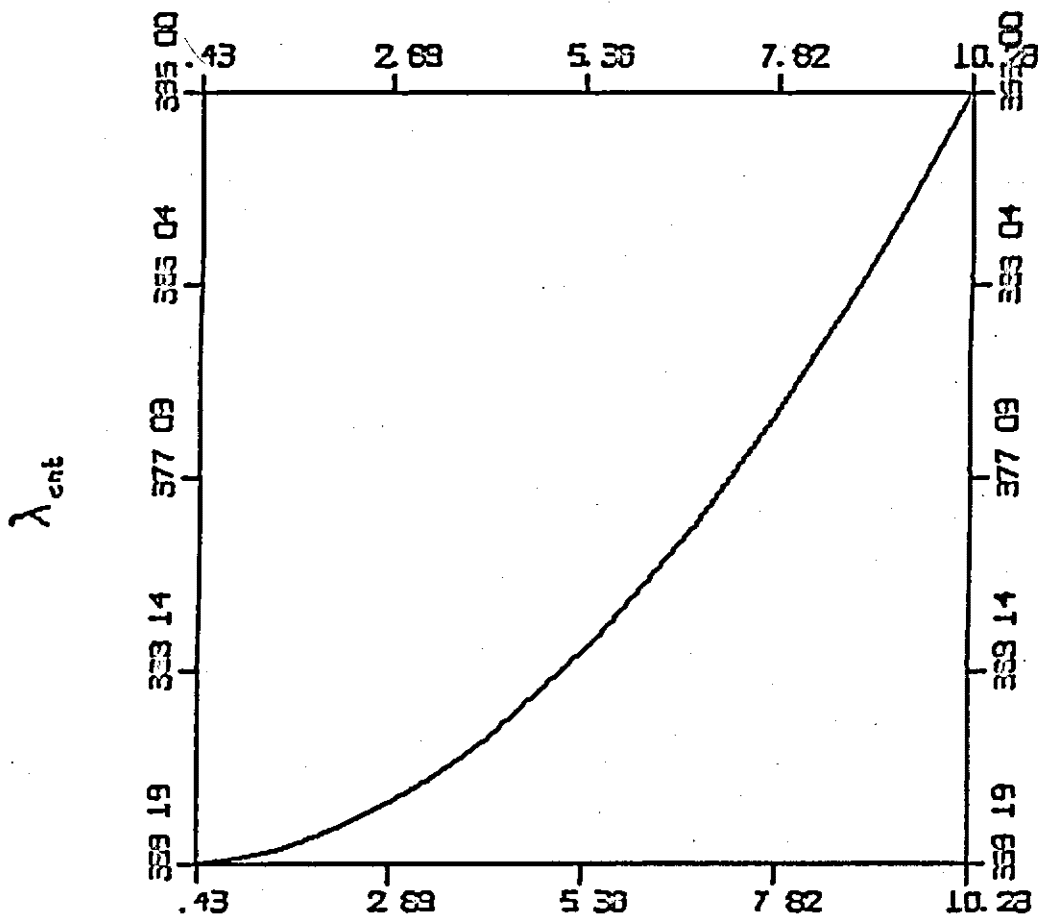


Figure 15. Effect of Damping on Flutter, Boron-Epoxy, $\phi=90^\circ$



9

Figure 16. Effect of Damping on Flutter, Graphite-Epoxy, $\phi=0^\circ$

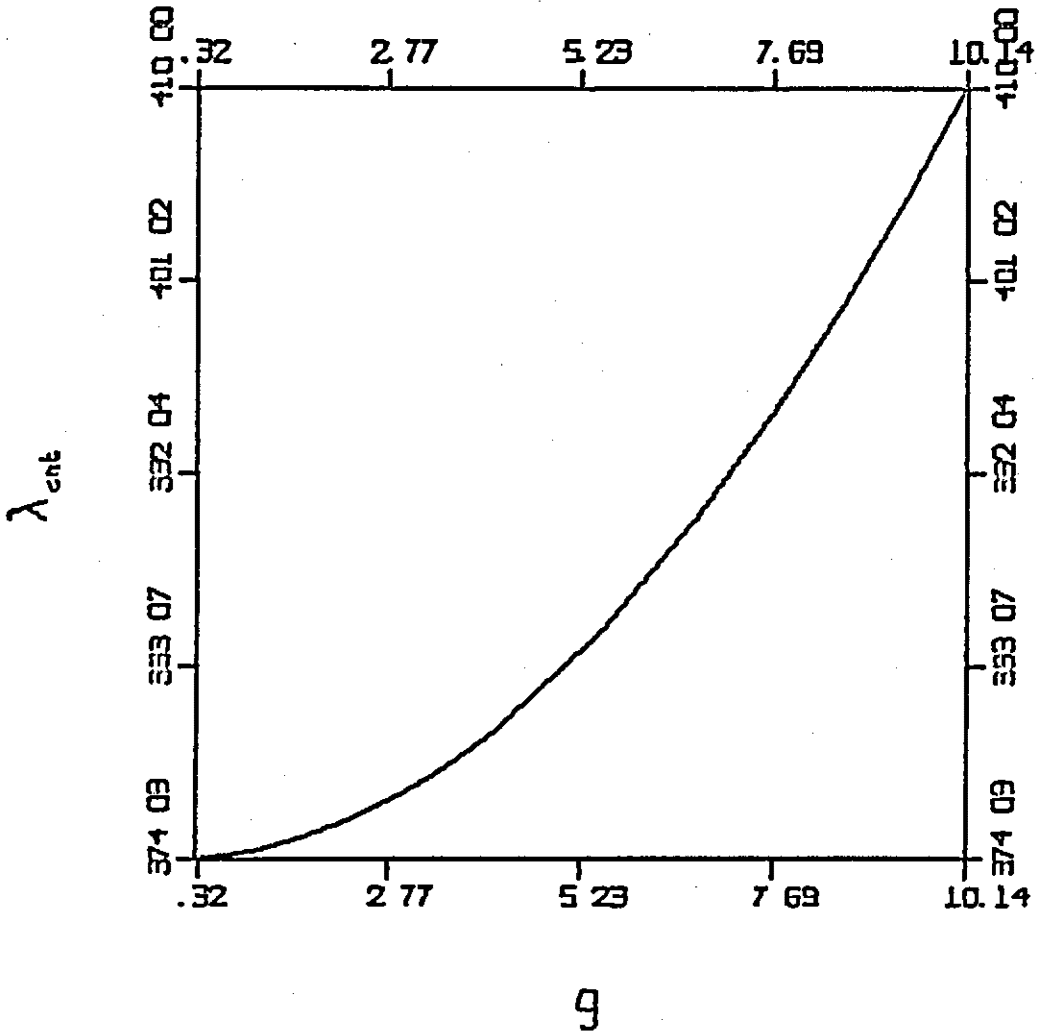


Figure 17. Effect of Damping on Flutter, Graphite-Epoxy, $\phi=10^\circ$

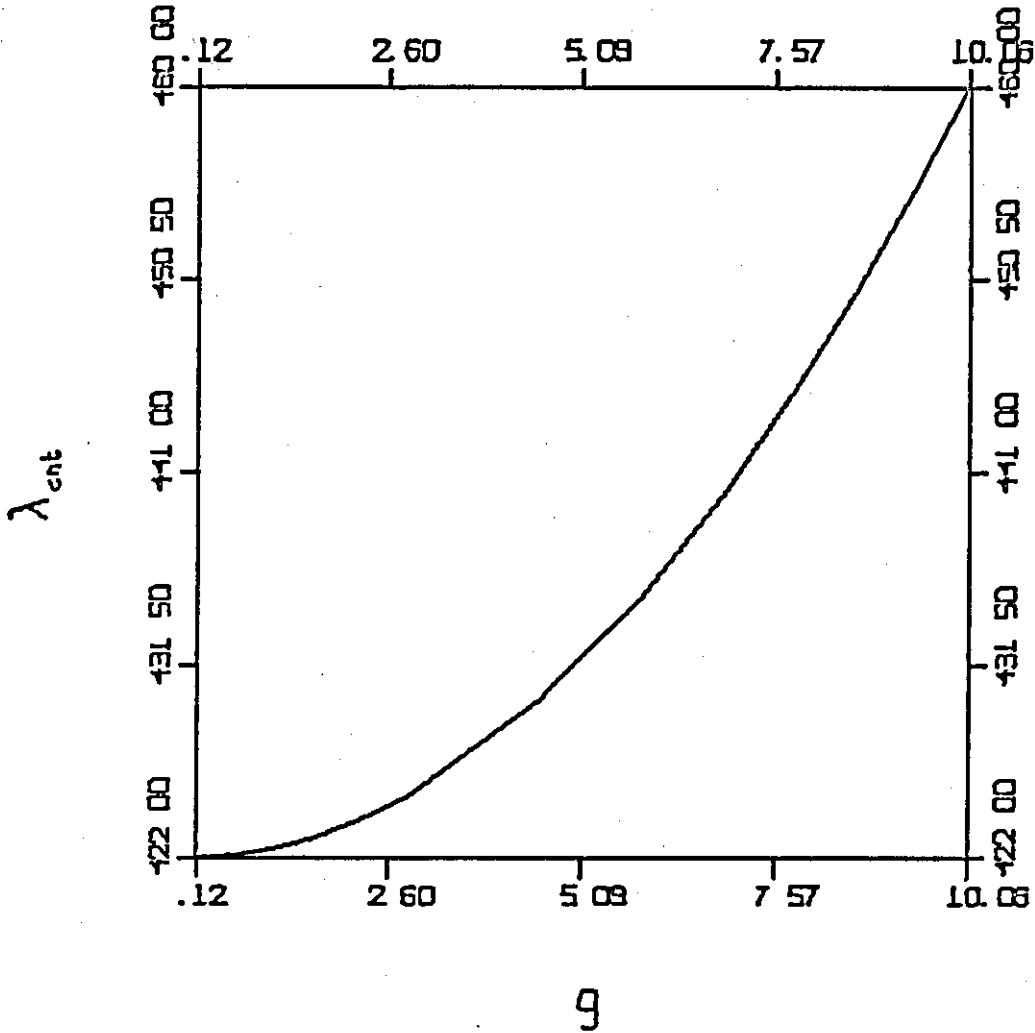


Figure 18. Effect of Damping on Flutter, Graphite-Epoxy, $\phi=20^\circ$

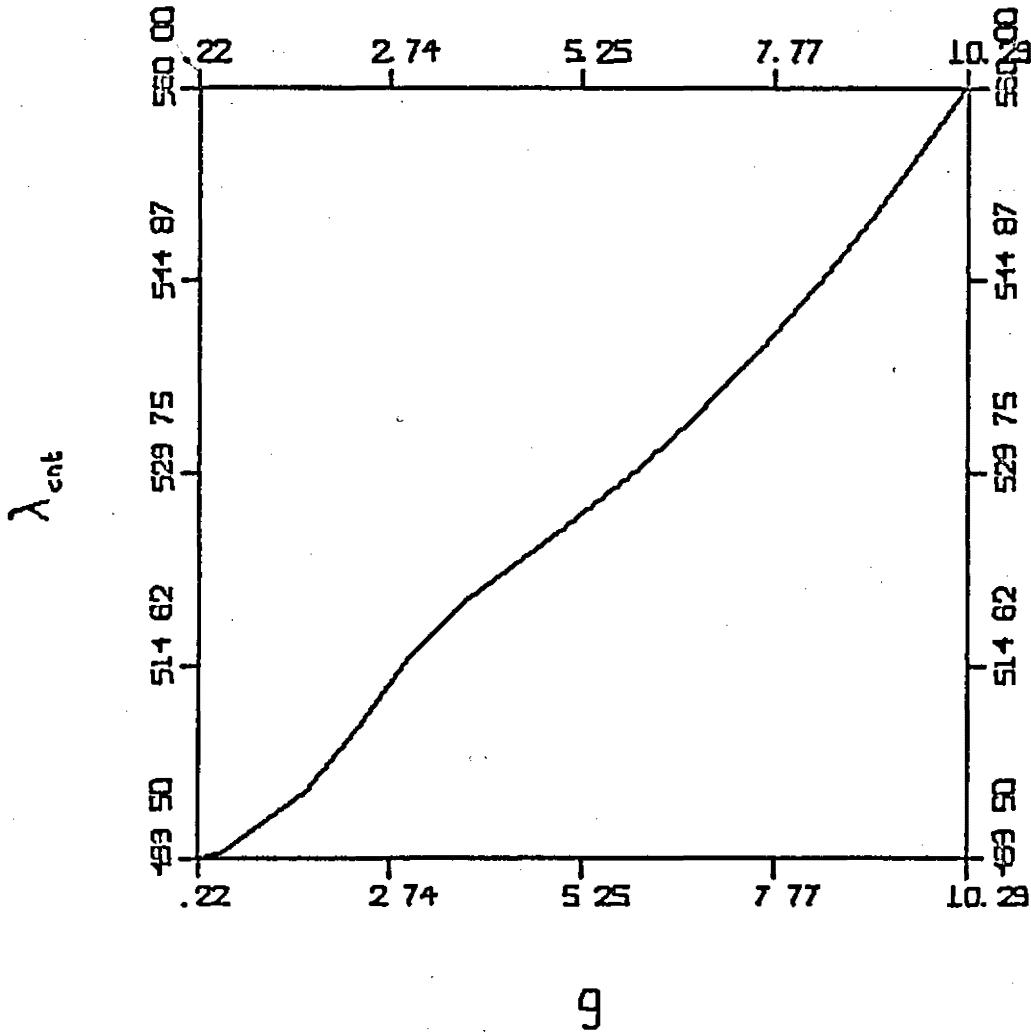


Figure 19. Effect of Damping on Flutter, Graphite-Epoxy, $\phi=30^\circ$

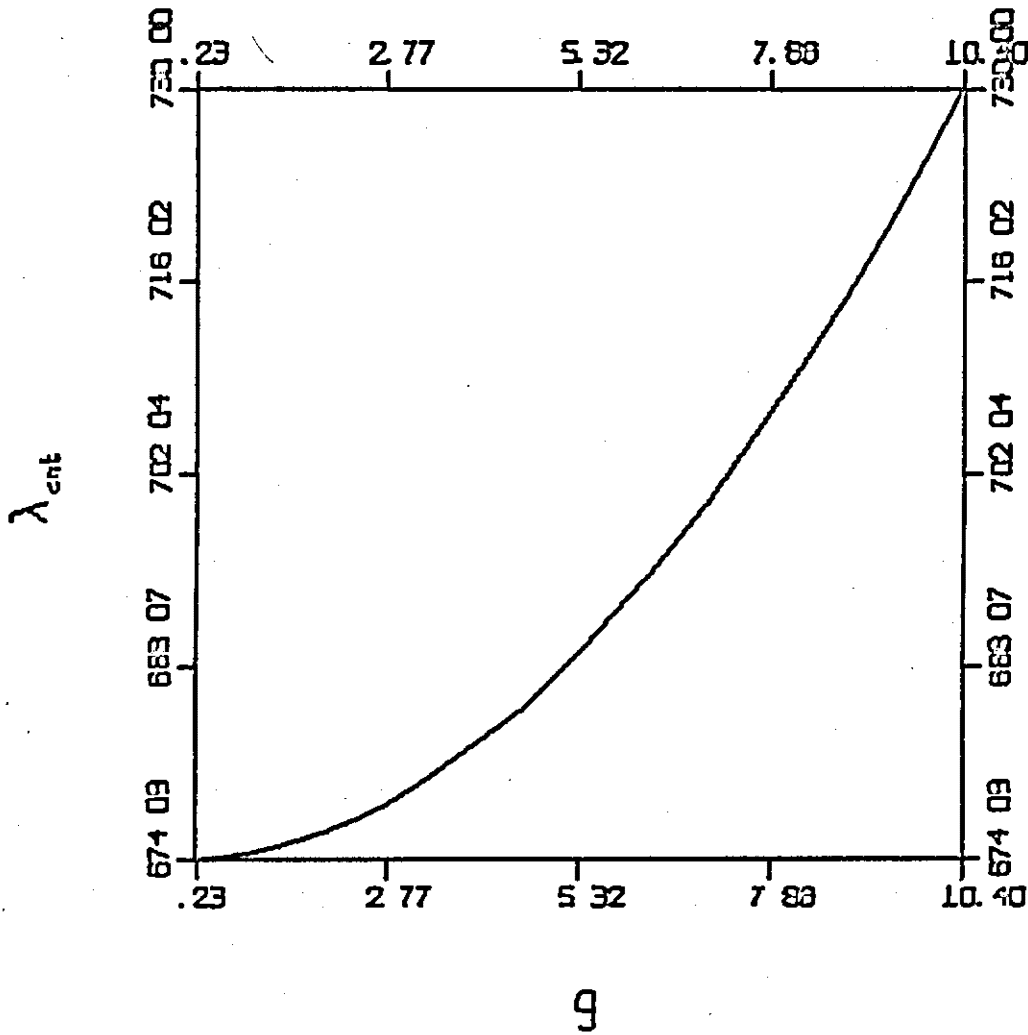


Figure 20. Effect of Damping on Flutter, Graphite-Epoxy, $\phi=40^\circ$

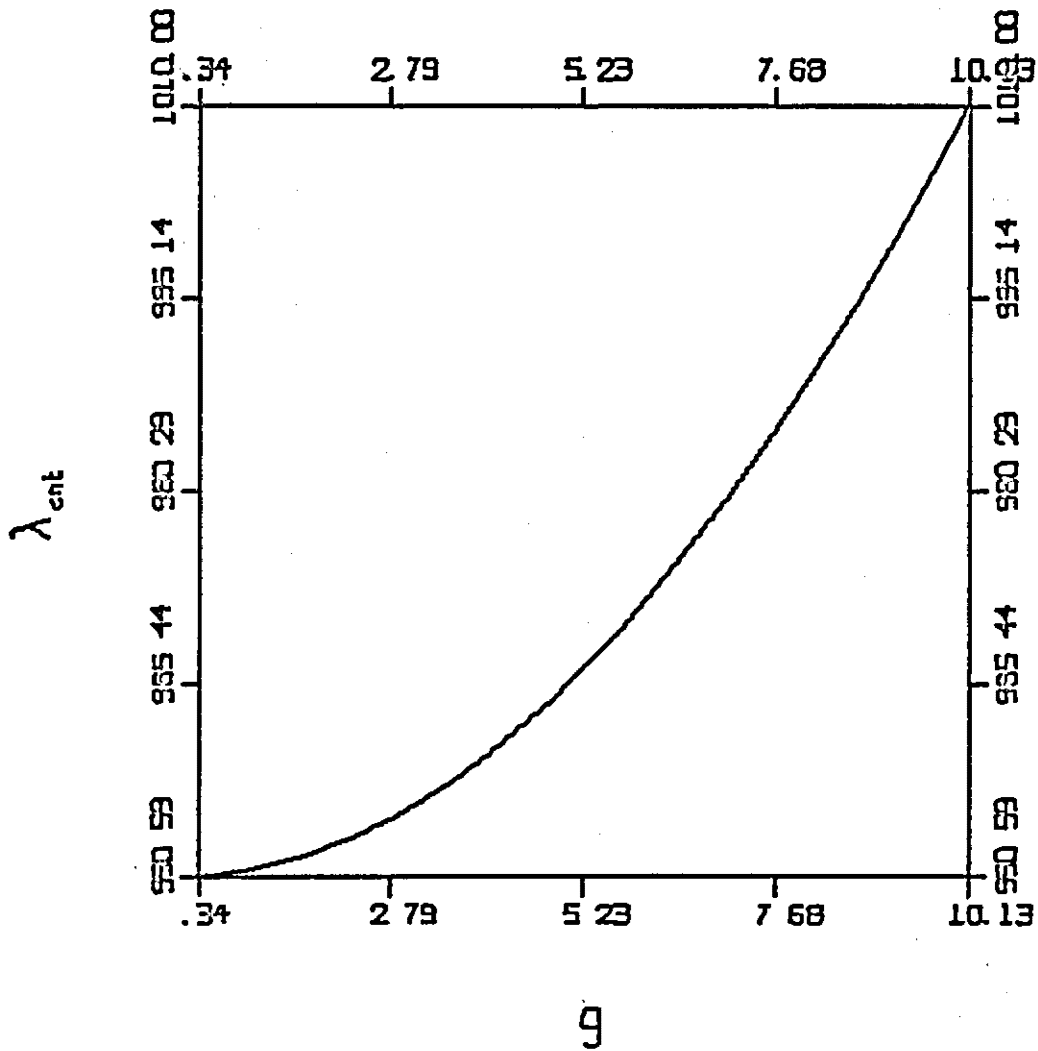


Figure 21. Effect of Damping on Flutter, Graphite-Epoxy, $\phi=50^\circ$

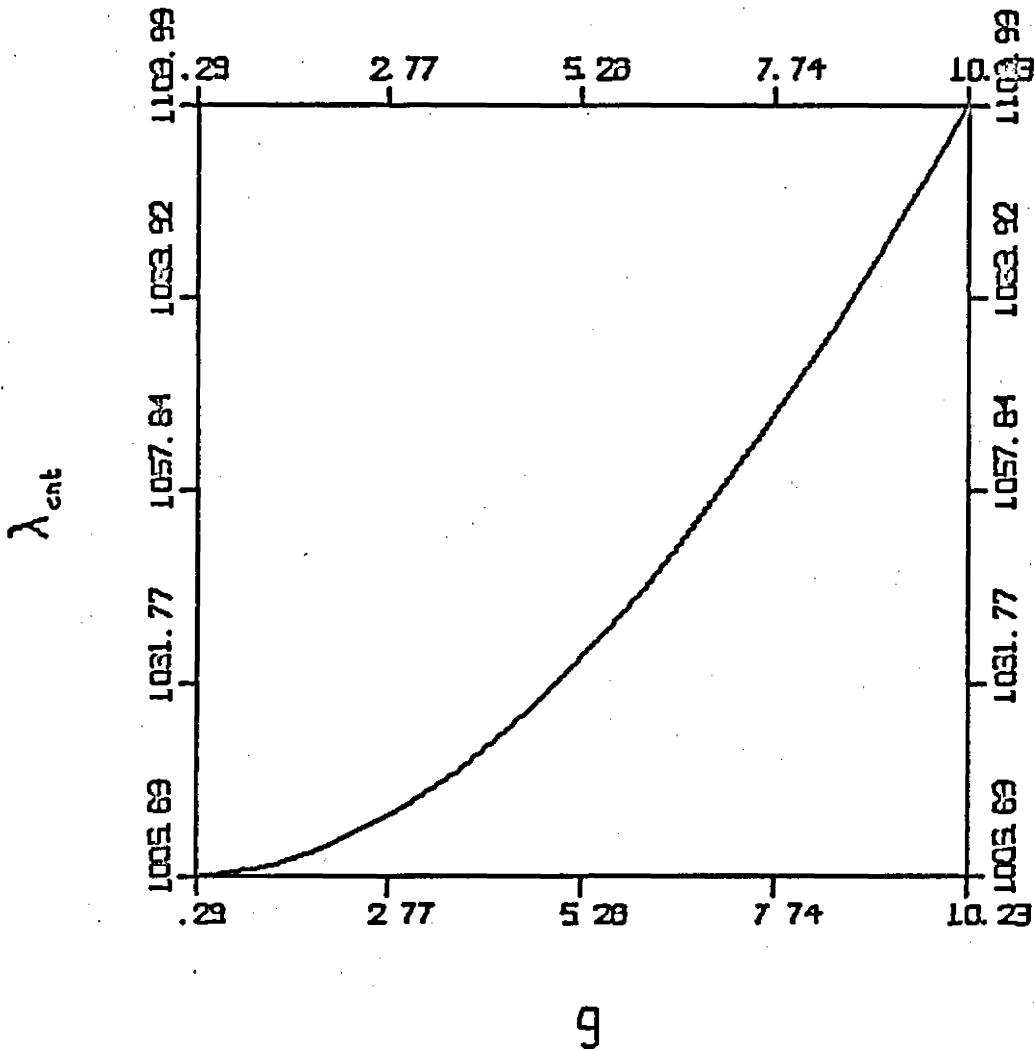


Figure 22. Effect of Damping on Flutter, Graphite-Epoxy, $\phi=60^\circ$.

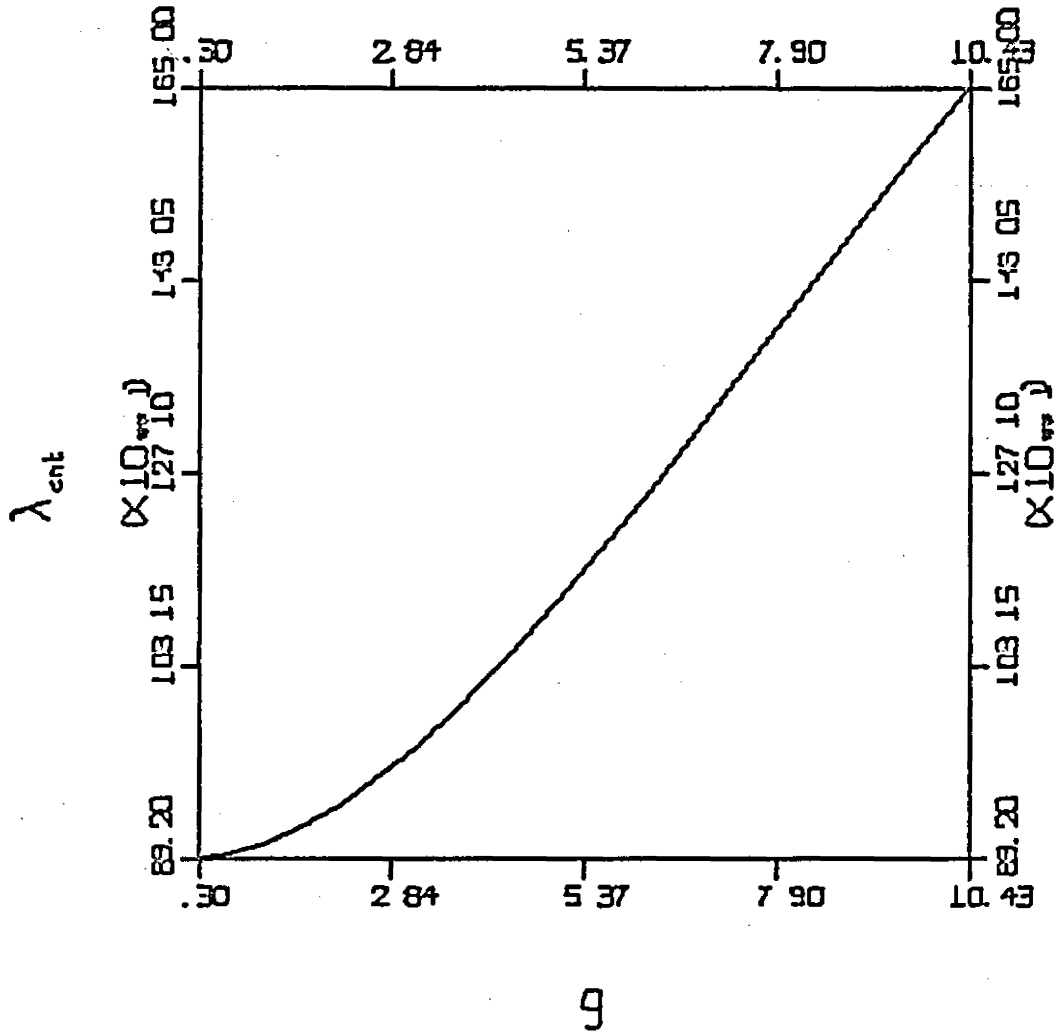


Figure 23. Effect of Damping on Flutter, Graphite-Epoxy, $\phi=70^\circ$

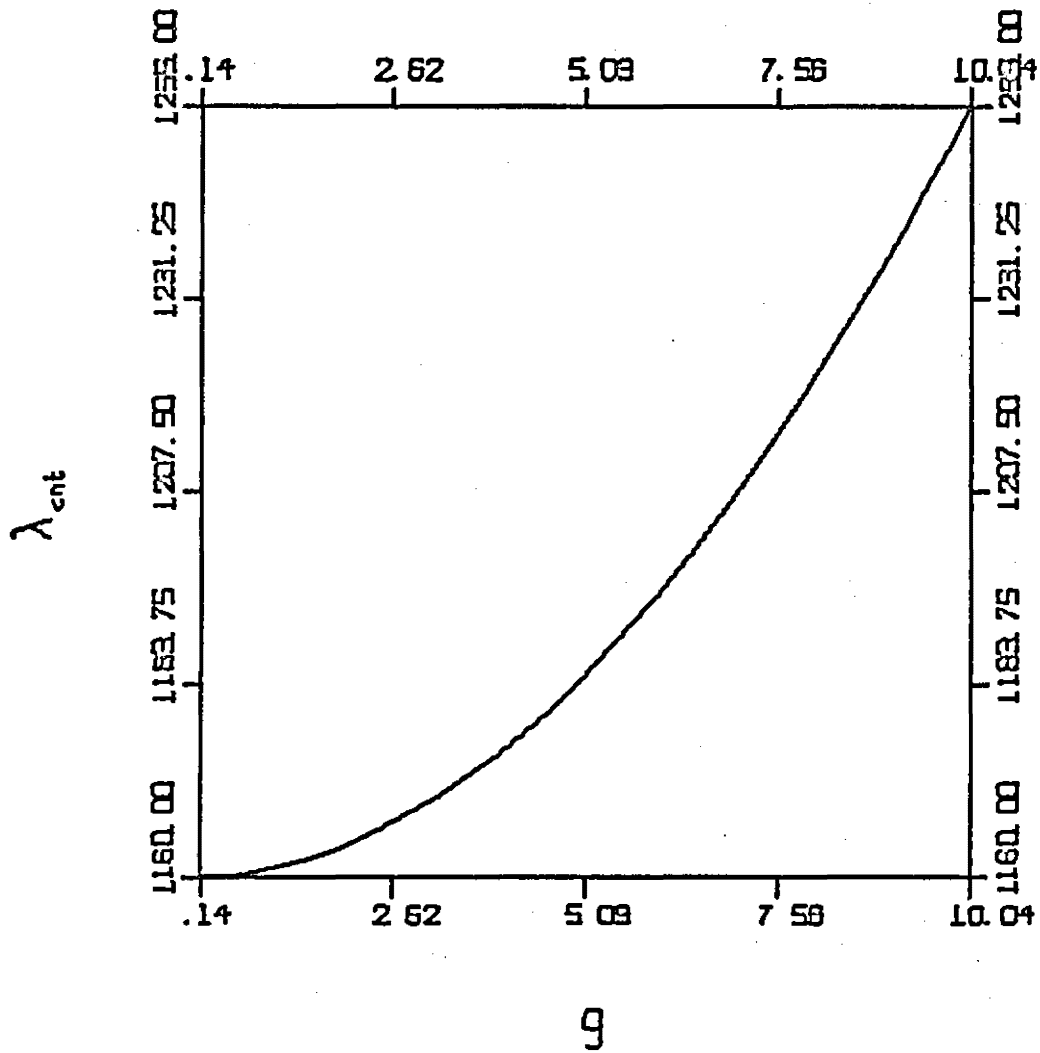


Figure 24. Effect of Damping on Flutter, Graphite-Epoxy, $\phi=80^\circ$

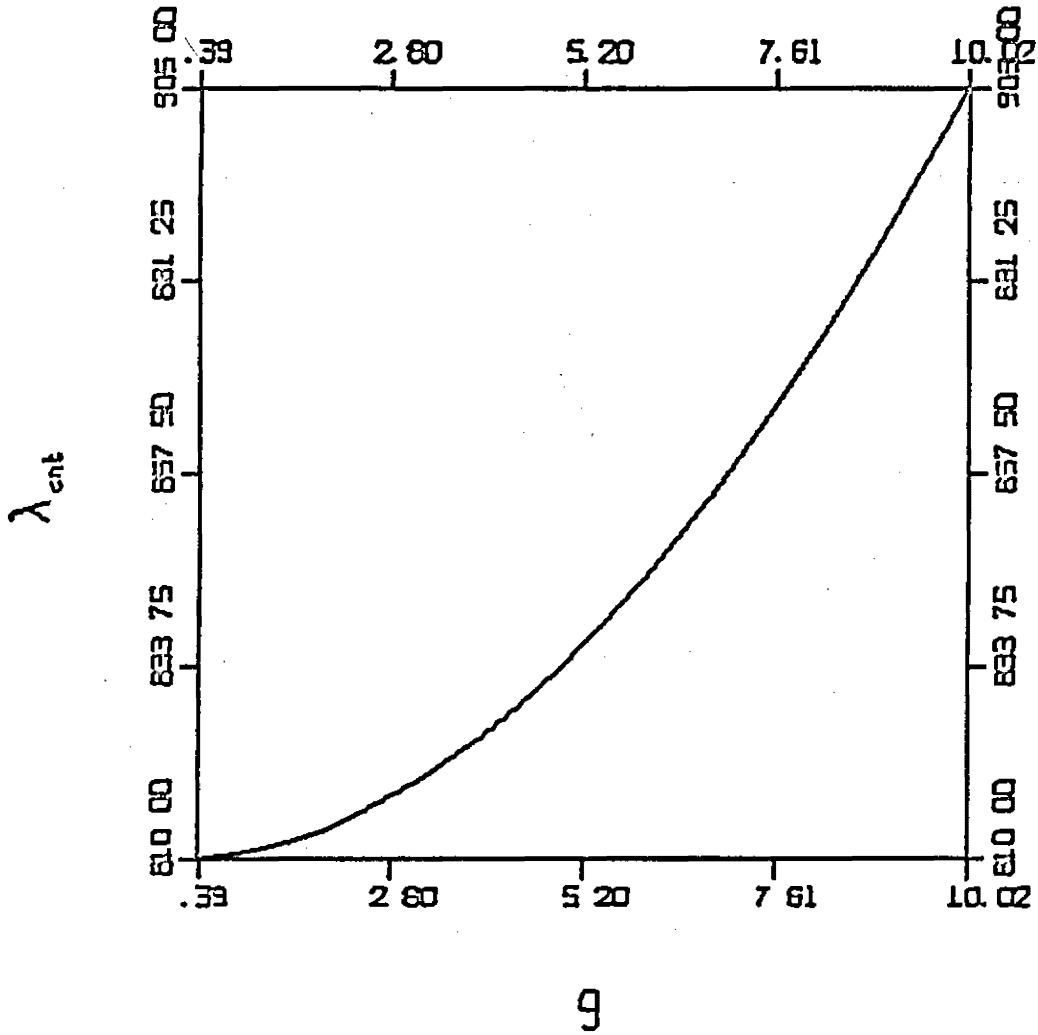


Figure 25. Effect of Damping on Flutter, Graphite-Epoxy, $\phi=90^\circ$

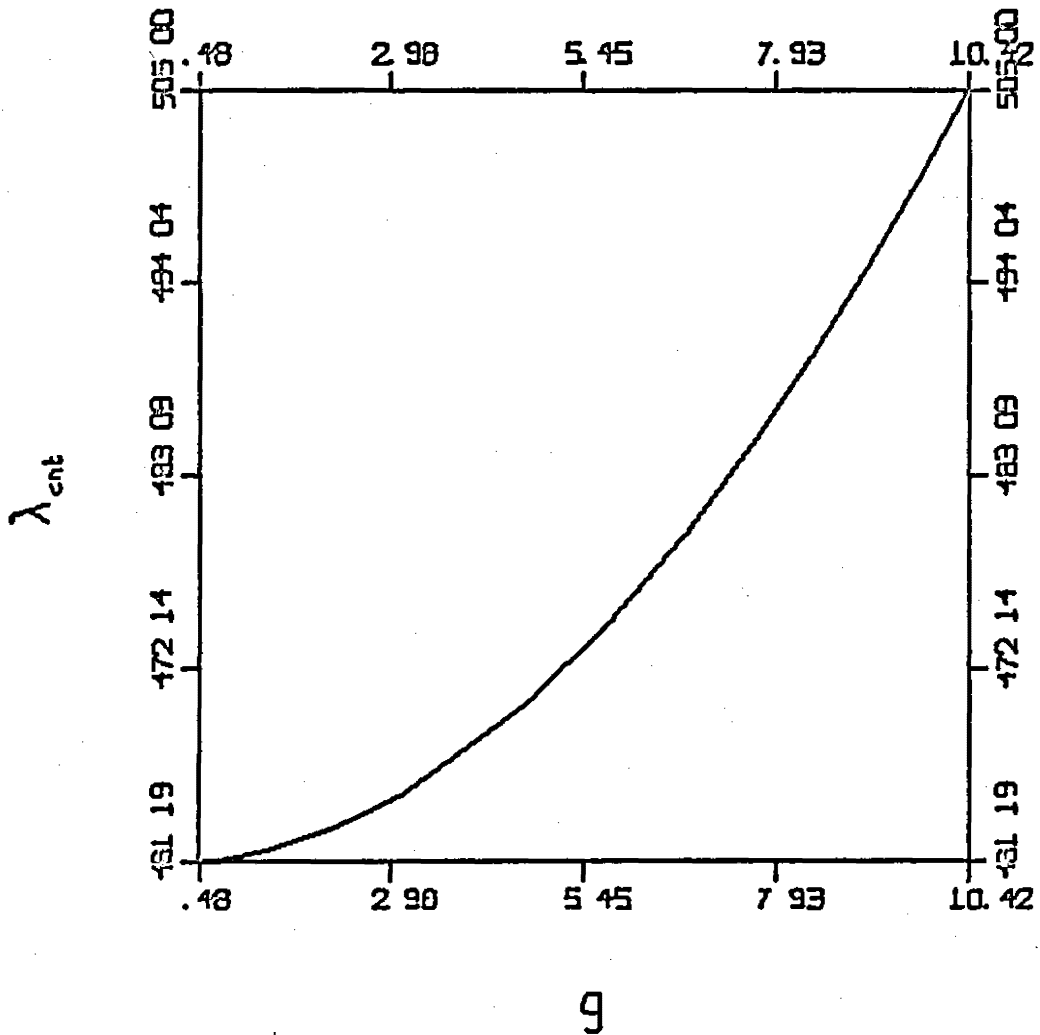


Figure 26. Effect of Damping on Flutter, Boron-Aluminium, $\phi=0^\circ$

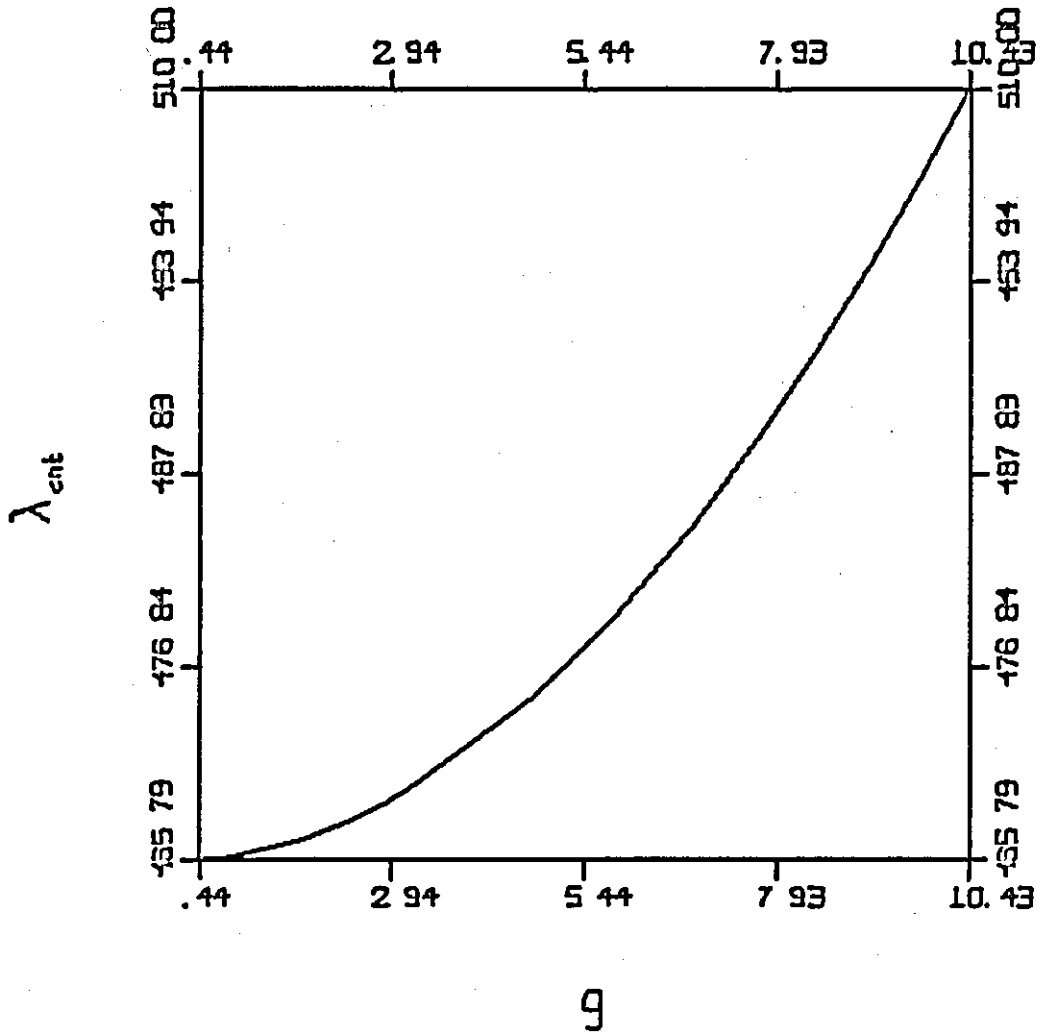


Figure 27. Effect of Damping on Flutter, Boron-Aluminium, $\phi=10^\circ$

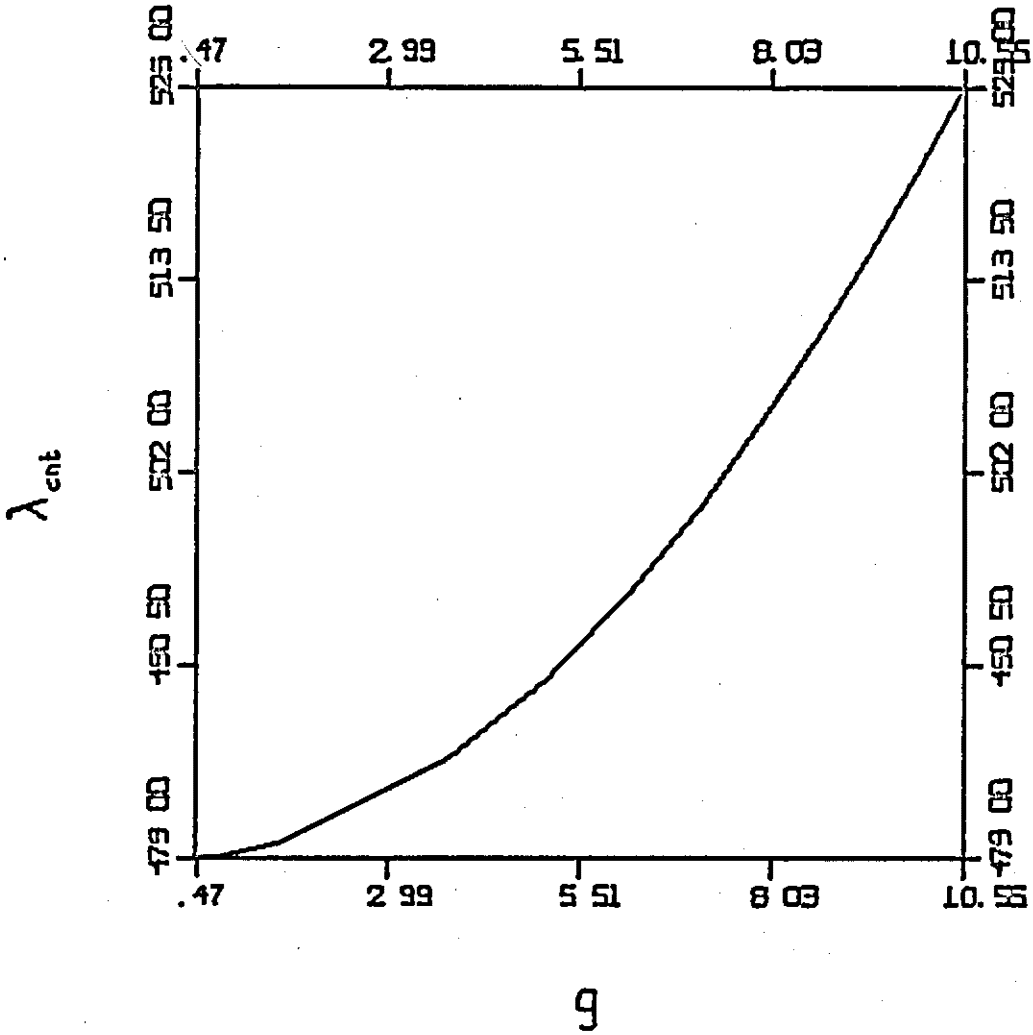


Figure 28. Effect of Damping on Flutter, Boron-Aluminium, $\phi=20^\circ$

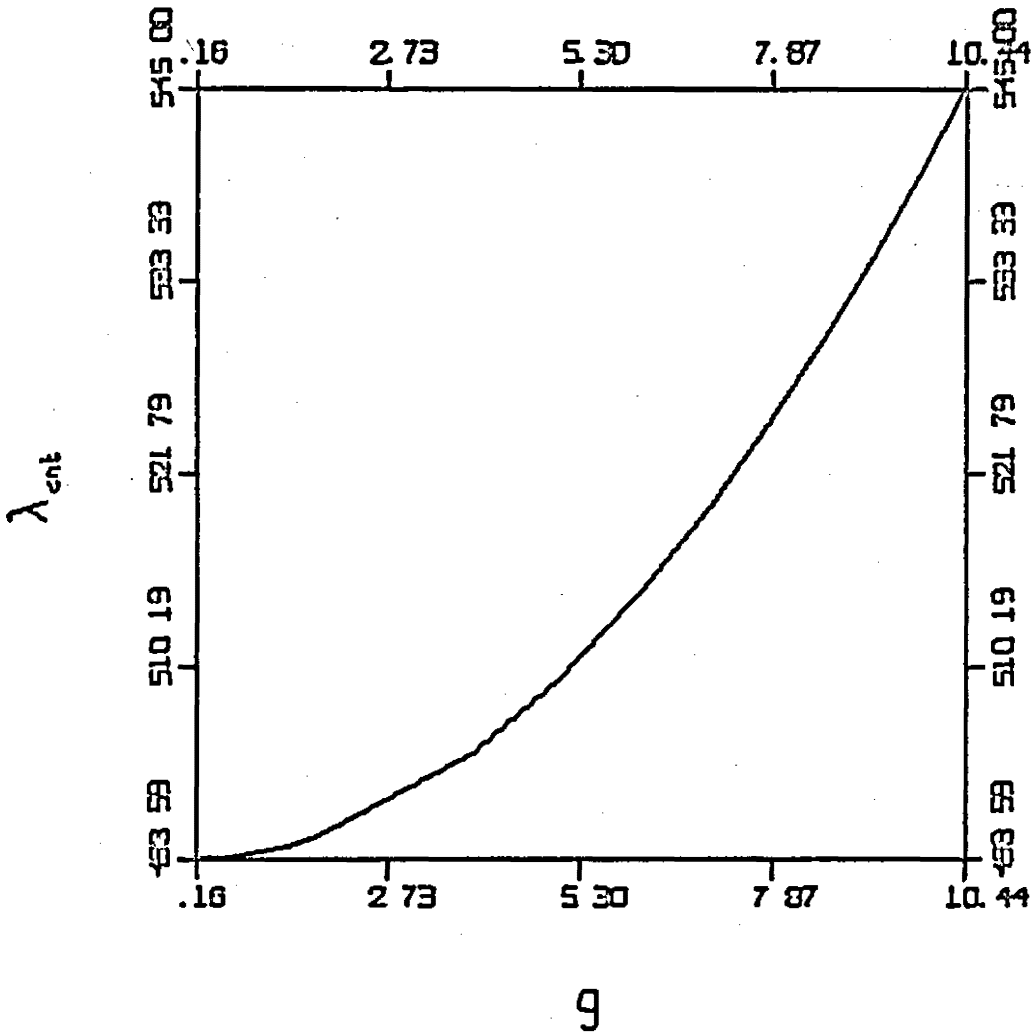


Figure 29. Effect of Damping on Flutter, Boron-Aluminium, $\phi=30^\circ$

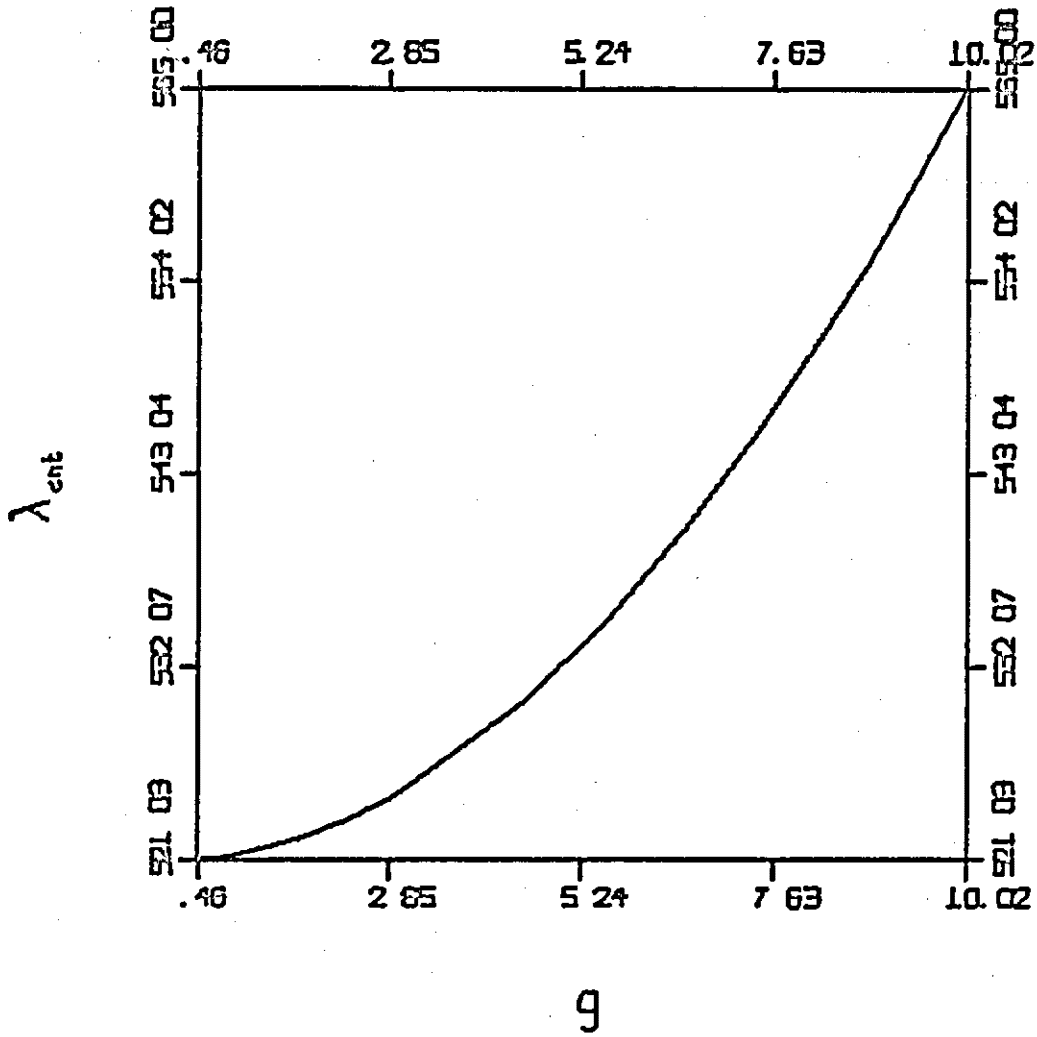


Figure 30. Effect of Damping on Flutter, Boron-Aluminium, $\phi=40^\circ$

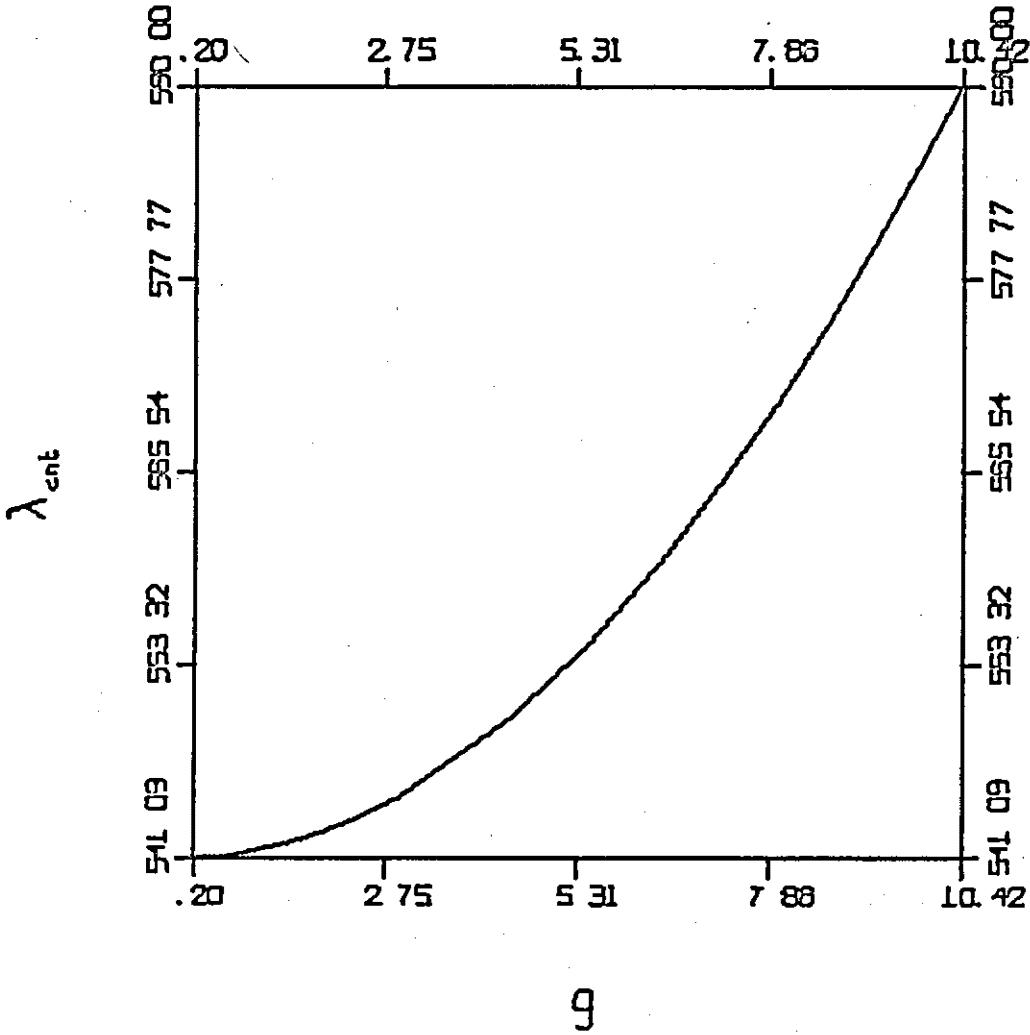


Figure 31. Effect of Damping on Flutter, Boron-Aluminium, $\phi=50^\circ$

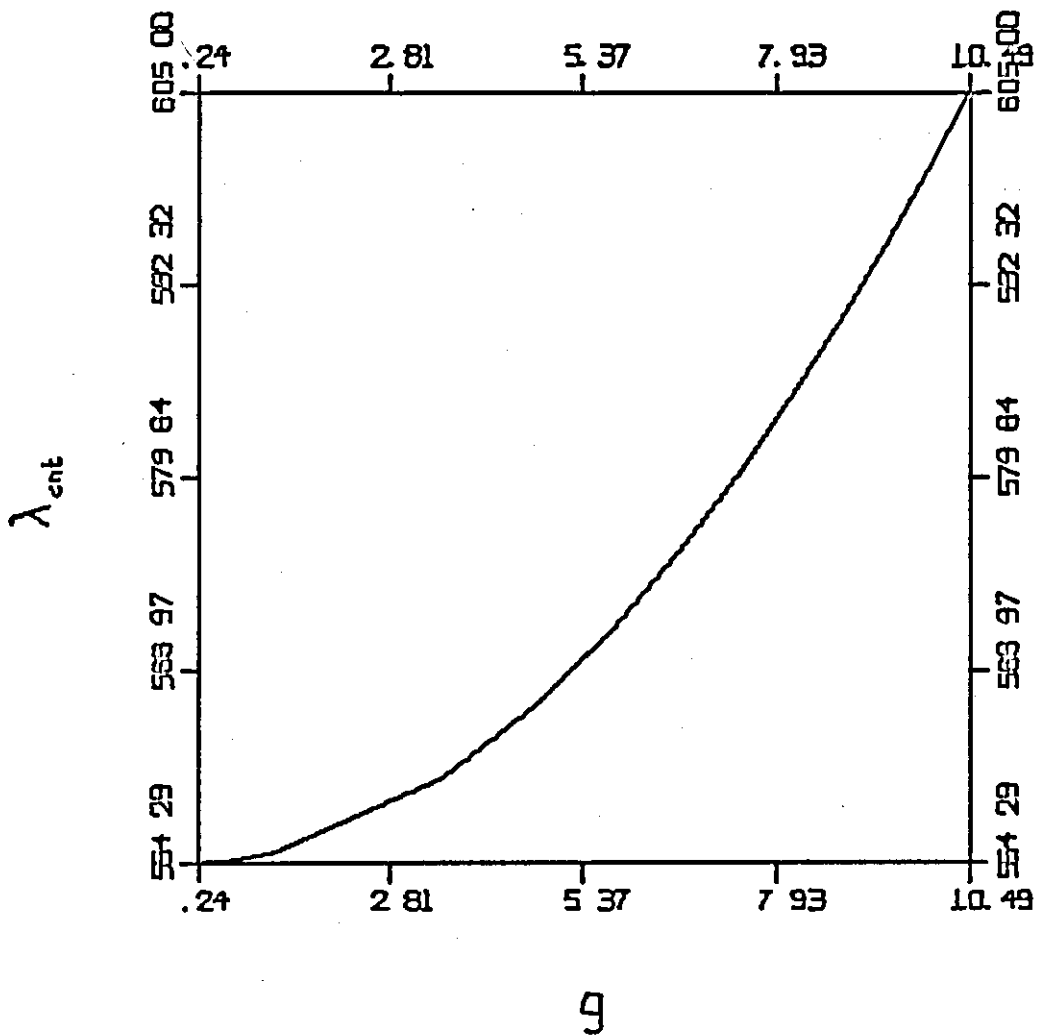


Figure 32. Effect of Damping on Flutter, Boron-Aluminium, $\phi=60^\circ$

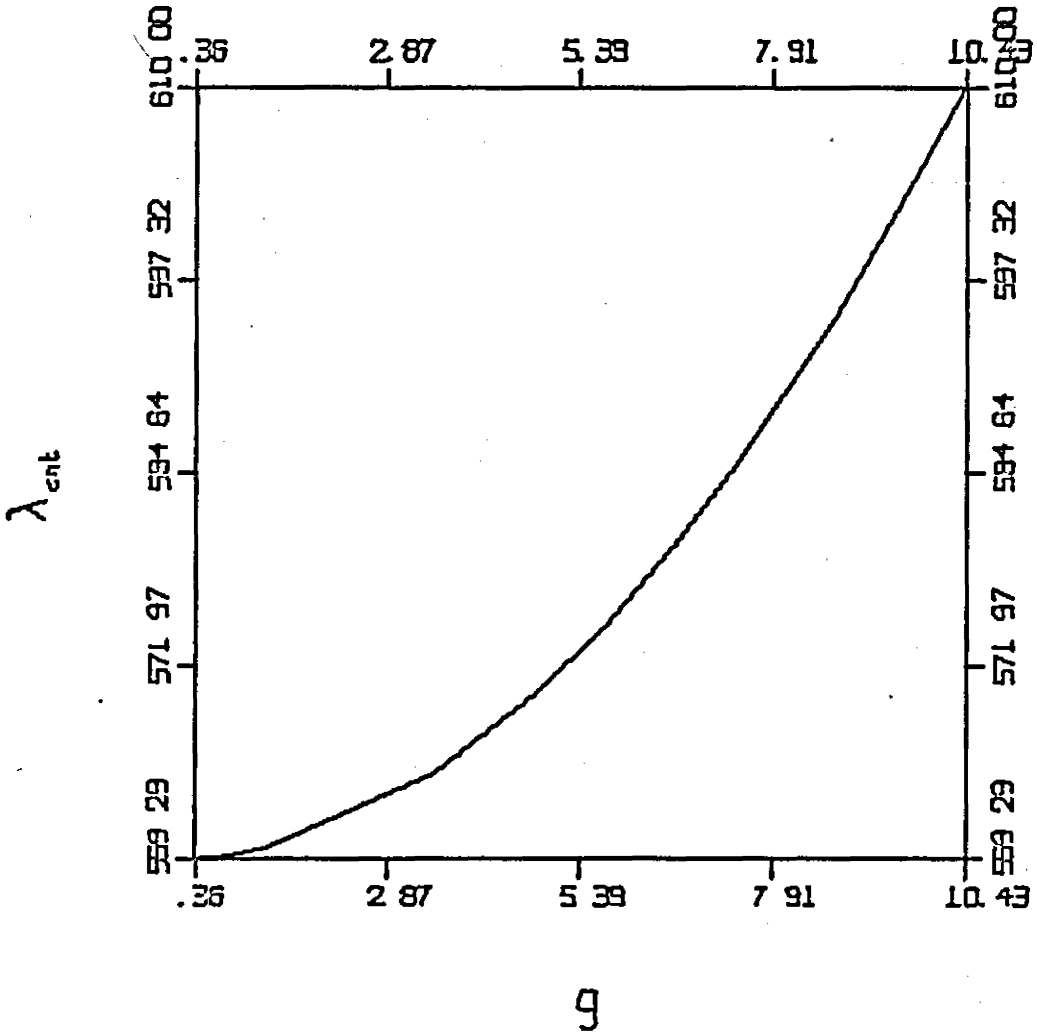


Figure 33. Effect of Damping on Flutter, Boron-Aluminium, $\phi=70^\circ$

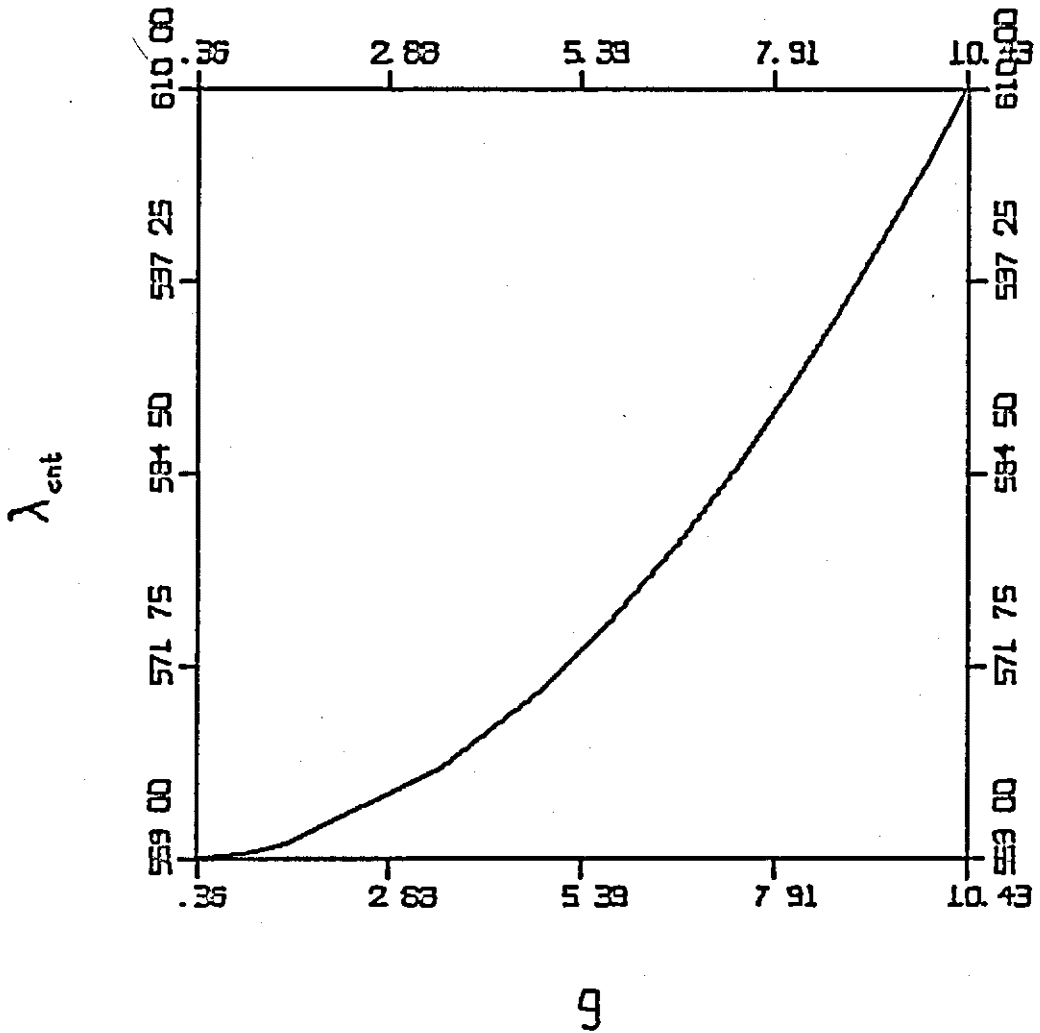


Figure 34. Effect of Damping on Flutter, Boron-Aluminium, $\phi=80^\circ$

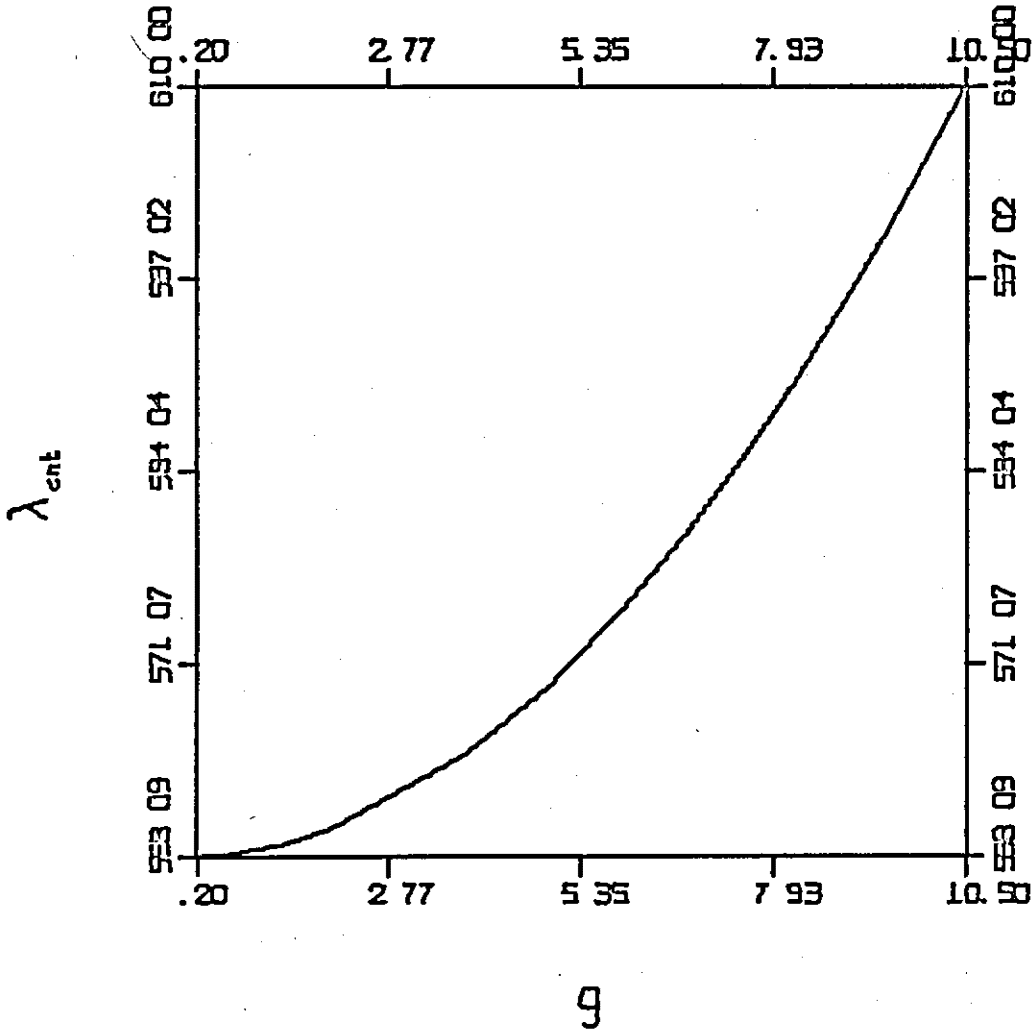


Figure 35. Effect of Damping on Flutter, Boron-Aluminium, $\phi=90^\circ$

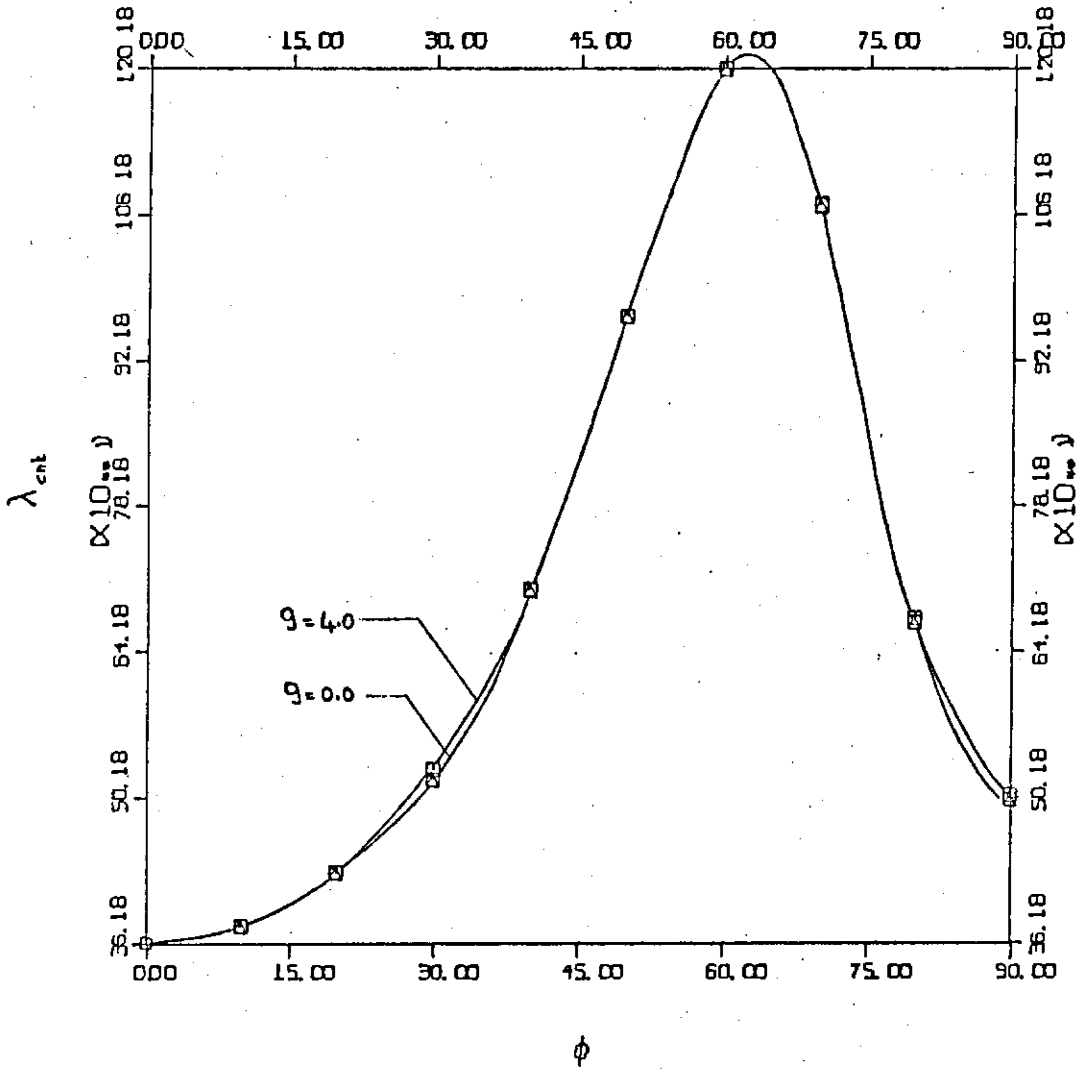


Figure 36. Variation in Flutter Boundary with Damping, Boron-Epoxy

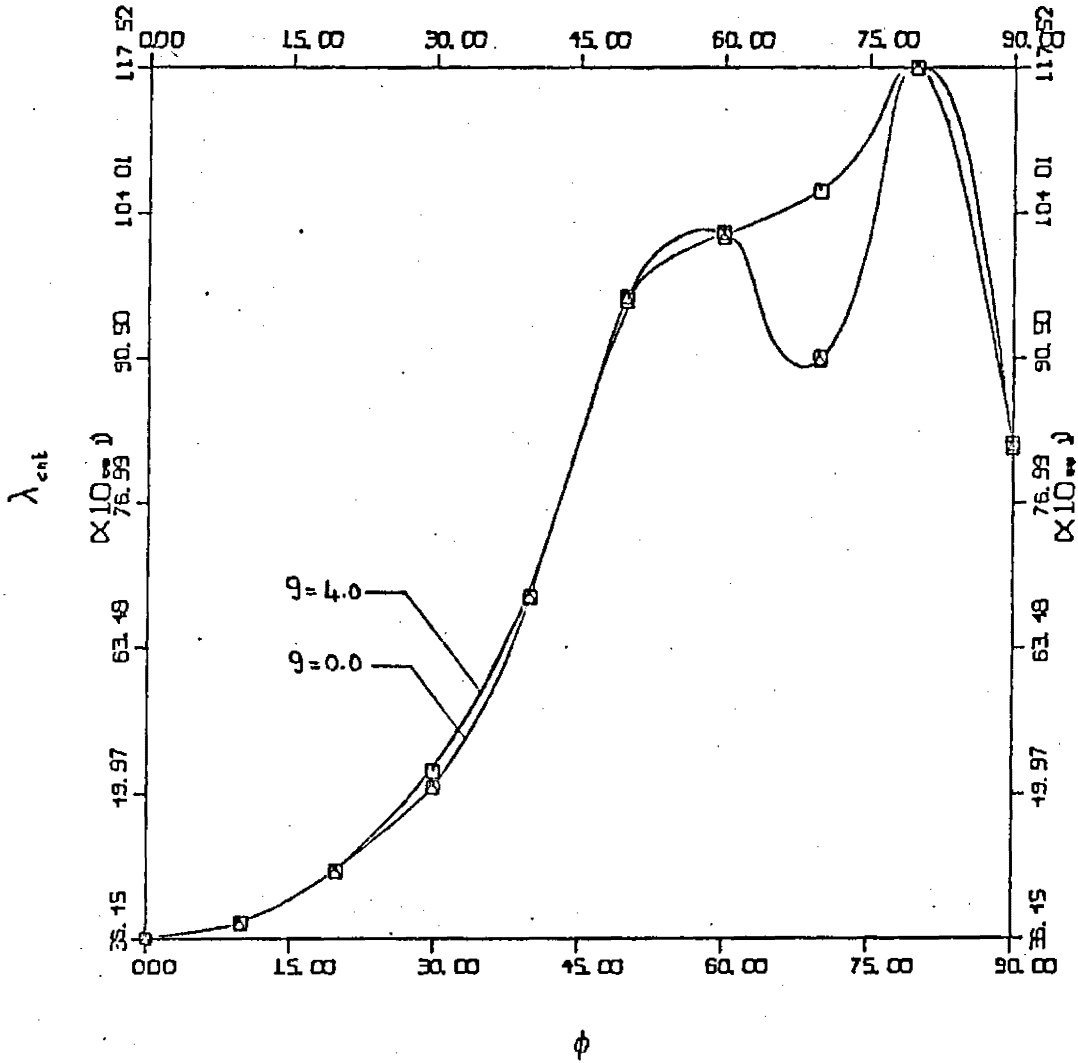


Figure 37. Variation in Flutter Boundary with Damping, Graphite-Epoxy

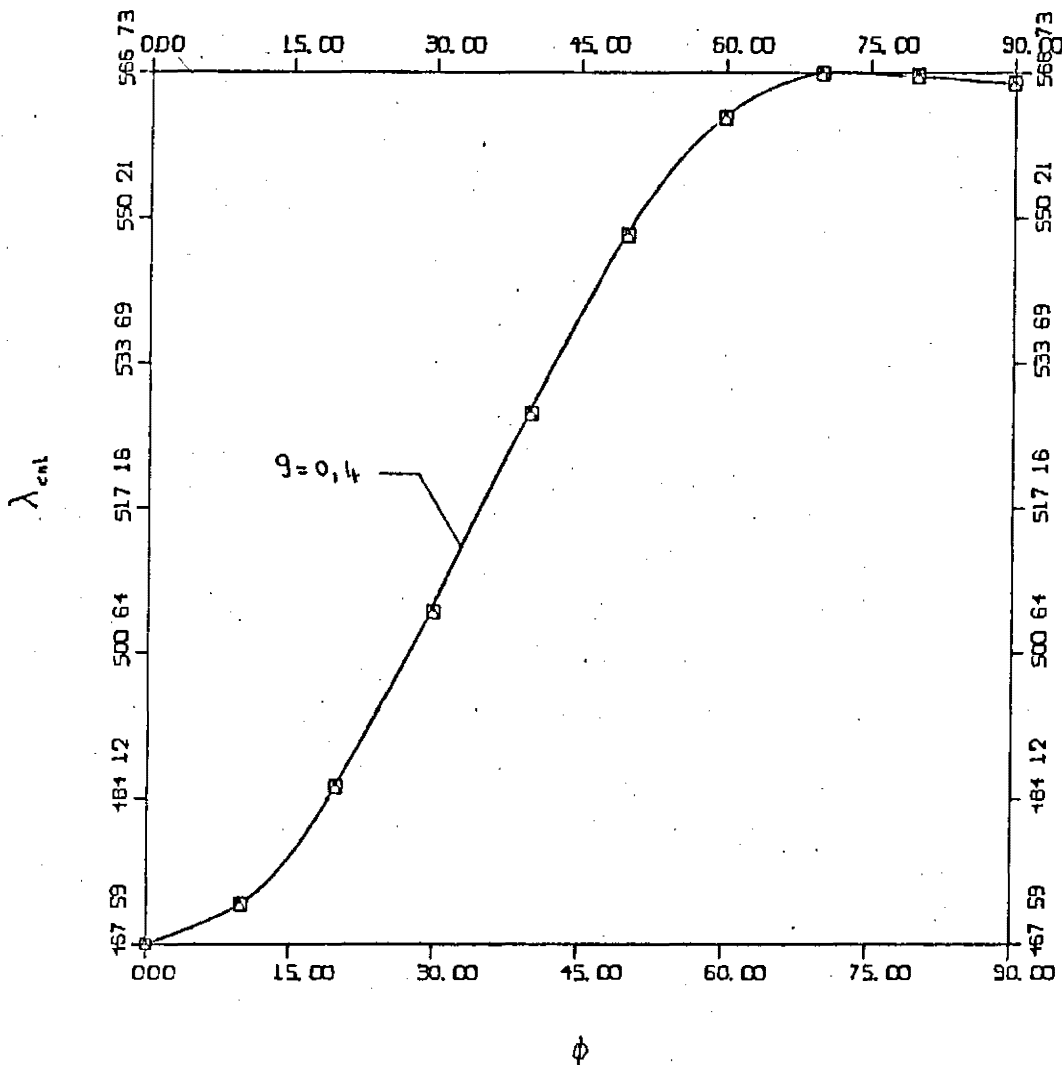


Figure 38. Variation in Flutter Boundary with Damping, Boron-Aluminium

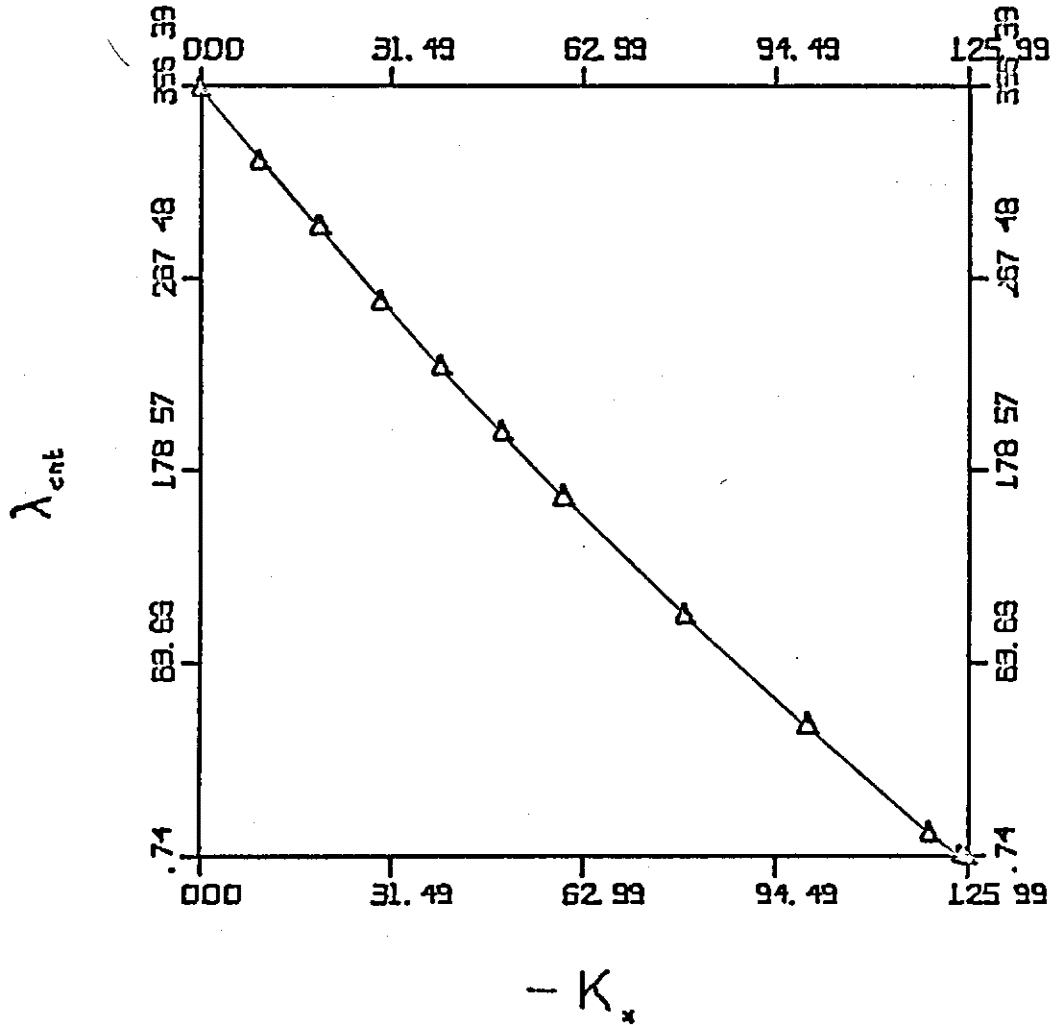


Fig. 39. Effect of Streamwise Inplane Compressive Stress on Flutter, Boron-Epoxy, $\phi=0^\circ$

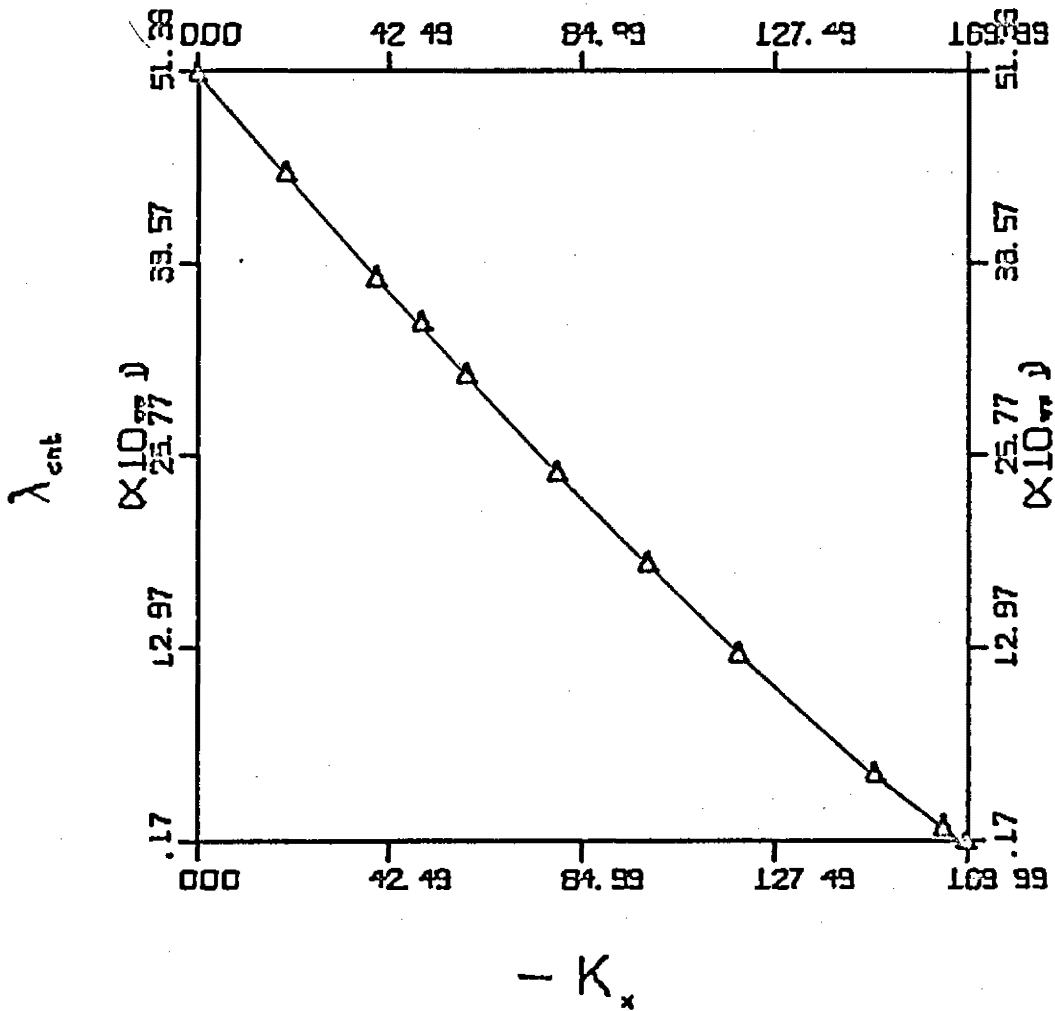


Fig. 40. Effect of Streamwise Inplane Compressive Stress on Flutter, Boron-Epoxy, $\phi=30^\circ$

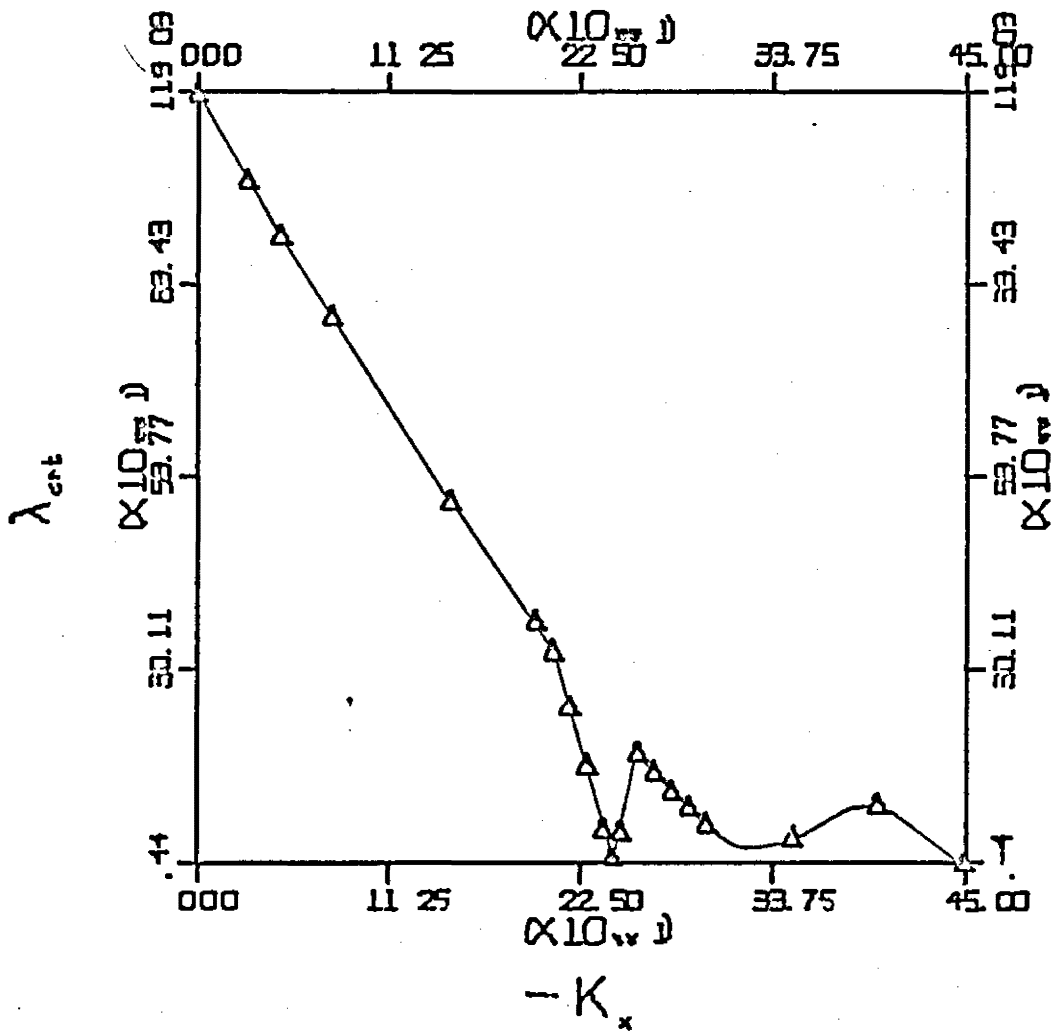


Fig. 41. Effect of Streamwise Inplane Compressive Stress on Flutter, Boron-Epoxy, $\phi=60^\circ$

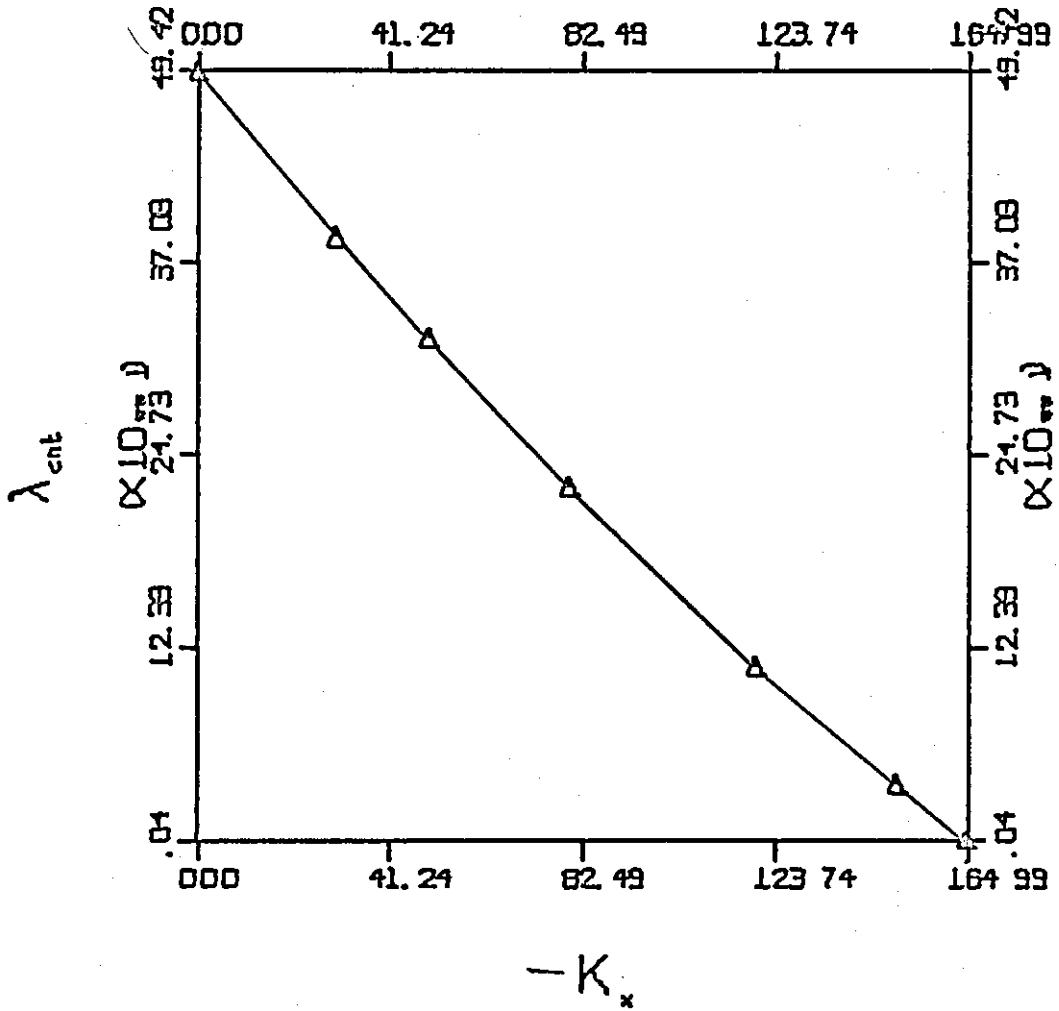


Fig. 42. Effect of Streamwise Inplane Compressive Stress on Flutter, Boron-Epoxy, $\phi=90^\circ$

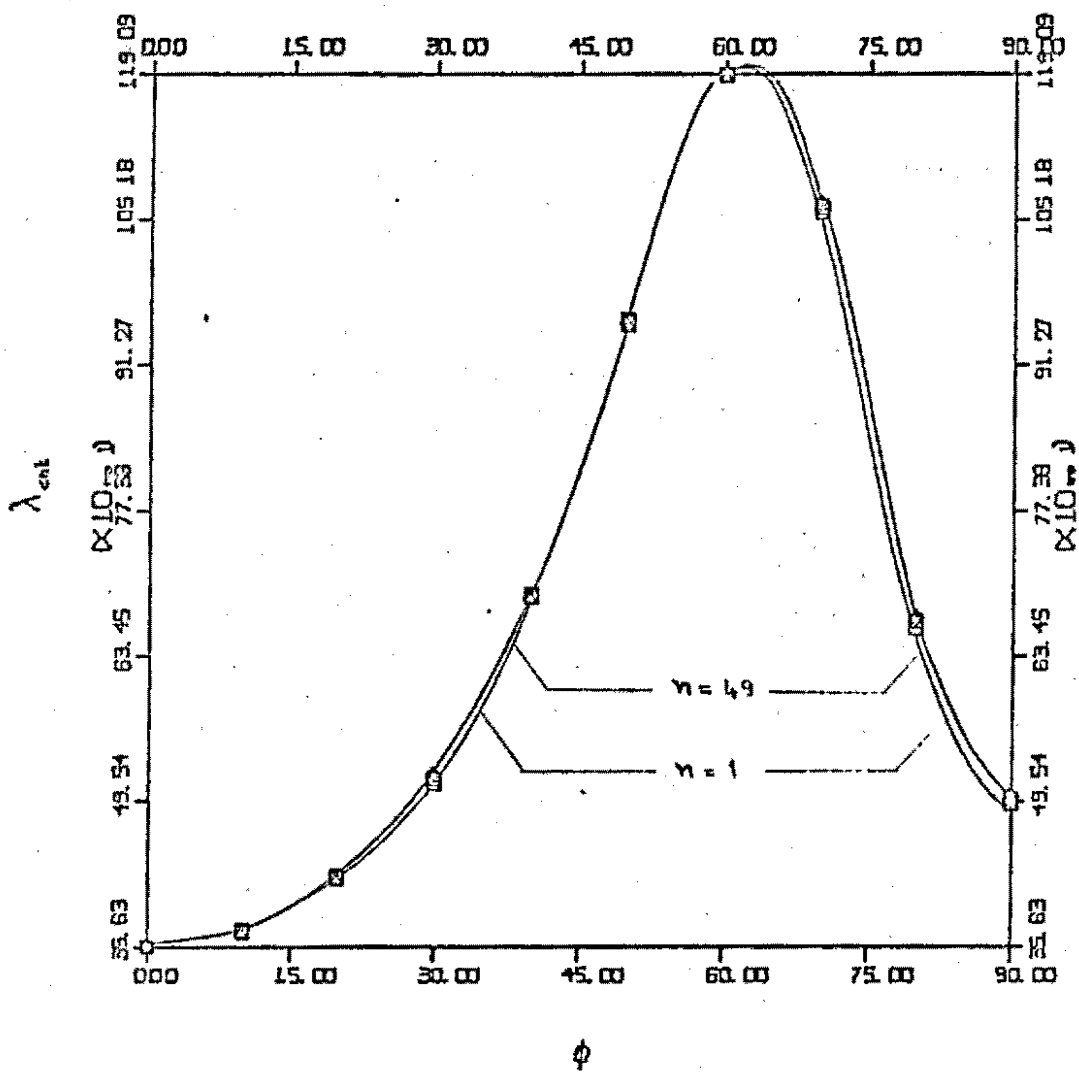


Fig. 43. Effect of Number of Plies on Flutter Boundary, Boron-Epoxy Angle-Ply Panel

Attention Patron:

The one-page vita has been removed
from the scanned document

FLUTTER ANALYSIS OF FLAT RECTANGULAR ANISOTROPIC PANELS

IN A HIGH MACH NUMBER SUPERSONIC FLOW

by

R. L. RAMKUMAR

(ABSTRACT)

A study of the flutter of a flat, simply supported, rectangular, anisotropic panel, exposed to supersonic flow on one side, is carried out using small deflection thin-plate theory and two-dimensional piston theory aerodynamics. The effect on flutter of the following items are examined : individual orthotropic ply orientation with respect to the freestream; inplane compressive stresses in the streamwise direction; aerodynamic and/or structural damping; and the number of layers in an angle-ply panel, with plies of the same orientation angle but alternating signs. Solutions are obtained using a twenty term Rayleigh-Ritz procedure. Three different fiber-matrix combinations for the individual orthotropic plies are used. These are : boron-epoxy, graphite-epoxy and boron-aluminium.

The results indicate that the parallel alignment of the ply principal axis with the freestream direction does not necessarily raise the flutter boundary. The flutter value is dependent on the relative stiffnesses of the individual plies, their orientation with respect to the freestream, and the panel aspect ratio. Increasing the number of plies in the panel and the addition of inplane compressive stresses lowers the flutter boundary while the addition of damping always raises it.